藥學博士 學位論文

Endogenous ω-3 fatty acid production in *fat-1* transgenic mice protects against experimentally induced inflammation and carcinogenesis

fat-1 형질전환 마우스를 이용한 오메가 3 지방산의 대장 염증질환 및 광유도 피부암 보호효과 기전 연구

2017 年 8 月

서울大學校 大學院

藥學科 醫藥生命科學專攻

廉 惠 媛

Endogenous ω-3 fatty acid production in *fat-1* transgenic mice protects against experimentally induced inflammation and carcinogenesis

fat-1 형질전환 마우스를 이용한 오메가3 지방산의 대장 염증질환 및 광유도 피부암 보호효과 기전 연구

指導敎授 徐 榮 俊

이 論文을 藥學博士 學位論文으로 提出함

2017 年 8 月

서울大學校 大學院

藥學科 醫藥生命科學專攻

廉 惠 媛

廉惠媛의 藥學博士 學位論文을 認准함

2017 年 8 月

委 員 長 _____ (印)

副委員長 _____ (印)

委 員 _____ (印)

委 員 _____ (印)

委 員 _____ (印)

Endogenous ω-3 fatty acid production in *fat-1* transgenic mice protects against experimentally induced inflammation and carcinogenesis

by

Hye-Won Yum

A thesis submitted in partial fulfillment of the requirements

for the degree of

DOCTOR OF PHILOSOPHY

(Pharmacy: Pharmaceutical bioscience major)

under the supervision of Professor Young-Joon Surh

at the

College of Pharmacy,

Seoul National University

August 2017

ABSTRACT

Endogenous ω-3 fatty acid production in *fat-1* transgenic mice protects against experimentally induced inflammation and carcinogenesis

HYE-WON YUM

Under the supervision of Professor Young-Joon Surh
at the College of Pharmacy, Seoul National University

Omega-6 (ω-6) and omega-3 (ω-3) polyunsaturated fatty acids (PUFAs) are known to have opposite effects on the inflammatory and carcinogenesis processes. In general, ω-6 PUFAs promote inflammation and tumor development, whereas ω-3 PUFAs possess anti-inflammatory as well as anti-oxidative activity and enhance host immune response.

In the present study, I investigated the protective effects of ω-3 PUFAs on experimentally induced inflammation and carcinogenesis using *fat-1* transgenic mice harboring ω-3 desaturase gene capable of converting ω-6 to ω-3 PUFAs. The ω-3/ω-6 PUFA ratio was significantly higher in the dorsal skin of *fat-1* mice than that in the wild-type (WT) C57BL/6 mice. *fat-1* mice expressed heme

oxygenase-1 (HO-1) and NAD(P)H:quinone oxidoreductase-1 and their mRNA transcripts to a greater extent than did WT mice, which was attributable to the elevated activation of nuclear factor erythroid-related factor 2 (Nrf2) responsible for upregulation of cytoprotective and stress-responsive proteins.

Exposure to solar radiation, especially ultraviolet B (UVB), is the most prevalent cause of skin photocarcinogenesis. Upon single exposure to UVB (500 mJ/cm^2) irradiation, *fat-1* mice exhibited a significantly lower degree of skin inflammation and phototoxicity and the expression of the pro-inflammatory enzyme, cyclooxygenases-2 (COX-2) as compared to those observed in WT mouse skin. The protection of *fat-1* mice from UVB-induced skin inflammation was associated with decreased phosphorylation of signal transducer and activator of transcription 3 (STAT3), one of the major pro-inflammatory transcription factors.

To determine whether the elevated ω-3 PUFA level also protects against UVB-induced skin papillomagenesis, hairless *fat-1*$^{-/-}$ and *fat-1*$^{+/-}$ mice were generated by cross-breeding of male *fat-1*$^{+/-}$ transgenic mice with female SKH-1 hairless mice. After repeated UVB irradiation (180 mJ/cm^2) thrice a week for 23 weeks, the incidence and the multiplicity of papillomas were markedly reduced in the *fat-1*$^{+/-}$ group as compared to the *fat-1*$^{-/-}$ group. Moreover, the expression of COX-2 and activation of STAT3 in papillomas from *fat-1*$^{+/-}$ mice were significantly lower than those found in UVB-irradiated *fat-1*$^{-/-}$ mice.

In another study, I also found that an increased ω-3 PUFA tissue status in the *fat-1* mice led to effective protection against inflammatory tissue injury in

colitis induced by 2,4,6-trinitrobenzene sulfonic acid. The endogenous increase in ω-3 PUFAs in *fat-1* mice lso attenuated lipid peroxidation (malondialdehyde) and protein oxidation (4-hydroxy-2-nonenal). The observed protection against inflammatory and oxidative tissue damages in the *fat-1* mouse colon was associated with decreased nuclear factor kappa B (NF-κB) activity and expression of COX-2 and with elevated activation of Nrf2 and expression of its target gene, *ho-1*.

Taken together, these observations indicate that functional *fat-1* potentiates cellular defense against experimentally induced inflammation and tumor development through elevated activation of Nrf2 and subsequent upregulation of cytoprotective gene expression as well as suppression of pro-inflammatory signaling mediated by STAT3 and/or NF-κB.

Keywords

2,4,6-Trinitrobenzene sulfonic acid; Colitis; *fat-1* transgenic mice; Inflammation; NF-κB; Nrf2; Omega-3 polyunsaturated fatty acids; Photocarcinogenesis; STAT3; Ultraviolet B

Student Number: 2012-30464

TABLE OF CONTENTS

LIST OF FIGURES

Chapter Ⅰ

Chapter Ⅱ

Chapter Ⅲ

Chapter Ⅳ

LIST OF TABLES

Chapter Ⅱ

Chapter Ⅲ

LIST OF ABBREVIATIONS

NSAID, nonsteroidal anti-inflammatory drug

PUFA, polyunsaturated fatty acid

AA, arachidonic acid

EPA, eicosapentaenoic acid

DHA, docosahexaenoic acid

WT, wild-type

LA, linoleic acid

UVB, ultraviolet B

TNBS, 2,4,6-trinitrobenzene sulfonic acid

STAT3, signal transducer and activator of transcription 3

Nrf2, nuclear factor erythroid-related factor 2

ROS, reactive oxygen species

4-HNE, 4-hydroxynonenal

MDA, malondialdehyde

COX-2, cyclooxygenase-2

iNOS, inducible nitric oxide synthase

HO-1, heme oxygenase-1

NQO1, NAD(P)H:quinone oxidoreductase-1

PI3K, phosphoinositide 3-kinase

H&E, hematoxylin and eosin

TUNEL, terminal deoxynucleotidyl transferase dUTP nick-end labeling

IHC, immunohistochemical analysis

DTT, dithiothreitol

PMSF, phenylmethyl sulfonylfluoride

EDTA, ethylenediaminetetraacetic acid

HEPES, 4-(2-hydroxyethyl)-1-piperazineethanesulfonic acid

NP-40, Nonidet P-40

SDS, sodium dodecyl sulfate

PAGE, polyacrylamide gel electrophoresis

PVDF, polyvinylidene difluoride

TBST, tris-buffered saline containing 0.1% tween 20

ECL, enhanced chemiluminescent

RT-PCR, reverse transcription-polymerase chain reaction analysis

SE, standard error

NF-κB, nuclear factor kappa B

ARE, antioxidant response element

MEF, mouse embryonic fibroblast

DMEM, Dulbecco's modified Eagle's medium

FBS, fetal bovine serum

MEM, minimum essential medium

PBS, phosphate-buffered saline

DCF-DA, 2',7'-dichlorofluorescein diacetate

HBSS, Hanks' balanced salt solution

SD, standard deviation

IBD, inflammatory bowel diseases

Chapter Ⅰ

Anti-inflammatory effects of ω-3 fatty acids: Implications for its cancer chemopreventive potential

1. Introduction

Inflammation underlies both physiological and pathological processes. Physiological or acute inflammation has been largely considered as the body's innate and adaptive immune responses triggered by divergent noxious stimuli and conditions (Medzhitov 2008). Upon infection and tissue injury, a distinct set of substances (*e.g.*, cytokines, chemokines, lymphokines, lipid mediators, etc.) are released in inflamed sites, triggering recruitment of leuokocytes and subsequent inflammatory reactions. While self-limited acute inflammation is protective, the defects in resolving the inflammation at an early stage results in a failure to return to the tissue homeostasis. This can cause persistent inflammatory conditions implicated in various pathologic conditions, such as rheumatoid arthritis, obesity, diabetes, cardiovascular diseases, neurodegenerative disorders, etc (Ricciotti & FitzGerald 2011, Nathan & Ding 2010). The emerging role of chronic inflammation that may occur as a consequence of failure to resolve acute inflammation in multistage carcinogenesis has been extensively explored at both cellular and molecular levels (Kundu & Surh 2012).

Due to poor cost-effectiveness and side effects of current anticancer therapy, attention has been paid to preventive strategies, especially by use of natural products (Harnack *et al.* 1997, Beaglehole *et al.* 2011, Manca *et al.* 2012, Sher *et al.* 2011). Besides a plethora of adverse effects reported for some chemotherapeutic drugs (Monsuez *et al.* 2010, Monje & Dietrich 2012, Eschenhagen *et al.* 2011, Ihbe-Heffinger *et al.* 2013, Love *et al.* 1989), use of

some anti-inflammatory agents for the purpose of cancer chemoprevention has been hampered by the abrupt finding of unpredictable serious side effects (Arber *et al.* 2006, Bertagnolli *et al.* 2006, Burn *et al.* 2011b, Burn *et al.* 2011a). Thus, the use of nonsteroidal anti-inflammatory drugs (NSAIDs) in clinical practice for cancer chemoprevention has always been outweighed by the possibility of serious complications. Furthermore, some currently used anti-inflammatory drugs were developed without appreciation of their potential impact in resolution, and proved to be resolution-toxic (Gilroy *et al.* 1999, Bannenberg *et al.* 2005, Serhan *et al.* 2007) whereas others, such as glucocorticoids (Coutinho & Chapman 2011), cyclin-dependent kinase inhibitors (Rossi *et al.* 2006) and aspirin (Serhan *et al.* 1995, Serhan 2007), possess proresolving actions.

A wide spectrum of natural products, especially those present in dietary and medicinal plants, have potent anti-inflammatory properties and have been shown to prevent tumor occurrence in several organs of experimental animals and inhibit the growth of neoplastic cells (Kim *et al.* 2009b, Pan *et al.* 2009, Gupta *et al.* 2010, Neergheen *et al.* 2010, Bishayee *et al.* 2012). A large number of chemopreventive phytochemicals capable of inhibiting the inflammatory cascade are known to modulate various signaling pathways implicated in cancer initiation, promotion and progression (Kundu & Surh 2005, Khor *et al.* 2008).

Additionally, interest in natural proresolving mechanisms has been heightened in recent years (Henson 2005, Luster *et al.* 2005, Serhan & Savill 2005). Polyunsaturated fatty acids (PUFAs) are precursors of biologically

active lipid mediators, including eicosanoids that play an important role in modulating pro-inflammatory and/or anti-inflammatory/proresolving processes. Arachidonic acid (AA), a key member of the ω-6 PUFAs, produces the eicosanoids that are essential mediators of inflammation (Calder 2006). These include prostaglandins, leukotrienes, and thromboxanes. Some pro-inflammatory prostaglandins (e.g., PGE_2) promote carcinogenesis and stimulate tumor growth, metastasis and angiogenesis (Wang & Dubois 2010a). However, eicosanoids and some other bioactive lipid mediators produced from ω-3 PUFAs have opposing effects (**Fig. 1-1**).

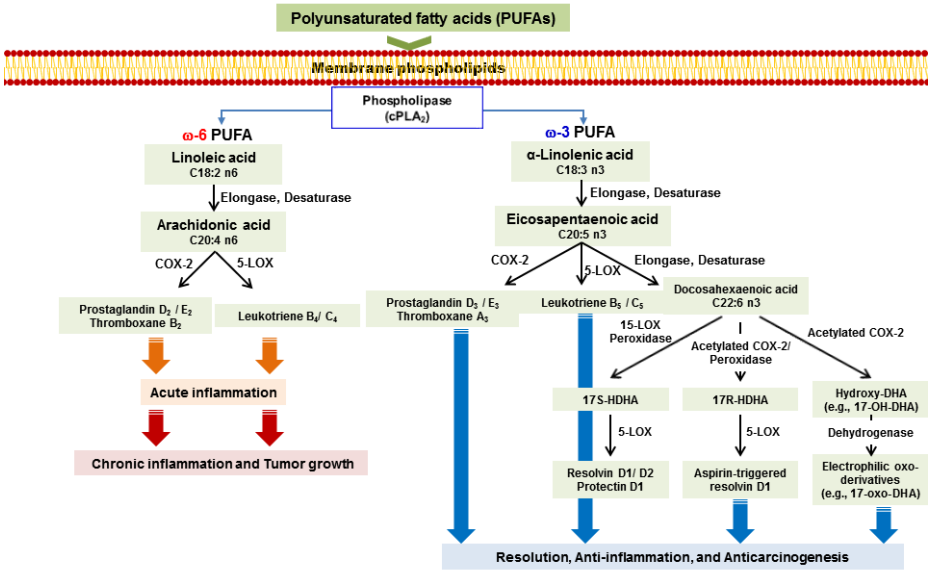

Fig. 1-1. Differential roles of ω-6 and ω-3 PUFAs in inflammation and carcinogenesis. Adopted from: Yum *et al.* (2016).

2. The health beneficial effects associated with ω-3 PUFAs

One major dietary source of anti-inflammatory ω-3 PUFAs is fish oil containing eicosapentaenoic acid (EPA; C20:5) and docosahexaenoic acid (DHA; C22:6). Numerous studies have demonstrated the protective effects of dietary supplementation with EPA and DHA against pathogenesis of multi-organ cancer (Toriyama-Baba *et al.* 2001) as well as other ailments, including cardiovascular disorders (Holub & Holub 2004), retinal degenerations (Souied *et al.* 2013), and neurodegenerative diseases (Connor & Connor 2007). Mammals are unable to synthesize EPA and DHA, but they can be formed from the shorter-chain ω-3 PUFA, α-linolenic acid (C18:3) obtained from the plant diet through elongation and desaturation (Calder 2008). Recently, attention has focused on a group of endogenous bioactive lipid mediators derived from DHA because of their powerful proresolving as well as anti-inflammatory activities. Examples are resolvins, protectins and maresins which are generated during the spontaneous resolution phase of inflammation (Dalli *et al.* 2013, Serhan & Savill 2005).

Recommendations for dietary intake of ω-3 PUFAs are often provided for the combination of EPA and DHA. Both have a similar spectrum of biological properties. However, several studies have reported differential effects of EPA, DHA and their metabolites on organization, fluidity and permeability of plasma membrane, modulation of signaling pathways related to cellular pro- or anti-inflammatory mechanisms, leukocyte functions (*e.g.*, phagocytosis, chemotactic response and cytokine production), endothelial cell functions, cell

proliferation and differentiation, etc (Russell & Burgin-Maunder 2012, Ma *et al.* 2012, Gorjao *et al.* 2009)**.** This may be attributable to the differences in their carbon backbone structure in terms of the length and the degree of unsaturation. While EPA has 20 carbon atoms and 5 double bonds (20:5), DHA has a longer chain of 22 carbon atoms and 6 double bonds (22:6). The higher degree of unsaturation in DHA, compared with EPA, is considered to yield greater proton selectivity and conductance by increasing the membrane permeability in planar phospholipid bilayer preparations (Gorjao *et al.* 2009). Such structural differences may also contribute to different potency of DHA and EPA in modulating cellular inflammatory and anti-inflammatory/proresolving processes. Under certain experimental conditions, DHA was shown to be more effective than EPA in terms of anticancer effects (Serini *et al.* 2011) and capability of decreasing blood pressure, heart rate, and platelet aggregation (Cottin *et al.* 2011, Ibrahim *et al.* 2011). **Fig. 1-2** illustrates the various health benefits that can be achieved by DHA intake. Transcription factors have also been proposed as molecular targets of DHA in exerting its anti-inflammatory effects and immune modulation (**Fig. 1-3**).

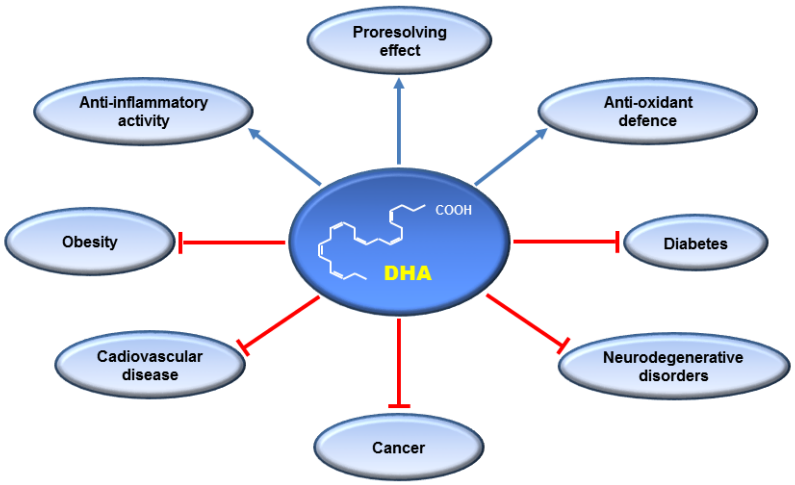

Fig. 1-2. The health beneficial effects associated with DHA derived from fish oil. Adopted from: Yum *et al.* (2016).

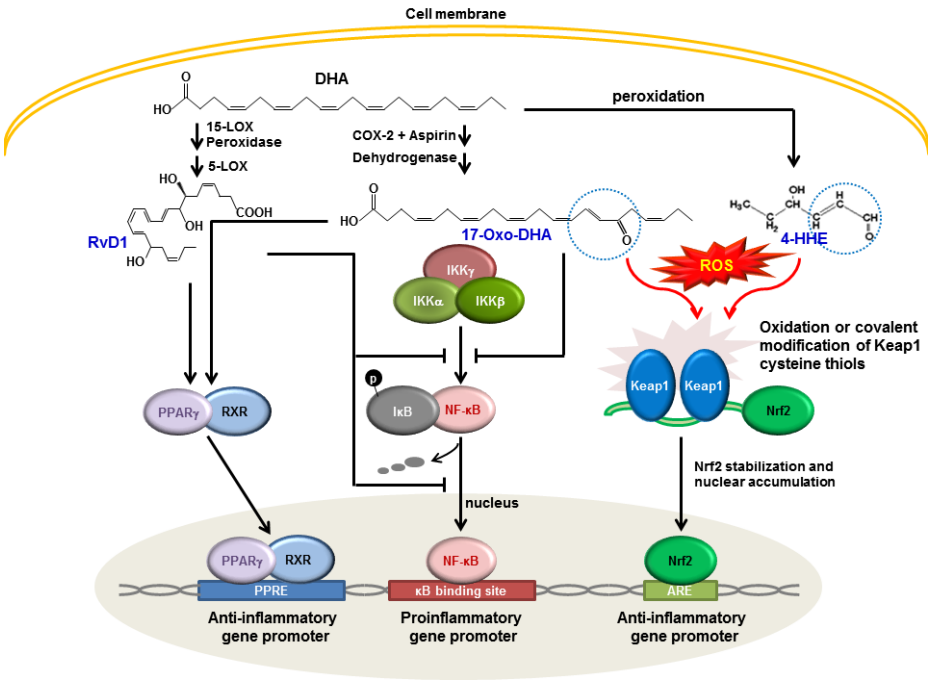

Fig. 1-3. Effects of some DHA-derived bioactive species on activation of representative transcription factors involved in pro-/anti-inflammatory signaling. 15-Lipoxygenase (15-LOX) transforms DHA into 17S-hydroperoxy-DHA, which is converted into RvD1 by 5-LOX activity of neighbouring leukocytes. Some electrophilic species (e.g., 4-HHE and 17-oxo-DHA) formed through peroxidation or oxidative metabolism of DHA activate Nrf2-mediated anti-inflammatory signaling. They can also inhibit pro-inflammatory transcription factors including NF-κB. The roles for these reactive species in the resolution of inflammation are largely elusive. **Adopted from: Yum *et al.* (2016).**

3. The *fat-1* transgenic mouse

An appropriate animal model that can eliminate confounding factors of diet has been delevoped for precise evaluation of the health effects of ω-3 PUFAs. Mammals normally lack the enzyme that can convert ω-6 to ω-3 PUFAs. However, *Caenorhabditis elegans* and some other lower life animas harbor a gene called *fat-1* (Spychalla *et al.* 1997). *fat-1* gene encodes an ω-3 fatty acid desaturase that can introduce a double bond into ω-6 PUFAs at the ω-3 position of their hydrocarbon chains to form ω-3 counterparts (Kang *et al.* 2001, 2007). Kang *et al.* generated a transgenic mouse capable of converting ω-6 to ω-3 fatty acids with the *fat-1* gene (Kang *et al.* 2004, 2007 ; see **Fig. 1-4** for illustration). This will eliminate the need of two different diets for a comparative study so that the potential variations of the impurities, flavor, caloric and other components in the supplemented oils can be avoided. Both transgenic and wild-type (WT) mice are maintained on just a single diet rich in ω-6 PUFAs, mainly linoleic acid (LA) with very little ω-3 PUFAs. Under this dietary regime, WT mice have little or no ω-3 fatty acid in their tissues because they cannot naturally produce ω-3 from ω-6 PUFAs, whereas the *fat–1* transgenic mice have significant amounts of ω-3 PUFAs derived from ω-6 PUFAs in their tissues (Kang *et al.* 2004, 2007). This ω-3 rich profile of lipid with a balanced ratio of ω-6 to ω-3 can be observed in all of the organs and tissues, without changing the mass of tissue fatty acids and the need of a dietary ω-3 supply (Kang *et al.* 2004, 2007).

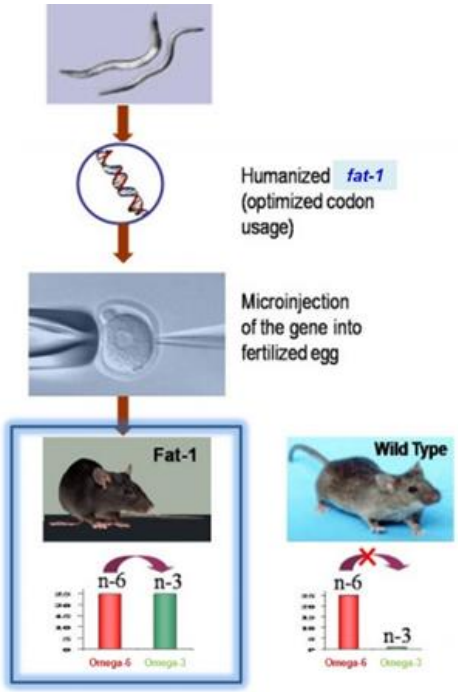

Fig. 1-4. Generation of *fat-1* transgenic mice expressing the gene encoding an ω-3 fatty acid desaturase that converts ω-6 to ω-3 fatty acids. Adopted from: http://www.llmt.org/research_*fat-1*_mouse_model.html.

STATEMENT OF PURPOSE

Inflammation is closely linked to oxidative stress in the pathogenesis of cancer and many other human ailments. The majority of health beneficial effects of ω-3 fatty acids have been ascribed to its anti-inflammatory as well as anti-oxidative properties, but the underlying molecular mechanisms, particularly in relation to their chemopreventive potential, remain largely elusive.

The modulation of the intracellular signal transduction involved in aberrant induction of pro-inflammatory enzymes is considered as a rational approach for chemoprevention. A detailed understanding of the signaling network involved in an inappropriate expression of pro-inflammatory enzymes in ultraviolet B (UVB)-induced inflammation, photocarcinogenesis and 2,4,6-trinitrobenzene sulfonic acid (TNBS)-stimulated colitis is yet to be elucidated.

The purpose of the present study was to investigate whether an increased ω-3 fatty acid tissue level in *fat-1* mice protects against experimentally induced disease models and to elucidate the molecular mechanisms underlying cellular adaptive or defensive response to pro-inflammatory and oxidative damages by focusing on the role of upregulation of cytoprotective proteins.

Chapter Ⅱ

The increased ω-3 fatty acid tissue level in *fat-1* mice protects against UVB-induced inflammatory and oxidative skin damages

1. Abstract

Exposure to solar radiation, especially ultraviolet B (UVB), is the main cause of photocarcinogenesis. Omega-3 (ω-3) polyunsaturated fatty acids (PUFAs), which occur at high levels in some fish oils, are known to scavenge lipid peroxyl radicals and increase host immunoresponsiveness. As UVB-induced oxidative stress and oxidative stress–mediated inflammation have been implicated in photocarcinogenesis, this study was designed to investigate the anti-inflammatory and anti-oxidative capacity of ω-3 PUFAs using *fat-1* transgenic mice that are capable of converting ω-6 to ω-3 PUFAs. Wild-type (WT) C57BL/6 mice and *fat-1* mice were maintained on the AIN-93 diet supplemented with 10% safflower oil rich in ω-6 PUFAs for 5 weeks. The ω-6/ω-3 PUFA ratio was significantly lower in the dorsal skin of *fat-1* mice than that in the WT mice. Upon single exposure to UVB (5.0 kJ/m^2) radiation, WT mice showed higher degree of skin inflammation, phototoxicity, and the expression of pro-inflammatory enzymes, cyclooxygenases-2 and inducible nitric oxide synthase, which were significantly decreased in *fat1* mouse skin. The protection of *fat-1* mice from UVB-induced skin inflammation resulted from decreased phosphorylation of signal transducer and activator of transcription 3 (STAT3) and Akt. In comparison to WT animals, higher levels of cytoprotective proteins, such as heme oxygenase-1 and NAD(P)H:quinone oxidoreductase-1, were found in skin of *fat-1* mice. Furthermore, the elevated activation of nuclear factor erythroid-related factor 2 (Nrf2), which regulates

transcriptional activation of cytoprotective proteins and hence protects against inflammatory and oxidative responses, was observed in the *fat-1* mouse skin. In conclusion, these results show that *fat-1* gene confers a protective effect against UVB-induced inflammatory and oxidative skin damages through elevation of endogenous ω-3 PUFA production and Nrf2-mediated upregulation of cytoprotective gene expression in mouse skin.

Keywords

fat-1 transgenic mice; Inflammation; Omega-3 polyunsaturated fatty acids; Oxidative stress; Ultraviolet B

2. Introduction

Ultraviolet B (UVB) radiation is an important environmental factor responsible for the pathogenesis of skin aging and photocarcinogenesis (Afaq *et al.* 2005, Halliday 2005). Excessive exposure to UVB causes a variety of adverse skin reactions, such as erythema, edema, sunburn, hyperplasia, inflammation and immunosuppression (Afaq *et al.* 2005, Halliday 2005, Yaar & Gilchrest 2007, Matsumura & Ananthaswamy 2004). Multiple lines of evidence suggest that UVB exerts its detrimental effect mainly through generation of reactive oxygen species (ROS) (Cerutti *et al.* 1994, Del Prete *et al.* 2011) causing oxidative modification of cellular macromolecules and increasing accumulation of lipid peroxidation products, such as 4-hydroxynonenal (4-HNE) and malondialdehyde (MDA) (Oberley *et al.* 2004, Petersen & Doorn 2004, Tyrrell 1995). In addition, UVB exposure impairs the antioxidant defense system by decreasing the activity of various antioxidant enzymes (Sander *et al.* 2004). The UVB-induced oxidative stress triggers epidermal inflammation through inappropriate modulation of intracellular signaling pathways, thereby predisposing skin cells to carcinogenesis (Katiyar *et al.* 1999) and increasing the risk of skin carcinogenesis (Halliday 2005). As UVB-induced oxidative stress triggers photo-inflammation and photocarcinogenesis, the optimal maintenance or potentiation of antioxidant defense capacity can help protect against oxidative damage, covalent modification, inflammatory injury and tumor development caused by UVB.

Two representatives of pro-inflammatory enzymes, cyclooxygenase-2 (COX-2) (Kundu *et al.* 2008, Tripp *et al.* 2003) and inducible nitric oxide synthase (iNOS) (Chang *et al.* 2011) are overexpressed aberrantly in the epidermis upon exposure to UVB radiation. Whereas *cox-2* transgenic mice are prone to develop experimentally induced skin tumors (Muller-Decker *et al.* 2002), genetic ablation of *cox-2* protects animals against skin papillomagenesis (Tiano *et al.* 2002). Likewise, mice genetically deficient in *inos* are relatively less susceptible to phorbol ester-induced skin inflammation (Medeiros *et al.* 2009), and pharmacological inhibition of iNOS decreases the multiplicity of chemically induced papilloma formation (Chun *et al.* 2004). Since abnormally elevated COX-2 (An *et al.* 2002, Fischer *et al.* 2007) and iNOS (Chun *et al.* 2004) expression has been frequently observed in murine and human nonmelanoma skin cancers, the COX-2 and iNOS signaling pathways are considered as a potential target for achieving chemoprevention against photocarcinogenesis.

The expression of COX-2 (Koon *et al.* 2006) and iNOS (Lo *et al.* 2005, Ziesche *et al.* 2007) is regulated by an eukaryotic transcription factor, signal transducer and activator of transcription 3 (STAT3). Previous studies have demonstrated that UVB irradiation activates STAT3 in mouse skin (Kim *et al.* 2009a). Furthermore, transient levels of ROS can activate cellular proliferation or survival signaling pathways, including the phosphoinositide-3-kinase–protein kinase B/Akt (PI3K-PKB/Akt) pathway. The aberrant expression of COX-2 and iNOS in UVB-irradiated cultured cells as well as in mouse skin *in*

vivo results, at least in part, from the inappropriate amplification of intracellular signaling pathways comprising upstream kinase PI3K/Akt (Tang *et al.* 2001b, Carpenter & Cantley 1996). Therefore, interference with the signaling cascades mediated by these upstream regulators may block aberrant overexpression of COX-2 and iNOS, thereby ameliorating UVB-induced skin inflammation and oxidative damages.

On the other hand, cellular redox homeostasis is maintained by the constitutive induction of cytoprotective genes that encode distinct set of anti-oxidative and other cytoprotective proteins such as heme oxygenase-1 (HO-1) and NAD(P)H:quinone oxidoreductase-1 (NQO1) (Nguyen *et al.* 2005). The induction of these cytoprotective proteins can confer protection against oxidative stress and inflammation, thereby preventing the development of cancer (Kundu & Surh 2010). HO-1 and NQO1 knockout mice were more prone to skin tumor development (Was *et al.* 2011, Long *et al.* 2001). The robust induction of aforementioned cytoprotective proteins is known to be mediated by nuclear factor erythroid-related factor 2 (Nrf2) (Surh *et al.* 2008). Thus, one of the potential strategies to prevent skin tissue damages and related abnormal disorders is to enhance the Nrf2-mediated induction of cytoprotective gene expression.

There is competition between ω-6 and ω-3 polyunsaturated fatty acids (PUFAs) for the same metabolic enzymes. The availability of ω-6 and ω-3 PUFAs and their ratio in cellular lipids determine the cellular eicosanoid profiles. A balanced ω-6/ω-3 PUFA ratio of body lipids is essential for normal

growth and development and plays an important role in prevention as well as treatment of many clinical problems (Simonsen *et al.* 1998, Gago-Dominguez *et al.* 2003, Maillard *et al.* 2002, Xia *et al.* 2005). Transgenic *fat-1* mice expressing the *fat-1* gene derived from *Caenorhabditis elegans*, are capable of producing ω-3 PUFAs from ω-6 PUFAs and thereby maintain a balanced ratio of ω-6/ω-3 PUFAs in their tissues and organs (Kang *et al.* 2004). In the present study, *fat-1* mice also show a marked increase in ω-3 PUFAs and decrease in ω-6 PUFAs, exhibiting a lower ω-6/ω-3 PUFA ratio in their skin tissues. This prompted me to investigate an impact of an enhanced ω-3 PUFA tissue status on UVB-induced inflammatory and oxidative damages and the underlying molecular mechanisms.

3. Materials and Methods

Animals and diets

Male transgenic *fat-1* mice (Kang *et al.* 2004) were backcrossed female mice with wild-type (WT) C57BL/6 background (Charles River Laboratories, Wilmington, MA). Animals were kept in standard cages under specific pathogen-free conditions. Each cage housed age and weight-matched mice, combining one WT and one *fat-1* transgenic mouse. They were fed a special diet (10% safflower oil), high in ω-6 and low in ω-3 PUFAs. All studies were approved by the Institutional Animal Care and Use Committee at Seoul National University. The offsprings were determined by genotyped for *fat-1*$^{+/-}$ heterozygosity using the Tissue-Direct^{TM} PCR Kit (Lamda Biotech, Inc. St. Louis, MO). The genotyping primers of *fat-1* were as follows: *fat-1,* 5'-CTG CAC CAC GCC TTC ACC AAC C-3' (forward) and 5'-ACA CAG CAG CAG ATT CCA GAG ATT-3' (reverse). In this study, transgenic *fat-1* mice used were female heterozygous.

Analysis of fatty acid composition

Fatty acid profiles were investigated using gas chromatography as described previously (Kang & Wang 2005). Briefly, fresh skin tissues were grounded to powder under liquid nitrogen and subjected to extraction of total lipids and fatty acid methylation by heating at 100°C for 1 h under 14% boron trifluoride-methanol reagent. Fatty acid methyl esters were analyzed by gas

chromatography using a fully automated Agilent 7890A system (Agilent, Santa Clara, CA) equipped with a flame-ionization detector. Peaks of resolved fatty acids were identified by comparison with the fatty acid methyl ester reference standard (Sigma Aldrich, St. Louis, MO), and area percentage for all resolved peaks was measured by using the ChemStation software (Agilent Technologies, Palo Alto, CA).

Source of UVB radiation

The dorsal hair of haired mice was trimmed 2 days before exposure to UVB radiation. The UVB radiation source was a 5×8 Watt tube, which emits an energy spectrum with high fluency in the UVB region (with a peak at 312 nm). A Biolink BLX-312 UV crosslinker (Vilbert Lourmat, Marne-la-Valle´ e, France) was used to irradiate mouse skin (5.0 kJ/m^2 dose of UVB).

Hematoxylin and eosin (H&E) staining and terminal deoxynucleotidyl transferase dUTP nick-end labeling (TUNEL) assay

The skin was removed from euthanized mice at 24 h after UVB exposure. Sections of harvested mouse skin were fixed with 10% neutral buffered formalin and embedded in paraffin. Mounted sections (4 μm) were stained with H&E for light microscopy. Apoptotic cells were detected in paraffin-embedded skin sections by the TUNEL assay with the ApopTag® peroxidase *in situ* apoptosis detection kit (Millipore, Billerica, MA). The apoptotic cells were visualized by light microscopy.

Immunohistochemical analysis (IHC)

The dissected skin was prepared for IHC of the expression patterns of 4-HNE- or MDA-modified protein, COX-2, P-STAT3 (Tyr^{705}) and Nrf2. Four-μm sections of 10% formalin-fixed, paraffin-embedded tissues were cut on silanized glass slides, deparaffinized three times with xylene and rehydrated through graded alcohol bath. The deparaffinized sections were heated by using microwave and boiled twice for 6 min in 10 mM citrate buffer (pH 6.0) for antigen retrieval. To diminish nonspecific staining, each section was treated with 3% hydrogen peroxide and 4% peptone casein blocking solution for 15 min. For the detection of respective protein expression, slides were incubated with proteins modified with 4-HNE or MDA (JaICA, Nikken SEIL Co. Ltd., Shizuoka, Japan), COX-2 (Cayman Chemical Co., Ann Arbor, MI), P-STAT3 (Cell Signaling Technology, Beverly, MA) and Nrf2 (Santa Cruz Biotechnology, Inc., Santa Cruz, CA) antibodies at room temperature for 40 min in Tris-buffered saline containing 0.05% Tween 20, and then developed using horseradish peroxidase-conjugated secondary antibodies (rabbit or mouse; Dako, Glostrup, Denmark). The peroxidase binding sites were detected by staining with 3,3'-diaminobenzidine tetrahydrochloride. Finally, counterstaining was performed using Mayer's hematoxylin.

Tissue lysis and protein extraction

The UVB irradiated dorsal skin was collected and fat was removed on ice to

get the epidermis. Collected epidermis was homogenized in an ice-cold lysis buffer [150 mM NaCl, 0.5% Triton-X 100, 50 mM Tris–HCl (pH 7.4), 20 mM ethylene glycol tetra-acetic acid, 1 mM dithiothreitol (DTT), 1 mM Na_3VO_4 and protease inhibitors, 1 mM phenylmethyl sulfonylfluoride (PMSF) and ethylenediaminetetraacetic acid (EDTA)-free cocktail tablet] followed by periodical vortex for 30 min at 0°C. The lysates were centrifuged at 14,800 *g* for 15 min at 4ºC. The supernatants were collected and stored at -70°C until use.

Fractionation of cytosolic and nuclear extracts

Scraped dorsal skin of mice was homogenized in 800 μL of hypotonic buffer A [10 mM 4-(2-hydroxyethyl)-1-piperazineethanesulfonic acid (HEPES, pH 7.8), 1.5 mM $MgCl_2$, 10 mM KCl, 1 mM DTT, 0.1 mM EDTA and 0.1 mM PMSF]. To the homogenates was added 80 μL of 10% Nonidet P-40 (NP-40) solution, and the mixture was then centrifuged for 15 min at 14,800 *g*. The supernatant was collected as a cytosolic fraction. The precipitated nuclei were washed once with 500 μL of buffer A plus 50 μL of 10% NP-40, centrifuged, resuspended in 200 μL of buffer C [50 mM HEPES (pH 7.8), 50 mM KCl, 300 mM NaCl, 0.1 mM EDTA, 1 mM DTT, 0.1 mM PMSF and 20% glycerol] and centrifuged for 15 min at 14,800 *g*. The supernatant containing nuclear proteins was collected and stored at -70°C until use.

Western blot analysis

For Western blot analysis, the total protein concentration was quantified by

using the bichinconinic acid protein assay kit (Pierce, Rockford, IL). Cell lysates (30 μg protein) were mixed and boiled in sodium dodecyl sulfate (SDS) sample buffer for 5 min before 8-15% SDS–polyacrylamide gel electrophoresis (SDS-PAGE). They were separated by SDS-PAGE and transferred to a polyvinylidene difluoride (PVDF) membrane (Gelman Laboratory, Ann Arbor, MI). The blots were blocked in 5% fat-free dry milk in tris-buffered saline containing 0.1% tween 20 (TBST) for 1 h at room temperature. The membranes were incubated for 12-24 h at 4°C with dilutions of primary antibodies for proteins modified with 4-HNE (JaICA, Nikken SEIL Co. Ltd., Shizuoka, Japan), actin (Sigma Aldrich, St. Louis, MO), COX-2 (Cayman Chemical Co., Ann Arbor, MI), iNOS (BD Biosciences, San Jose, CA), P-STAT3 (Tyr^{705}), STAT3, P-Akt (Ser^{473}), Akt (Cell Signaling Technology, Danvers, MA), lamin B (Invitrogen, Carlsbad, CA), HO-1 (Stressgen Biotechnologies Co., San Diego, CA), NQO1 (Abcam Inc., Cambridge, MA) and Nrf2 (Santa Cruz Biotechnology, Inc., Santa Cruz, CA). Membranes were washed followed by incubation with 1:3000 dilutions of respective horseradish peroxidase conjugated secondary antibodies (rabbit or mouse; Zymed Laboratories Inc., San Francisco, CA) for 2 h and again with TBST. Protein expressed was visualized with an enhanced chemiluminescent (ECL) detection kit (Amersham Pharmacia Biotech, Buckinghamshire, UK) and LAS-4000 image reader (Fujifilm, Tokyo, Japan) according to the manufacturer's instructions.

Reverse transcription-polymerase chain reaction analysis (RT-PCR)

Total RNA was isolated from mouse skin tissues using TRIzol® reagent (Invitrogen, Carlsbad, CA) according to the manufacturer's protocol. To generate the cDNA from RNA, 1 μg of total RNA was reverse transcribed with murine leukemia virus reverse transcriptase (Promega, Madison, WI) for 50 min at 42°C and again for 15 min at 72°C. About 1 μl of cDNA was amplified with a PCR mixture (HS Prime Taq 2X Premix, Daejeon, South Korea) in sequential reactions. The primers used for each RT-PCR reactions are as follows: *cox-2*, 5'-CTG GTG CCT GGT CTG ATG ATG-3' and 5'-GGC AAT GCG GTT CTG ATA CTG-3'; *actin*, 5'-AGA GCA TAG CCC TCG TAG AT-3' and 5'-CCC AGA GCA AGA GAG GTA TC-3'; *ho-1*, 5'-TAC ACA TCC AAG CCG AGA AT-3' and 5'-GTT CCT CTG TCA GCA TCA CC-3'; *nqo1*, 5'-TCG GAG AAC TTT CAG TAC CC-3' and 5'-TGC AGA GAG TAC ATG GAG CC-3'; *nrf2,* 5'-CCT CTG TCA CCA AGC TCA AGG-3' and 5'-TTC TGG GCG GCG ACT TTA TT-3' (forward and reverse, respectively). Amplification products were analyzed by 2-3% agarose gel electrophoresis, followed by staining with SYBR Green (Invitrogen, Carlsbad, CA) and photographed using fluorescence in LAS-4000 (Fujifilm, Tokyo, Japan).

Statistical analysis

All the values were expressed as the mean ± standard error (SE) of at least three independent experiments. Statistical significance was determined by the Student's *t*-test and $p < 0.05$ was considered to be statistically significant.

4. Results

fat-1 *transgenic mice had higher amounts of ω-3 PUFAs in skin tissues as compared to those of WT mice*

The *fat-1* gene of *C. elegans* encodes an ω-3 fatty acid desaturase enzyme that converts ω-6 PUFAs to ω-3 PUFAs (Kang 2007). We performed gas chromatography to determine an effect of *fat-1* transgene on fatty acid profiles of their skin (**Fig. 2-1**). Both WT and *fat*-1 transgenic mice born to the same mother were fed an identical diet that was high in ω-6 PUFAs, but deficient in ω-3 PUFAs. During this dietary regime, the *fat-1* mice had significantly higher amounts of ω-3 fatty acids, particularly docosahexaenoic acid (DHA) in skin tissues as compared to those of WT mice. However, the reduction of ω-6 fatty acids was not as dramatic as increases in ω-3 fatty acids. The results showed a decrease in ω-6/ω-3 fatty acid ratio (18:2n-6 + 18:3n-6 + 20:3n-6 + 20:4n-6)/(18:3n-3 + 20:3n-3 + 20:5n-3 + 22:6n-3) in the skin from *fat-1* mice (**Table 2-1 and Fig. 2-1C**).

UVB-induced inflammation and oxidative stress were attenuated in **fat-1** ***mice compared with those in WT mice***

Exposure to UVB radiation induces skin hyperplasia and apoptosis as a consequence of inflammatory tissue injury (Halliday 2005). As illustrated in **Fig. 2-2A**, UVB-induced skin inflammation was less severe in *fat-1* transgenic mice than that in WT mice upon exposure to UVB (5.0 kJ/m^2 radiation) for 24 h.

The results showed a dramatic attenuation of the skin hyperplasia in the *fat-1* mice. **Fig. 2-2A** also represents results of an independent study comparing the extent of apoptosis in the mouse skin. The UVB-exposed *fat-1* mice had less apoptotic epidermal cells than the UVB-exposed WT mice. UVB irradiation produces ROS, which leads to lipid peroxidation (Sander *et al.* 2004, Halliday 2005) and photodamage (Tyrrell 1995). 4-HNE and MDA are two representative lipid peroxidation products (Oberley *et al.* 2004, Petersen & Doorn 2004). The levels of 4-HNE and MDA-modified proteins were much lower in the skin from *fat-1* mice than those from WT animals upon UV irradiation (**Fig. 2-2A and B**).

UVB-induced expression of COX-2 and iNOS was decreased in the skin of* fat-1 mice *as compared to that in the WT mouse skin

According to previous studies, irradiation with UVB induced the abnormal expression of two representative pro-inflammatory enzymes, COX-2 (Kundu *et al.* 2008) and iNOS (Chang *et al.* 2011), in mouse skin. To assess whether the *fat-1* transgene-mediated protection against UVB-induced inflammation involves alteration in the expression of pro-inflammatory enzymes, skin tissue samples were subjected to immunoblot analysis to detect their levels. UVB-induced expression of COX-2 and iNOS was increased significantly in the WT mouse skin, but this was markedly reduced in the skin of *fat-1* mice (**Fig. 2-3B**). Immunohistochemical analysis further confirmed the inhibitory effect of endogenously produced ω-3 fatty acids on UVB-induced COX-2 expression in

the *fat-1* mouse skin (**Fig. 2-3C**). In unirradiated WT and *fat-1* mice, specific COX-2 immunostaining was barely detectable in the mouse skin. In response to UVB exposure, the number of COX-2 positive cells increased in the WT mouse skin; however, an elevated ω-3 PUFA production attenuated UVB-induced COX2 expression in the *fat-1* mouse skin.

UVB-induced phosphorylation of STAT3 and Akt was diminished in the* fat-1 *mouse skin compared with that in the WT mouse skin

The protein expression of COX-2 and iNOS is transcriptionally regulated by ubiquitous eukaryotic transcription factors. Since, STAT3 is the one of the representative transcription factors known to regulate COX-2 (Koon *et al.* 2006) and iNOS expression (Lo *et al.* 2005, Ziesche *et al.* 2007), activation of the aforementioned transcription factor in the UVB-stimulated mouse skin was assessed. The phosphorylation of STATs at the tyrosine 705 residue has generally been accepted as a prerequisite for their DNA binding and transactivation (Ramsauer *et al.* 2002). We determined the level of phosphorylated as well as total STAT3 protein in the mouse skin using monoclonal antibodies. The total STAT3 levels remained unchanged during these events. As illustrated in **Fig. 2-4A**, exposure of the *fat-1* mice to UVB radiation resulted in a significant inhibition of STAT3 phosphorylation at the tyrosine 705 residue. In addition, Western blot analysis with nuclear extract from skin tissues showed UVB induced nuclear translocation of phosphorylated STAT3, which was blunted in the *fat-1* mice. A significantly lower level of

phospho-STAT3 (Tyr^{705}), an activated form of STAT3, in the skin from *fat-1* mice was verified by immunohistochemical analysis (**Fig. 2-4B**). Bito *et al.* have suggested that STAT3 activation is one of the initial events in UV-exposed human skin along with ROS generation and apoptotic cell death (Jean *et al.* 2007). There are several pathways by which keratinocytes might protect themselves from apoptosis. The PI3K/Akt signaling pathway is thought to be initiated and prolonged by ROS release in response to UVB irradiation (Zhang *et al.* 2001). Our data showed that UVB caused significant phosphorylation of Akt at Ser^{473} whereas the total Akt levels remained unchanged (**Fig. 2-4A**). A significant decrease in the levels of phosphorylated Akt was noted, which is attributable to an increased ω-3 fatty acid level in the skin of *fat-1* mice.

The Nrf2-mediated induction of cytoprotective gene expression was elevated in the skin of* fat-1 *mice

Oxidative stress plays a major role in the induction and progression of inflammation and its level depends on the balance between ROS production and cytoprotective protein expression (Kundu & Surh 2010). The Nrf2-mediated induction of HO-1 and NQO1 expression was significantly increased in the skin of *fat-1* mice as compared to that of WT mice (**Fig. 2-5A and B**). There was a slight increase in the expression of Nrf2 was seen in the *fat-1* mouse skin (**Fig. 2-5B and C**), but more pronounced enhancement was observed in nuclear translocation of Nrf2 in the skin tissue from *fat-1* mice (**Fig. 2-5B**). However, there was no difference found in the Nrf2 mRNA level in the

skin between WT and *fat-1* mice (**Fig. 2-5A**). This result indicates that the *nrf2* gene transcription or its mRNA stability is not affected in the *fat-1* mouse skin. An increased ω-3 fatty acid tissue level can augment the Nrf2-mediated induction of cytoprotective gene expression, which will neutralize ROS and reduce the oxidative damage to lipids and proteins, thereby ameliorating pathological conditions of the skin.

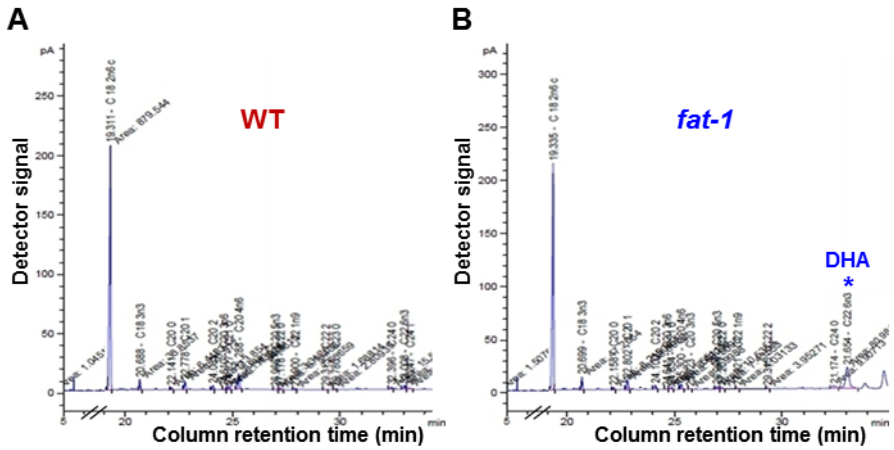

Table 2-1. PUFA composition in the skin of *fat-1* and wild-type mice.

		WT	*fat-1*
Linoleic acid	C18:2	31.52 ± 0.53	26.78 ± 1.51[a]
γ-Linolenic acid	C18:3	0.44 ± 0.04	0.23 ± 0.03[a]
Dihomo-γ-linolenic acid	C20:3	1.27 ± 0.08	0.63 ± 0.02[b]
Arachidonic acid	C20:4	0.21 ± 0.02	0.03 ± 0.01[b]
ω-6 PUFAs (%)		33.45 ± 0.53	27.68 ± 1.47[a]
α-Linolenic acid	C18:3	0.61 ± 0.05	1.94 ± 0.10[c]
Eicosatrienoic acid	C20:3	0.75 ± 0.01	1.06 ± 0.04[b]
Eicosapentaenoic acid	C20:5	0.21 ± 0.04	1.22 ± 0.02[c]
Docosahexaenoic acid	C22:6	0.53 ± 0.06	3.33 ± 0.07[c]
ω-3 PUFAs (%)		2.09 ± 0.08	7.55 ± 0.15[c]
ω-6/ω-3 PUFAs		16.05 ± 0.53	3.66 ± 0.13[c]
ω-3/ω-6 PUFAs		0.06 ± 0.002	0.28 ± 0.01[c]

Data are expressed as means ± SE ($n = 3$).

[a]$p < 0.05$, [b]$p < 0.01$ and [c]$p < 0.001$ versus WT mice.

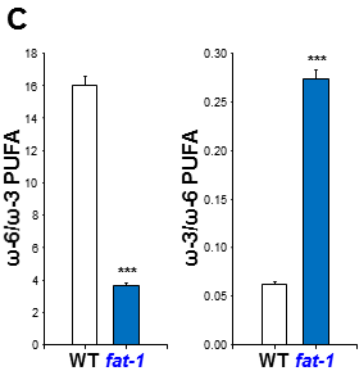

Fig. 2-1. *fat-1* transgenic mice had higher amounts of ω-3 PUFAs in skin tissue as compared to that of WT mice. Both WT and *fat-1* transgenic littermates born to the same mother were maintained on a diet (10% safflower oil) high in ω-6 and low in ω-3 fatty acids. (A) After the dietary regimen, the PUFAs profiles of mouse skin were analyzed using gas chromatography. Whereas high levels of ω-6 fatty acids characterized the WT samples, ω-3 fatty acids were nearly undetectable. (B) An abundance of docosahexaenoic acid,

DHA (22:6 n-3) was found in the *fat-1* mouse skin. The DHA is marked with asterisks. (C) A significantly decreased level of ω-6 vs. ω-3 fatty acids was observed in the skin of *fat-1* mice as compared to that of WT mice. Data are expressed as means ± SE. ***p <0.001 versus WT mice.

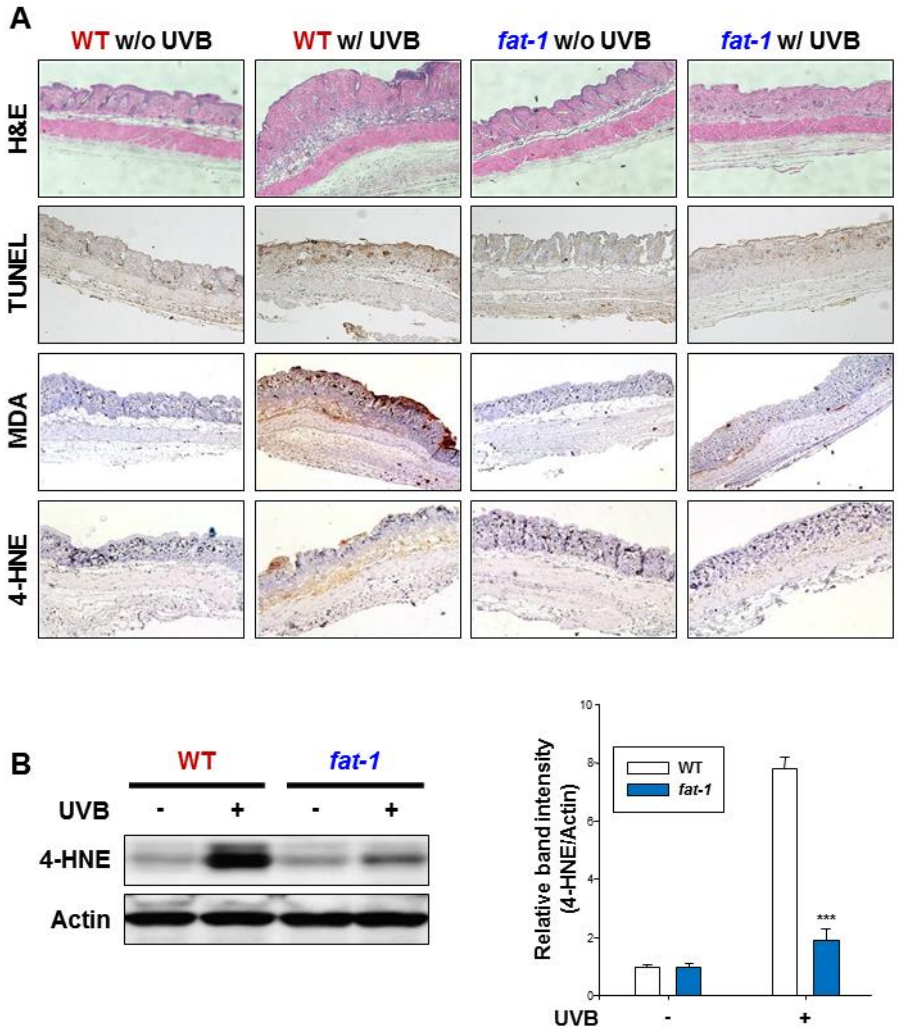

Fig. 2-2. UVB-induced inflammation and oxidative stress were attenuated in *fat-1* mice compared with those in WT mice. (A) Skin thickness and apoptotic cells in WT and *fat-1* mice were detected by H&E staining and the TUNEL assay, respectively at 24 h following 5.0 kJ/m^2 UVB exposure. Formalin-fixed and paraffin-embedded tissues from the UVB-irradiated mice were also immunostained for MDA and 4-HNE. Magnifications ×100. (B) Isolated protein extracts were electrophoresed, transferred to a PVDF

membrane, and the membranes were probed using antibodies for 4-HNE. Quantification of 4-HNE was normalized to that of actin followed by statistical analysis of relative band density. Result is expressed as means ± SE. ***p <0.001 versus UVB-irradiated WT mice.

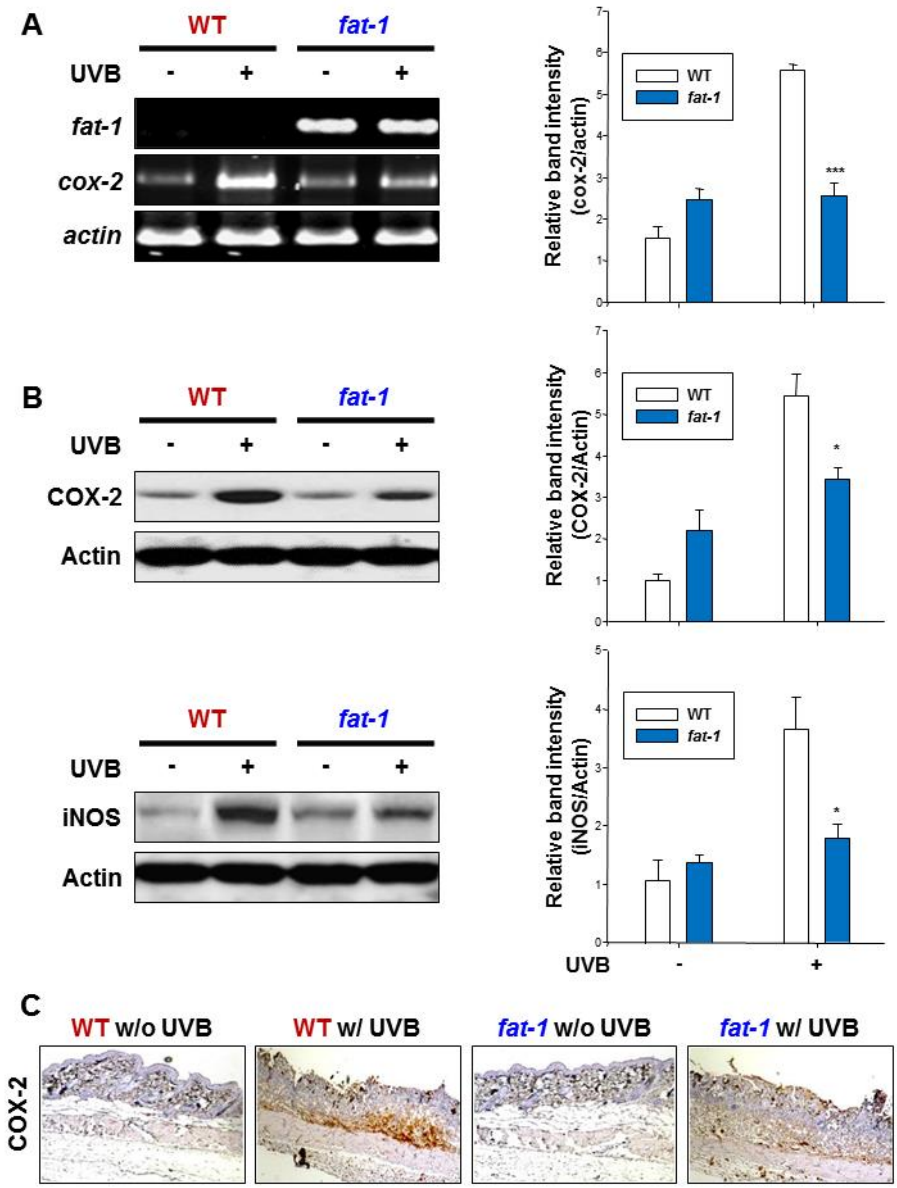

Fig. 2-3. UVB-induced expression of COX-2 and iNOS was decreased in the skin of *fat-1* mice as compared to that in the WT mouse skin. Animal treatment and other experimental details are same as described in the legend to **Fig. 2-2**. (A) Total RNA was isolated from the skin tissues using TRIzol® reagent according to the manufacturer's protocol. RT-PCR analysis was

performed to detect the mRNA expression of *cox-2*. (B) Collected skin tissues were placed on ice and fat was removed to get an epidermal layer. Whole tissue extracts were analyzed for the protein expression of COX-2 and iNOS by immunoblotting. Quantification of COX-2 and iNOS was normalized to those of actin followed by statistical analysis of relative band density. Data are expressed as means ± SE. *p <0.05 and ***p <0.001 versus UVB-irradiated WT mice. (C) The respective sections were immunostained for COX-2 and counterstained with hematoxylin. Positive COX-2 staining yielded a brown-colored product. Magnifications ×100.

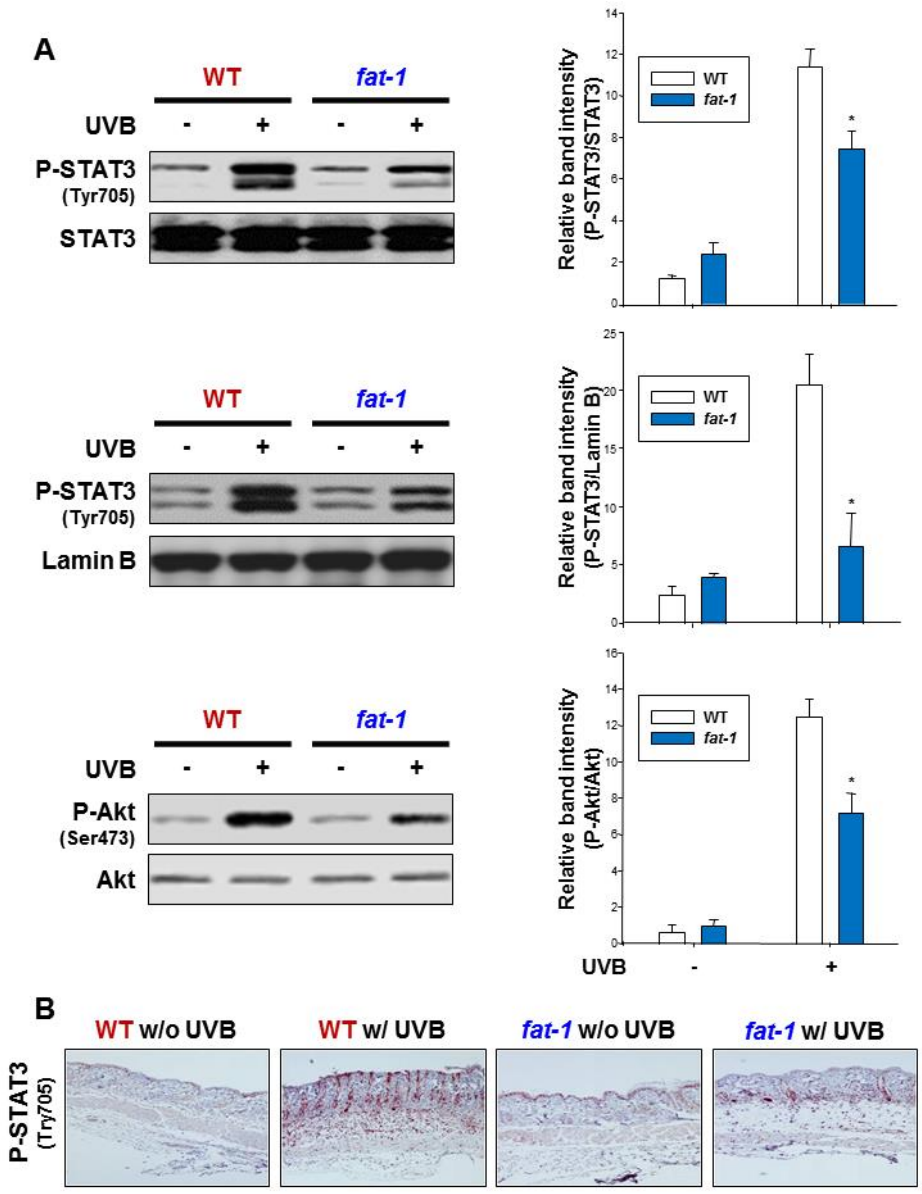

Fig. 2-4. UVB-induced phosphorylation of STAT3 and Akt was diminished in the *fat-1* mouse skin compared with that in the WT mouse skin. Animal treatment and other experimental conditions are same as described in the **Fig. 2-2** legend section. (A) Whole lysates and nuclear extracts from the different groups were separated by electrophoresis on SDS-PAGE and immunoblotted to

detect total and phosphorylated forms of STAT3 (Tyr^{705}) and Akt (Ser^{473}). Quantification of P-STAT3 and P-Akt was normalized to those of STAT3 and Akt, respectively. Results are expressed as means ± SE. *p <0.05 versus UVB-irradiated WT mice. (B) The sections of skin tissues were subjected to immunohistochemical analysis of phosphorylated of STAT3 at Tyr^{705}. Magnifications ×100.

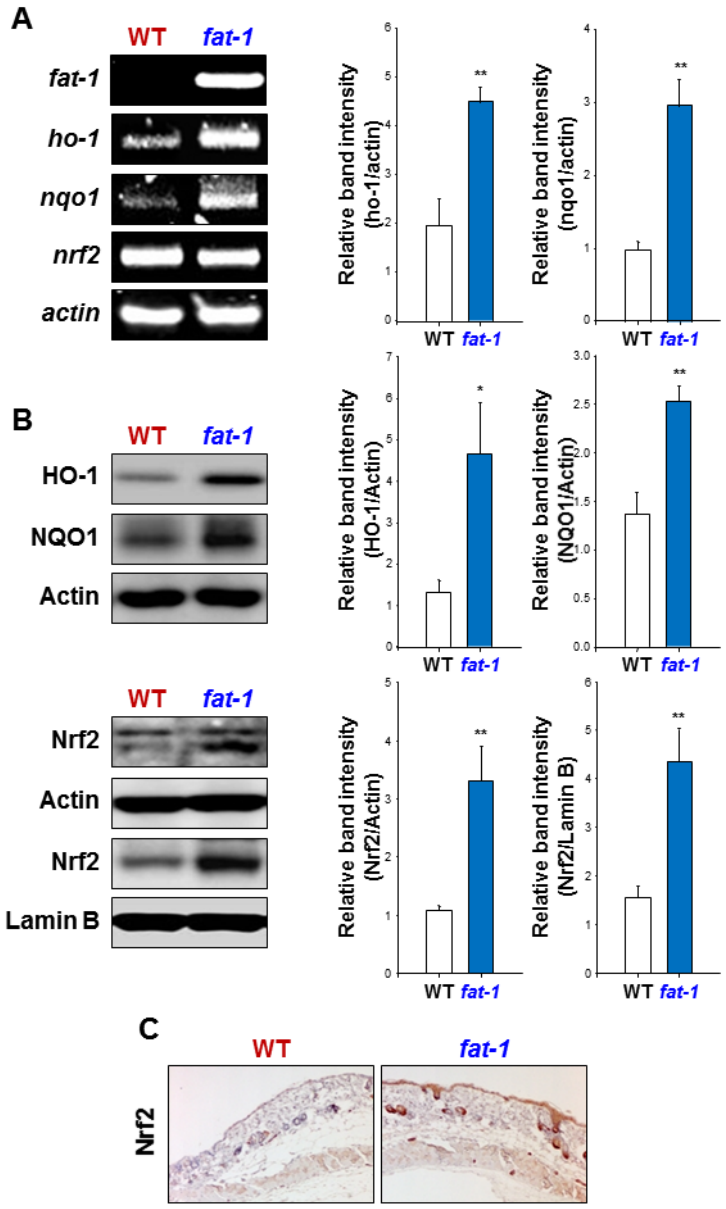

Fig. 2-5. The Nrf2-mediated induction of cytoprotective gene expression was elevated in the skin of *fat-1* mice. Both WT and *fat-1* mice had access to AIN-93 diet supplemented with 10% safflower oil (rich in ω-6 fatty acids) *ad libitum* for 5 weeks. The The dorsal hair of mice was trimmed 2 days before sacrifice. (A) Total RNA was isolated from the skin tissues and the mRNA

expression of *ho-1*, *nqo1* and *nrf2* was examined by RT-PCR analysis. Quantification of *ho-1* and *nqo1* was normalized to those of *actin*, followed by statistical analysis of relative band density. (B) The epidermal lysates were subjected to Western blot analysis to detect the protein expression of HO-1, NQO1 and Nrf2. Data are expressed as means ± SE. **p* <0.05 and ***p* <0.01 versus WT mice. (C) Paraffin-embedded skin tissue blocks were analyzed by immunohistochemistry and the levels of Nrf2 were compared between WT and *fat-1* mice. Magnifications ×100.

5. Discussion

The ω-6 PUFAs, especially arachidonic acid (AA), is a precursor of prostaglandins, leukotrienes and related compounds, which enhance inflammation (Jia *et al.* 2008). The western diet is abundant in ω-6 PUFAs, mainly from vegetable oils. In contrast, ω-3 PUFAs have anti-inflammatory and anti-oxidative properties of ω-3 PUFAs. The consumption of fish, rich in ω-3 PUFAs, is recommended for its health benefits to protect against heart disease, diabetes and potentially cancer (Connor 2000). Consuming increased amounts of long chain ω-3 PUFAs results in a partial replacement of the AA in cell membranes by eicosapentanoic acid and DHA (Kang 2007). This leads to a decreased production of AA-derived pro-inflammatory mediators. Studies by Kang *et al.* (2004) suggested a new strategy for producing food that is enriched in ω-3 fatty acids from livestock carrying *fat-1*, an ω-3 fatty acid desaturase gene. Production of ω-3 fatty acids by the animals themselves would be a cost-effective and sustainable way of meeting the increasing demand for ω-3 PUFAs and the ideal ω-6/ω-3 PUFA ratio. Thus, we utilized the *fat-1* transgenic mice to investigate the effect of ω-3 PUFAs and ω-6/ω-3 PUFA ratio on inflammatory and oxidative skin damages without providing exogenous ω-3 PUFAs in the their diet. There was a remarkable difference in the ω-6/ω-3 PUFA ratio between WT and *fat-1* mouse skin. When both WT and *fat-1* mice were maintained on the identical diet high in ω-6 but low in ω-3 fatty acids, the WT mice exhibited substantially high contents of ω-6 PUFAs but much lesser

amounts of ω-3 PUFAs, whereas the *fat-1* mice capable of spontaneously generating ω-3 fatty acids had a lower ω-6/ω-3 PUFA ratio in their skin. Notably, the level of DHA, derived from the α-linolenic acid, was markedly higher, whereas the level of AA, derived from the ω-6 PUFA linoleic acid, was significantly lower in the skin from *fat-1* mice. Thus, this allowed us to produce two different fatty acid profiles in the animals by using just a single diet and therefore eliminated the need of two different diets for a comparative study.

The major cause of dermatologic disorders is acute or chronic exposure to UVB radiation. Since UVB radiation induces oxidative modification of cellular macromolecules through increased generation of ROS (Tyrrell 1995, Oberley *et al.* 2004, Petersen & Doorn 2004), we initially examined the effect of endogenously produced ω-3 PUFAs on the levels of proteins modified by MDA and 4-HNE. The UVB-induced peroxyl and hydroxyl radicals were rapidly scavenged, thereby reducing the accumulation of lipid peroxidation products in the *fat-1* mouse skin. UVB-induced ROS generation triggers amplification of cellular survival signaling and contributes to cell proliferation (Afaq *et al.* 2005). Since the endogenous ω-3 fatty acids were effective in preventing UVB-induced epidermal thickness, hyperplasia and lipid peroxidation, it would be worthwhile to examine the anti-tumor promoting effect of *fat-1* gene on experimentally induced photocarcinogenesis.

The pathologic basis of UVB-induced tumor development is partially attributed to the local tissue inflammation. The aberrant induction of pro-inflammatory enzymes has been implicated in inflammation-associated

carcinogenesis (Kundu & Surh 2012). The demonstration of COX-2 downregulation in UVB-exposed *fat-1* mouse skin *in vivo* is in good agreement with a previous study demonstrating the inhibition of UVB-induced expression of COX-2 and NAD(P)H oxidase-4, an enzyme involved in the generation of ROS, in mouse skin topically treated with DHA (Rahman *et al.* 2011).

Oxidative stress occurs when the balance between ROS and antioxidant enzymes favors toward the former. That means the more production of antioxidant enzymes, the less generation of oxidative stress, thereby preventing chronic inflammatory tissue damage and neoplastic transformation of cells. For instance, the induction of HO-1 protected mice against experimental colitis (Paul *et al.* 2005) and chemically induced skin papillomagenesis (Paul *et al.* 2005). Topical application of hemin, a HO-1 inducer, abrogated 12-*O*-tetradecanoylphorbol-13-acetate-induced COX-2 expression and nuclear factor kappa B activation in mouse skin (Park *et al.* 2008). NQO1-null mice are more susceptible to benzo[*α*]pyrene (Long *et al.* 2000)- or 7,12-dimethylbenz[*a*]anthracene (Long *et al.* 2001)-induced skin carcinogenesis. The beneficial effect of ω-3 PUFAs in health and diseases is due mainly to its powerful anti-inflammatory resistance against oxidative stress and ability to maintain a proper cellular redox status (Romieu *et al.* 2008). Others have shown that ω-3 PUFAs enhance the antioxidant defense system of animals and humans by increasing the production of antioxidant enzymes (Bhattacharya *et al.* 2005, Bhattacharya *et al.* 2007, Ramaprasad *et al.* 2005). In a previous study, higher levels of catalase and superoxide dismutase were found in muscle and liver of

fat-1 mice (Rahman *et al.* 2009). These data suggested that an enhanced ω-3 PUFA tissue level potentially enhanced the antioxidant defense system, thereby helping reduce pathological conditions. The study presented here was also designed to examine the effect of an increased ω-3 PUFA status on the anti-oxidative property of *fat-1* mouse skin. Significant augmentation of antioxidant enzymes production, along with enhanced expression of Nrf2, was observed in the skin tissue of *fat-1* mice.

In conclusion, the present study demonstrates that the inflammation of mouse skin irradiated by UVB is significantly less severe in *fat-1* transgenic mice than that in WT littermates. The protection from UVB-induced skin inflammation in *fat-1* mice is correlated with the formation of anti-inflammatory as well as anti-oxidative ω-3 PUFAs including DHA, down-regulation of pro-inflammatory markers and up-regulation of cytoprotective proteins in the skin of these animals.

Chapter Ⅲ

Endogenous ω-3 fatty acid production in hairless *fat-1* transgenic mice protects against photocarcinogenesis

1. Abstract

Ultraviolet B (UVB) radiation is the most prevalent environmental carcinogen that increases the risk of skin cancer. Persistent inflammation caused by oxidative tissue damage is a key pathologic event in UVB-induced skin photocarcinogenesis. Omega-6 (ω-6) and omega-3 (ω-3) polyunsaturated fatty acids (PUFAs) exert differential effects on the inflammatory and carcinogenesis processes. While ω-6 PUFAs promote inflammation and tumor development, ω-3 PUFAs possess anti-inflammatory and chemopreventive properties. Here, we investigated the effects of endogenously produced ω-3 PUFAs on UVB-induced skin inflammation and photocarcinogenesis using *fat-1* transgenic mice harboring ω-3 desaturase gene capable of converting ω-6 to ω-3 PUFAs. To avoid the inconvenience of removing hairs for inducing photocarcinogenesis by repeated long-term UVB irradiation, we generated hairless *fat-1*$^{+/-}$ and *fat-1*$^{-/-}$ mice by cross-breeding male *fat-1*$^{+/-}$ transgenic mice with female SKH-1 hairless mice. The ω-3/ω-6 PUFA ratio was significantly higher in the dorsal skin of hairless *fat-1*$^{+/-}$ mice than that in the *fat-1*$^{-/-}$ mice. Upon single exposure to UVB (180 mJ/cm^2) irradiation, hairless *fat-1*$^{+/-}$ transgenic mice exhibited a significantly lower degree of epidermal hyperplasia and oxidative skin damage as compared to those observed in the skin of *fat-1*$^{-/-}$ mice. After repeated UVB irradiation thrice a week for 23 weeks, the incidence and the multiplicity of papillomas were also markedly reduced in the hairless *fat-1*$^{+/-}$ mice. The protection of *fat-1*$^{+/-}$ mice from the pathogenesis of inflammation and subsequent development of skin cancer was associated with decreased

phosphorylation of signal transducer and activator of transcription 3 (STAT3). Moreover, *fat-1*$^{+/-}$ mice expressed heme oxygenase-1 and NAD(P)H:quinone oxidoreductase 1, and their mRNA transcripts to a greater extent than did *fat-1*$^{-/-}$ control mice, which were attributable to the elevated activation of nuclear factor erythroid-related factor 2 (Nrf2). Embryo fibroblasts from *fat-1* mice were much less responsive to UVB than those from wild type animals, in terms of inducing pro-inflammatory enzyme expression and intracellular generation of reactive oxygen species. While the protein expression of Nrf2 was enhanced, the steady-state level of the Nrf2 mRNA transcript was barely changed in the *fat-1* embryo fibroblasts. Furthermore, transient overexpression of *fat-1* gene and incubation with docosahexaenoic acid in mouse epidermal JB6 cells resulted in the inhibition of Nrf2 ubiquitination, leading to stabilization of Nrf2 protein. Taken together, our results indicate that functional *fat-1* potentiates cellular defense against UVB-induced skin inflammation and photocarcinogenesis through elevated activation of Nrf2 and upregulation of cytoprotective gene expression.

Keywords

Docosahexaenoic acid; *fat-1* transgenic mice; Inflammation; Omega-3 polyunsaturated fatty acids; Photocarcinogenesis; Ultraviolet B

2. Introduction

Ultraviolet B (UVB) radiation is known to cause initiation as well as promote the clonal expansion of initiated cells to produce skin tumors. Exposure of skin to excessive UVB induces the production of reactive oxygen species (ROS) which results in massive infiltration of inflammatory cells, especially, neutrophils at the site of tissue injury (Wagener *et al.* 2013). ROS play important roles in the modulation of intercellular transduction pathways involved in each stage of carcinogenesis, i.e., initiation, promotion, and progression (Wittgen & van Kempen 2007). Thus, the blockade of abnormally activated inflammatory signaling through fortification of cellular anti-oxidative defense capacity can protect against UVB-induced skin carcinogenesis.

One of the key enzymes mediating inflammatory signal transduction is cyclooxygenase-2 (COX-2) that catalyzes the rate-limiting step in the biosynthesis of prostaglandins. Studies on the molecular mechanisms underlying UVB-induced COX-2 overexpression in cultured cells as well as in mouse skin have identified distinct upstream regulators of inflammatory signal transduction, such as nuclear factor kappa B (NF-κB) and signal transducer and activator of transcription 3 (STAT3) (Smith *et al.* 2000, Lukiw *et al.* 1998, Lo *et al.* 2010, Xiong *et al.* 2014, Carpenter & Lo 2014, Koon *et al.* 2006, Gong *et al.* 2014).

A battery of antioxidant enzymes play a central role in maintaining the cellular redox balance. Examples are hemeoxygenase-1 (HO-1) and

NAD(P)H:quinone oxidoreductase 1 (NQO1) that have been reported to protect skin from oxidative and inflammatory tissue injury and carcinogenesis. The proximal promoter regions of genes encoding HO-1 and NQO1 harbor a consensus sequence known as antioxidant response element (ARE), which is a preferred binding site of a redox-sensitive transcription factor, nuclear factor erythroid-related factor 2 (Nrf2) (Surh *et al.* 2008).

Multiple lines of evidence from laboratory and clinical studies suggest that some naturally occurring substances that can inhibit the oxidative and inflammatory tissue damage act as potential cancer chemopreventive agents (Surh 2003). Omega-3 polyunsaturated fatty acids (ω-3 PUFAs) present in fish oil and some plant-based diets have been reported to retain marked anti-inflammatory and anti-oxidative properties, which contribute to their chemopreventive potential (Jho *et al.* 2004, Rahman *et al.* 2011). The ω-6/ω-3 PUFA ratio has been considered essential for determining the risk for some human malignancies (Simonsen *et al.* 1998, Gago-Dominguez *et al.* 2003, Maillard *et al.* 2002, Xia *et al.* 2005). Kang *et al.* developed genetically engineered mice of C57BL6 background carrying a *fat-1* gene which encodes an ω-3 fatty acid desaturase derived from *Caenorhabditis elegans* (Chung *et al.* 2009, Kang *et al.* 2004). The transgenic mice are capable of converting ω-3 PUFAs from ω-6 PUFAs, thereby maintaining a significantly elevated ω-3/ω-6 PUFA ratio in their tissues and organs. In the present study, hairless *fat-1*$^{+/-}$ mice were generated by cross-breeding of male *fat-1*$^{+/-}$ transgenic mice with female SKH-1 hairless mice. By utilizing these hairless *fat-1*$^{+/-}$ transgenic mice

maintained on ω-6 PUFA containing diet, we investigated the effect of endogenously formed ω-3 PUFAs on the development of UVB-induced tumors as well as oxidative stress and inflammation in the skin.

3. Material and Methods

Development of an in vivo *hairless fat-1$^{+/-}$ model*

Male transgenic *fat-1*$^{+/-}$ mice (Kang *et al.* 2004) were backcrossed (at least five times) to female mice with Skh:hr-1 hairless background (Charles River Laboratories, Wilmington, MA). Animals were kept in standard cages under specific pathogen-free conditions and were fed with a special diet (10% safflower oil), high in ω-6 and low in ω-3 PUFAs. All studies were approved by the Institutional Animal Care and Use Committee of Seoul National University. The offsprings were examined for the hairless phenotypes and genotyped for *fat-1*$^{+/-}$ heterozygosity using the Tissue-Direct^{TM} PCR Kit (Lamda Biotech, Inc. St. Louis, MO). The genotyping primers of *fat-1* were as follows: *fat-1,* 5'-CTG CAC CAC GCC TTC ACC AAC C-3' (forward) and 5'-ACA CAG CAG CAG ATT CCA GAG ATT-3' (reverse).

Preparation and maintenance of mouse embryonic fibroblasts (MEFs)

fat-1 transgenic mice and wild-type (WT) C57BL/6 mice (Charles River Laboratories, Wilmington, MA) were maintained and housed in a climate-controlled quarters (24 ± 1°C at 50% humidity) with a 12-h light/12-h dark cycle. They were given *ad libitum* access to 10% safflower oil diets and water. Male *fat-1* and female WT mice were paired and the pregnancies were monitored. Embryos were obtained at the day 13.5 after paring and used to prepare fibroblasts after removing head, heart and legs. The tails of the embryos

were used to confirm the *fat-1* genotype by PCR, and the embryo bodies were minced into small pieces and cultured in high glucose Dulbecco's modified Eagle's medium (DMEM; Gibco BRL, Grand Island, NY) supplemented with 10% fetal bovine serum (FBS; Gibco BRL, Grand Island, NY) and kept at 37 °C with 5% CO_2.

Analysis of fatty acid composition

Fatty acid profiles were determined by using gas chromatography as described previously (Kang & Wang 2005). Briefly, samples were grounded to powder under liquid nitrogen. They were subjected to extraction of total lipids and fatty acid methylation by heating at 100°C for 1 h with 14% boron trifluoride-methanol reagent. Fatty acid methyl esters were analyzed by gas chromatography using a fully automated Agilent 7890A system (Agilent, Santa Clara, CA) equipped with a flame-ionization detector. Peaks of resolved fatty acids were identified by comparison with the fatty acid methyl ester reference standards (Sigma Aldrich, St. Louis, MO), and area percentage for all resolved peaks was measured by using the ChemStation software (Agilent Technologies, Palo Alto, CA).

JB6 Cl41 cell culture

The mouse epidermal cell line, JB6 Cl41, was obtained from the American Type Culture Collection (Manassas, VA), and its characterization was done by monitoring cell morphology, karyotyping, and the cytochrome *c* oxidase I assay.

The cells were maintained in minimum essential medium (MEM) containing 5% FBS, 25 μg/mL gentamicin, 0.01% sodium pyruvate and 1.5 mg/mL sodium bicarbonate in an atmosphere of 95% air and 5% CO_2 at 37°C. MEM and gentamicin were purchased from Gibco BRL (Grand Island, NY).

Source and protocols of UVB irradiation

The UVB radiation source was a 5×8 Watt tube, which emits an energy spectrum with high fluency in the UVB region (with a peak at 312 nm). A Biolink BLX-312 UV crosslinker (Vilbert Lourmat, Marne-la-Valle´ e, France) was used to irradiate mouse skin (180 mJ/cm^2 dose of UVB) and MEFs (20 mJ/cm^2 dose of UVB). The irradiated animals were allowed to move freely and with no more than five mice per cage. Dorsal skin samples were obtained for epidermal sheets 2 h later. In a skin papillomagenesis model, female hairless mice were irradiated with UVB (180 mJ/cm^2) three times a week for 23 weeks. The irradiated mice were sacrificed, and their skin and tumors were collected for subsequent studies.

Histological and immunohistochemical analyses of paraffin-embedded skin sections

Sections of harvested mouse skin were washed with phosphate-buffered saline (PBS) and fixed with 10% buffered formalin and embedded in paraffin. Each section (4 μm) was stained with hematoxylin and eosin (H&E). The H&E stained sections were examined under light microscope to detect the presence

of lesions. Immunohistochemistry (IHC) of formalin-fixed and paraffin-embedded tissue specimens were performed to detect the expression of P-STAT3, COX-2, 4-hydroxy-2-nonenal (4-HNE)-modified protein and Nrf2. The sections were cut on silanized glass slides, deparaffinized three times with xylene and rehydrated through graded alcohol bath. The deparaffinized sections were heated by using microwave and boiled twice for 6 min in 10 mM citrate buffer (pH 6.0) for antigen retrieval. To diminish nonspecific staining, each section was treated with 3% hydrogen peroxide and 4% peptone casein blocking solution for 15 min. For the detection of respective protein expression, slides were incubated with P-STAT3 (Cell Signaling Technology, Beverly, MA), COX-2 (Cayman Chemical Co., Ann Arbor, MI), proteins modified with 4-HNE (JaICA, Nikken SEIL Co. Ltd., Shizuoka, Japan) and Nrf2 (Santa Cruz Biotechnology, Inc., Santa Cruz, CA) antibodies at room temperature for 40 min in Tris-buffered saline containing 0.05% Tween 20, and then developed using horseradish peroxidase-conjugated secondary antibodies (rabbit or mouse) (Dako, Glostrup, Denmark). The peroxidase binding sites were detected by staining with 3,3'-diaminobenzidine tetrahydrochloride. Finally, counterstaining was performed using Mayer's hematoxylin.

Tissue lysis and protein extraction

For the preparation of mouse epidermal protein extract, fat and dermis were removed from the harvested skin samples kept on ice, and the fat-free epidermis was immediately placed in liquid nitrogen and pulverized in mortar. The

pulverized skin was homogenized on ice for 20 s with a polytron tissue homogenizer and lysed in 1 mL ice-cold lysis buffer [150 mM NaCl, 0.5% Triton-X 100, 50 mM Tris–HCl (pH 7.4), 20 mM ethylene glycol tetra-acetic acid, 1 mM dithiothreitol (DTT), 1 mM Na_3VO_4 and protease inhibitors, 1 mM phenylmethyl sulfonylfluoride (PMSF) and ethylenediaminetetraacetic acid (EDTA)-free cocktail tablet] followed by a periodical vortex for 30 min at 0°C. In other studies, MEFs and JB6 C141 cells were incubated with linoleic acid (LA), arachidonic acid (AA), docosahexaenoic acid (DHA; Cayman Chemical Co., Ann Arbor, MI), dimethyl sulfoxide (DMSO; Amresco, Solon, OH), cycloheximide (Sigma-Aldrich, St. Louis, MO) or MG132 (Enzo Life Sciences, Inc., Farmingdale, NY) for indicated durations. The treated cells were harvested, washed with PBS and suspended in the lysis buffer as mentioned above for 1 h on ice. The lysates were centrifuged at 14,800 *g* for 15 min at 4 ºC. The aliquots collected from the supernatant containing protein were stored at -70°C until use.

Preparation of cytosolic and nuclear extracts

Scraped dorsal skin of mice was homogenized in 800 μL of hypotonic buffer A [10 mM 4-(2-hydroxyethyl)-1-piperazineethanesulfonic acid (HEPES, pH 7.8), 1.5 mM $MgCl_2$, 10 mM KCl, 1 mM DTT, 0.1 mM EDTA and 0.1 mM PMSF]. To the homogenates was added 80 μL of 10% Nonidet P-40 (NP-40) solution, and the mixture was then centrifuged for 2 min at 14,800 *g*. The supernatant was collected as cytosolic fraction. The precipitated nuclei were washed once with 500 μL of buffer A plus 50 μl of 10% NP-40, centrifuged, resuspended in

200 μL of buffer C [50 mM HEPES (pH 7.8), 50 mM KCl, 300 mM NaCl, 0.1 mM EDTA, 1 mM DTT, 0.1 mM PMSF and 20% glycerol] and centrifuged for 5 min at 14,800 *g*. The supernatant containing nuclear proteins was collected and stored at -70°C.

Western blot analysis

For Western blot analysis, the protein concentration of whole cell lysates and cytosolic extract was measured by using the bichinconinic acid protein assay kit (Pierce, Rockford, IL), while that of nuclear extract was quantified by using the Bio-Rad protein assay kit (Bio-Rad Laboratories, Hercules, CA). Cell lysates (30 μg protein) were boiled in sodium dodecyl sulfate (SDS) sample loading buffer for 5 min before electrophoresis on 8-15% SDS-polyacrylamide gel (SDS-PAGE). After transfer to a polyvinylidene difluoride (PVDF) membrane (Gelman Laboratory, Ann Arbor, MI), the blots were blocked with 5% fat-free dry milk in tris-buffered saline containing 0.1% tween 20 (TBST) for 1 h at room temperature. The membranes were incubated for 12-24 h at 4°C with dilutions of primary antibodies for P-STAT3, STAT3, HA-tag (Cell Signaling Technology, Beverly, MA), lamin B, ubiquitin (Invitrogen, Carlsbad, CA), COX-2 (Cayman Chemical Co., Ann Arbor, MI), actin (Sigma Aldrich, St. Louis, MO), proteins modified with 4-HNE (JaICA, Nikken SEIL Co. Ltd., Shizuoka, Japan), HO-1 (Stressgen Biotechnologies Co., San Diego, CA), NQO1 (Abcam Inc., Cambridge, MA), Nrf2 and α-tubulin (Santa Cruz Biotechnology, Inc., Santa Cruz, CA). Blots were washed three times with

TBST at 7 min intervals followed by incubation with 1:3000 dilution of respective horseradish peroxidase conjugated secondary antibodies (rabbit, mouse or goat) in 3% fat-free dry milk-TBST for 2 h at room temperature. The blots were rinsed again three times with TBST. The immunoblots were visualized with an enhanced chemiluminescent (ECL) detection kit (Amersham Pharmacia Biotech, Buckinghamshire, UK) and LAS-4000 image reader (Fujifilm, Tokyo, Japan) according to the manufacturer's instructions.

Reverse transcription-polymerase chain reaction analysis (RT-PCR)

Total RNA was isolated from mouse skin tissues using TRIzol® reagent (Invitrogen, Carlsbad, CA) according to the manufacturer's protocol. To generate the cDNA from RNA, 1 μg of total RNA was reverse transcribed with murine leukemia virus reverse transcriptase (Promega, Madison, WI) for 50 min at 42°C and again for 15 min at 72°C. About 1 μL of cDNA was amplified with a PCR mixture (HS Prime Taq 2X Premix, Daejeon, South Korea) in sequential reactions. The primers used for each RT-PCR reactions are as follows : *cox-2*, 5'-CTG GTG CCT GGT CTG ATG ATG-3' and 5'-GGC AAT GCG GTT CTG ATA CTG-3'; *actin*, 5'-AGA GCA TAG CCC TCG TAG AT-3' and 5'-CCC AGA GCA AGA GAG GTA TC-3'; *ho-1*, 5'-TAC ACA TCC AAG CCG AGA AT-3' and 5'-GTT CCT CTG TCA GCA TCA CC-3'; *nqo1*, 5'-TCG GAG AAC TTT CAG TAC CC-3' and 5'-TGC AGA GAG TAC ATG GAG CC-3'; *nrf2,* 5'-CCT CTG TCA CCA AGC TCA AGG-3' and 5'-TTC TGG GCG GCG ACT TTA TT-3' (forward and reverse, respectively).

Amplification products were analyzed by 2-3% agarose gel electrophoresis, followed by staining with SYBR Green (Invitrogen, Carlsbad, CA) and photographed using fluorescence in LAS-4000 (Fujifilm, Tokyo, Japan).

Measurement of intracellular ROS accumulation

The accumulation of ROS in UVB-irradiated MEFs was monitored using the fluorescence-generating probe 2',7'-dichlorofluorescein diacetate (DCF-DA; Invitrogen, Carlsbad, CA). Treated cells were rinsed twice with Hanks' balanced salt solution (HBSS, Cellgro, Herndon, VA) and loaded with 10 μM DCF-DA for 30 min in a 5% CO_2 incubator to assess ROS-mediated oxidation of DCF-DA to the fluorescent compound DCF. Cells were washed twice with HBSS, suspended in the complete media and examined under a micromanipulator system (Leica Microsystems, Heidelberg, Germany).

Transient transfection with Nrf2 siRNA

Nrf2 siRNA and Stealth™ universal RNAi negative control duplexes were from Invitrogen (Carlsbad, CA). The target sequence for Nrf2 siRNA is as follow: forward 5'-AAG AGU AUG AGC UGG AAA AAC UU-3'and reverse 5'-GUU UUU CCA GCU CAU ACU CUU UU-3'. MEFs were seeded at a density of 4 x 10^4 cells/mL in 60-mm petridishes and grown to 60-70% confluence. Nrf2 siRNA (20 μM) was transfected into MEFs with Lipofectamine® RNAi-MAX reagent (Invitrogen, Carlsbad, CA) according to the manufacturer's instructions. After 48-h transfection, cells were treated with LA (50 μM) and AA (50 μM)

for additional 24 h, and cell lysates were prepared as described earlier.

Construction of plasmid pCMV-HA-N-fat-1

The murine full-length *fat-1* was amplified by RT-PCR from the total RNA obtained from the tails of *fat*-1 mice with primers 5'-CAT GGA GGC CCG AAT TCG GAT GGT CGC TCA TTC CTC A-3' (forward) and 5'- ATC CCC GCG GCC GCG GTA CCT TAC TTG GCC TTT GCC TT-3' (reverse) and subcloned into HA-tagged-pCMV expression vector (Clontech Laboratories, Inc., Mountain View, CA) as *EcoRI*/*KpnI* fragment. One day before transfection, JB6 C141 cells were seeded at a density of 3 x 10^4 cells/mL in a 60-mm dishes and grown to 40–50% confluence growth media without antibiotic at 37℃ in a humidified atmosphere of 5% CO_2/95% air. The *fat-1* overexpresion vector (50 nM) was transfected into JB6 Cl41 cells with Lipofectamine® 2000 reagent (Invitrogen, Carlsbad, CA) according to the manufacturer's instructions. After 24-h transfection, cells were treated with LA (25 μM) and AA (25 μM) for additional 48 h, and cell lysates were prepared as described earlier.

Immunoprecipitation

JB6 cells were treated with DHA and AA for indicated time and lysed in 250 mM sucrose, 50 mM Tris-HCl (pH 8.0), 25 mM KCl, 5 mM $MgCl_2$, 1 mM EDTA, 2 μM NaF, 2 μM sodium orthovanadate, 1 mM PMSF and 10 mM N-ethylmaleimide. Total protein (500 μg) was subjected to immunoprecipitation by shaking with Nrf2 primary antibody at 4℃ for 24 h followed by the addition

of 40 μL of 25% protein G-agarose bead slurry (Santa Cruz Biotechnology, Inc., Santa Cruz, CA) and additional shaking for 2 h at 4℃. After centrifugation at 10,000 *g* for 1 min, immunoprecipitated beads were collected by discarding the supernatant and washed with cell lysis buffer. After final wash, immunoprecipitate was resuspended in 50 μL of 2X SDS electrophoresis sample buffer and boiled for 5 min. Forty five-μL of supernatant from each sample was loaded on SDS-PAGE. The ubiquitinated Nrf2 was visualized by antibody against ubiquitin (Life Technologies, Carlsbad, CA).

Statistical analysis

Except for the data on the body weight change and multiplicity expressed as the mean ± standard deviation (SD), all other values were expressed as the mean ± standard error (SE) of at least three independent experiments. Statistical significance was determined by Student's *t*-test and a *p*-value of less than 0.05 was considered to be statistically significant.

4. Results

Generation of hairless* fat-1$^{+/-}$ *mice and fatty acid profiles of their skin tissues

Hairless animals are known to be more susceptible to the induction of squamous cell carcinomas than their haired littermates (Kim *et al.* 2012). The *fat-1* gene of *C. elegans* encodes an ω-3 fatty acid desaturase that converts ω-6 to ω-3 PUFAs, but this gene is absent in mammals (Kang 2007). To determine whether an increased ω-3 PUFA tissue accumulation is protective against repeated UVB-induced skin inflammation and photocarcinogenesis, we generated hairless *fat-1* mice by crossing *fat-1*$^{+/-}$ haired and SKH-1 hairless mice as shown in **Fig. 3-1A**. Thus, the '*fat-1*' transgenic mice of the C57BL6 strain were subsequently backcrossed five times to SKH-1 hairless mice. The *fat-1*$^{+/-}$ animals were segregated for the hairless phenotype. The resulting mice had the predominant genetic background of Skh:hr-1 hairless (>96.875%). All the experiments were performed by comparing mice of the same genetic background with or without carrying the *fat-1* transgene. The hairless mutation showed normal development of the hair coat in the first hair cycle. Starting at the 2 week of age, they lost their hair coat rapidly (Sundberg & King 2001). At weaning, they were completely hairless. Both hairless *fat-1*$^{-/-}$ and *fat-1*$^{+/-}$ littermates born to the same mother were maintained on an identical diet containing ω-6 PUFAs, but deficient in ω-3 ones. Analysis of the total lipids extracted from skin tissues of hairless *fat-1*$^{+/-}$ mice showed a PUFA profile distinct from that of hairless *fat-1*$^{-/-}$ (**Fig. 3-1B and Table 3-1**). There were

significantly lower levels of ω-6 PUFAs and much higher proportions of ω-3 PUFAs in the skin of hairless *fat-1*$^{+/-}$ mice compared to those *fat-1*$^{-/-}$ mouse skin. The ratios of the ω-6 (18:2n-6, 18:3n-6, 20:3n-6 and 20:4n-6) to the ω-3 PUFAs (18:3n-3, 20:3n-3, 20:5n-3 and 22:6n-3) in skin tissues of hairless *fat-1*$^{-/-}$ and *fat-1*$^{+/-}$ mice were 15.48:1 and 3.77:1, respectively. This indicates that the transgene is functionally active and transmittable.

UVB-induced inflammation was ameliorated in* fat-1$^{+/-}$ *mouse skin

First, we investigated whether an elevated ω-3 PUFA tissue level in hairless *fat-1*$^{+/-}$ mice protects against UVB-induced inflammation. Hairless *fat-1*$^{+/-}$ mice developed less severe skin hyperplasia compared with their *fat-1*$^{-/-}$ littermates (**Fig. 3-2A**, upper panels). Persistently activated STAT3 plays an important role in photocarcinogenesis through upregulation of genes involved in tumor-associated inflammation, anti-apoptosis and proliferation (Kim *et al.* 2009a). One of the essential events in activation of STAT3 signaling is phosphorylation at its tyrosine 705 residue (Tyr^{705}). As shown in **Fig. 3-2A** (lower panels), hairless *fat-1*$^{-/-}$ mice irradiated with UVB exhibited markedly increased expression of P-STAT3 (Tyr^{705}) which appeared as brown color staining. A significantly lower proportion of phosphorylated STAT3-positive cells was observed in *fat-1*$^{+/-}$ mouse skin irradiated with UVB. Lysates of both total and nuclear extracts of skin tissues were subjected to Western blot analysis of the phosphorylation of STAT3 at Tyr^{705}. Whole tissue lysates and nuclear extracts from *fat-1*$^{+/-}$ mouse skin showed markedly decreased nuclear translocation of

P-STAT3 after UVB irradiation compared with *fat-1*$^{-/-}$ mouse skin (**Fig. 3-2B**).

UVB-induced skin tumor development was suppressed in hairless* fat-1$^{+/-}$ *mice compared with that in* fat-1$^{-/-}$ *mice

After repeated UVB irradiation thrice a week for 23 weeks, representative photographs of mice from different groups were taken. **Fig. 3-3A** shows that the tumor burden in the hairless *fat-1*$^{+/-}$ mice was much lower than that in the hairless *fat-1*$^{-/-}$ mice. The smallest tumor in the hairless *fat-1*$^{-/-}$ mice was still bigger than the biggest one in the hairless *fat-1*$^{+/-}$ mice. We monitored the body weight of each mouse every week until termination of the experiment. The body weight change of UVB-exposed mice was decreased compared with the mice in the control group. However, hairless *fat-1*$^{+/-}$ mice exhibited body weight reduction caused by UVB to a lesser extent than the hairless *fat-1*$^{-/-}$ mice (**Fig. 3-3B**, upper left panel). As shown in the upper right panel of **Fig. 3-3B**, there is a marked difference in the onset of tumor formation between hairless *fat-1*$^{-/-}$ and *fat-1*$^{+/-}$ mice. About the half of hairless *fat-1*$^{-/-}$ mice irradiated with UVB developed skin papillomas at the 14th week which reached 100% at the 18th week. However, the first appearance of skin papillomas in hairless *fat-1*$^{+/-}$ mice was observed at the 16th week, and the 100% tumor incidence was attained at the 23th week. The tumor multiplicity between the two experimental groups was also significantly different (**Fig. 3-3B**, lower left panel). In the hairless *fat-1*$^{+/-}$ mice, the average number of tumors per mouse was 7 compared with 16.5 in the hairless *fat-1*$^{-/-}$ littermates. Likewise, the cumulative number of

papillomas was markedly reduced in hairless *fat-1*$^{+/-}$ mice (**Fig. 3-3B**, lower right panel). Our data clearly demonstrate a pronounced inhibition of inflammation and papilloma formation in UVB-irradiated skin of the hairless *fat-1*$^{+/-}$ mice, which is attributable to an increased ω-3 to ω-6 PUFA ratio.

UVB-induced expression of COX-2 and phosphorylation of STAT3 were diminished in the papillomas of hairless* fat-1$^{+/-}$ *mice compared with those in the* fat-1$^{-/-}$ *mice

COX-2 is an inducible prostaglandin synthase responsible for producing a distinct set of prostaglandins and thromboxanes involved in inflammatory processes. Inappropriate upregulation of COX-2 induces malignant changes in epidermal keratinocytes (Rundhaug & Fischer 2010) and prolongs the survival of malignant or transformed cells with metastatic potential (Surh *et al.* 2001). STAT3 is a well known transcription factor involved in the regulation of COX-2 (Koon *et al.* 2006). A significant decrease in expression of COX-2 at both transcriptional (**Fig. 3-4A**) and translational (**Fig. 3-4B**) levels was noted in the papillomas of the hairless *fat-1*$^{+/-}$ mice. Concomitant with downregulation of COX-2, the level of P-STAT3 (Tyr^{705}) was also markedly reduced in *fat-1*$^{+/-}$ mouse skin irradiated with UVB (**Fig. 3-4B**). The above findings were also verified by H&E staining and immunohistochemical analysis. The thickening of epidermal layer and inflammatory cell infiltration in UVB-irradiated *fat-1*$^{-/-}$ mouse skin were less severe in *fat-1*$^{+/-}$ skin (**Fig. 3-4C**, upper panels). Likewise, expression of COX-2 (**Fig. 3-4C**, middle panels) and P-STAT3 (**Fig. 3-4C**,

lower panels) in the skin of *fat-1*$^{+/-}$ mice was substantially reduced.

UVB-induced oxidative skin damage was attenuated in* fat-1$^{+/-}$ *mice

Multiple lines of evidence suggest that UVB-induced generation of ROS, such as superoxide anion, hydroxyl radical and hydrogen peroxide, is responsible for skin hyperplasia (Tyrrell 1995) as well as lipid peroxidation (Halliday 2005). 4-HNE is a representative lipid peroxidation product (Oberley *et al.* 2004, Petersen & Doorn 2004). There was lesser 4-HNE-induced protein modification in the hairless *fat-1*$^{+/-}$ mouse skin as compared to *fat-1*$^{-/-}$ one upon acute UVB irradiation (**Fig. 3-5A**). Moreover, repeated exposure to UVB up to 23 weeks increased the 4-HNE-modified protein expression, which was blunted in the skin of *fat-1*$^{+/-}$ mice (**Fig. 3-5B**).

The Nrf2-mediated induction of cytoprotective gene expression was elevated in the skin of* fat-1$^{+/-}$ *mice

Exposure to UVB is known to generate ROS which can cause oxidative stress. This may trigger an adaptive antioxidant response to protect cells from oxidative damage. To investigate whether the decreased number of papillomas formed by UVB irradiation is attributable to augmentation of cellular defense capacity that counteract excessive ROS accumulation, we analyzed the antioxidant gene expression in the skin of *fat-1*$^{+/-}$ mice. We found a robust enhancement in the expression of two representative cytoprotective enzymes HO-1 and NQO1, at both transcriptional and translational levels, in the *fat-1*$^{+/-}$

(**Fig. 3-6A and B**). Nrf2 plays a critical role in transcriptional activation of genes encoding HO-1 and NQO1. Enhanced nuclear accumulation of Nrf2 was observed in the skin of *fat-1*$^{+/-}$ (**Fig. 3-6B and C**). Consistently, the stabilization of Nrf2 protein was observed in the hairless *fat-1*$^{+/-}$ mouse skin at the 23rd week, as measured by Western blot analysis (**Fig. 3-6D**). Compared with their respective age-matched skin of *fat-1*$^{-/-}$ mice, no significant change in the epidermal level of Nrf2 mRNA was found in the *fat-1*$^{+/-}$ mice (**Fig. 3-6A**) which is in a good agreement with a previous finding (Yang *et al.* 2013). These findings suggest that the epidermal *nrf2* gene transcription is not affected by an increased ω-3 PUFA production in *fat-1*$^{+/-}$ and that its protein expression is likely to be regulated by post-transcriptional mechanisms.

UVB-induced inflammation and oxidative stress were less severe in* fat-1 *MEFs than those in WT MEFs

It has been reported that changes in fatty acid composition occur in the early stage of embryo-genesis and last for the whole life in the *fat-1* transgenic mice (Kang 2007). To further confirm the *in vivo* findings, MEF cells were isolated from both WT and *fat-1* transgenic mice. A significantly lower level of the ω-6/ω-3 fatty acid ratio was observed in *fat-1* MEF cells as compared to WT MEF cells (**Fig. 3-7A and Table 3-2**). Reduced levels of ω-6 PUFAs, especially LA and AA, were found in the *fat-1* MEF cells as compared to the WT MEF cells. However, the reduction of ω-6 PUFA levels in the *fat-1* MEF cells was not as dramatic as increases in ω-3 PUFA. To elucidate the role of the *fat-1* transgene

in UVB-induced inflammatory and oxidative insults, MEF cells were incubated with representative ω-6 PUFAs, LA and AA, followed by UVB irradiation. COX-2 expression was further enhanced in WT MEF cells with co-expression of an active form of STAT3 (P-STAT3). COX-2 expression and STAT3 phosphorylation were attenuated in UVB-exposed *fat-1* MEFs (**Fig. 3-7B**). Next, we examined the effect of *fat-1* gene against intracellular ROS production in UVB-irradiated MEF cells. As illustrated in **Fig. 3-7C**, UVB-irradiated MEF cells showed an enormous increase in the ROS accumulation as compared to control cells. The ROS generation was further enhanced in the *fat-1* deficient MEFs incubated with ω-6 PUFAs, LA and AA. However, the increased ω-6/ω-3 fatty acid ratio blocked UVB-induced ROS overproduction in the *fat-1* MEFs. The *fat-1* MEF cells exhibited upregulation of the two representative antioxidant enzymes, HO-1 and NQO1, at both transcriptional and translational levels, to a greater extent than WT MEF cells upon treatment with LA plus AA (**Fig. 3-7D**). Further, siRNA knock down of *nrf2* gene abrogated the expression of HO-1 and NQO1 in *fat-1*$^{+/-}$ MEF cells (**Fig. 3-7E**). This finding indicates that Nrf2 is essential for the induction of cytoprotective gene expression in *fat-1* MEF cells.

DHA increased the stability of Nrf2 protein in mouse epidermal JB6 cells

In another experiment, mouse epidermal JB6 cells were transfected with either pCMV-HA-control vector or pCMV-HA-*fat-1* vector. Overexpression of *fat-1* gene increased the Nrf2-mediated expression of cytoprotective enzymes (**Fig.**

3-8A). In contrast to the altered Nrf2 protein expression, JB6 cells transiently, transfected with pCMV-HA-*fat-1* vector exhibited no significant alteration in the steady state level of its mRNA transcript (**Fig. 3-8A**). To determine whether DHA stabilizes Nrf2 protein without inducing *de novo* synthesis, we monitored the degradation of basal and DHA-induced Nrf2 protein in JB6 cells after inhibition of protein synthesis by cycloheximide. As illustrated in **Fig. 3-8B**, Nrf2 protein in untreated control cells degraded rapidly after addition of cycloheximide, whereas Nrf2 in the DHA-treated JB6 cells underwent degradation more slowly. As shown in **Fig. 3-8C**, treatment of JB6 cells with the proteasome inhibitor, MG-132 significantly increased the level of Nrf2. Moreover, most proteins subjected to proteasomal degradation are marked by prior, covalent ligation of ubiquitin molecules to the ε-amino group of specific lysine residues. A ubiquitination assay revealed that the appearance of ubiquitinated Nrf2 was decreased with a concomitant increase in Nrf2 accumulation in cells treated with DHA (**Fig. 3-8D**).

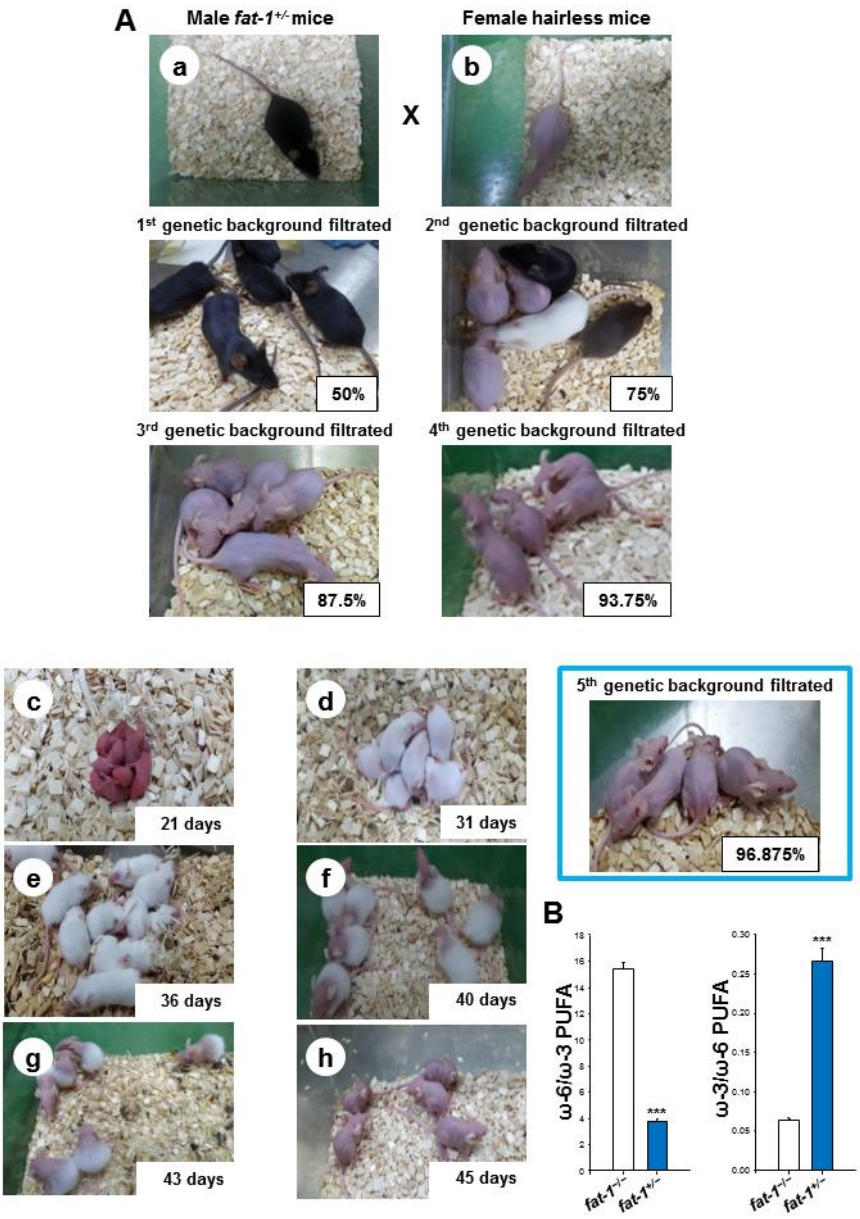

Fig. 3-1. Generation of hairless *fat-1*$^{+/-}$ mice and the analysis of their skin PUFA composition. (A) *fat-1*$^{+/-}$ haired mice (a) were crossed with SKH-1 hairless mice (b) to generate *fat-1*$^{-/-}$ and *fat-1*$^{+/-}$ progenies. Hairless *fat-1*$^{-/-}$ and *fat-1*$^{+/-}$ mice during (c–g) and after (h) first hair cycle. After an initial hair cycle, the skin became eventually hairless, suitable for all studies to be

undertaken. (B) Both hairless *fat-1*$^{-/-}$ and *fat-1*$^{+/-}$ littermates born to the same mother were maintained on a diet (10% safflower oil) high in ω-6 and low in ω-3 fatty acids. After the dietary regimen, the PUFA profiles of mouse skin were analyzed by gas chromatography. Significantly elevated levels of ω-3 vs. ω-6 fatty acids were observed in skin tissues of hairless *fat-1*$^{+/-}$ mice as compared to those of hairless *fat-1*$^{-/-}$ mice. Data are expressed as means ± SE. ***p <0.001 versus hairless *fat-1*$^{-/-}$ mice.

Table 3-1. PUFA composition in the skin of hairless *fat-1* transgenic and wild-type mice.

		***fat-1*$^{-/-}$**	***fat-1*$^{+/-}$**
Linoleic acid	C18:2	31.81 ± 0.62	27.06 ± 0.86[a]
γ-Linolenic acid	C18:3	0.46 ± 0.06	0.22 ± 0.01[a]
Dihomo-γ-linolenic acid	C20:3	1.03 ± 0.04	0.54 ± 0.06[b]
Arachidonic acid	C20:4	0.37 ± 0.02	0.04 ± 0.01[c]
ω-6 PUFAs (%)		**33.66 ± 0.60**	**27.86 ± 0.89[b]**
α-Linolenic acid	C18:3	0.90 ± 0.04	2.46 ± 0.13[c]
Eicosatrienoic acid	C20:3	0.56 ± 0.06	1.03 ± 0.01[b]
Eicosapentaenoic acid	C20:5	0.35 ± 0.04	1.29 ± 0.02[c]
Docosahexaenoic acid	C22:6	0.36 ± 0.01	2.63 ± 0.11[c]
ω-3 PUFAs (%)		**2.18 ± 0.03**	**7.41 ± 0.24[c]**
ω-6/ω-3 PUFAs		15.48 ± 0.48	3.77 ± 0.22[c]
ω-3/ω-6 PUFAs		0.06 ± 0.004	0.27 ± 0.02[c]

Data are expressed as means ± SE (n = 3).

[a]p <0.05, [b]p <0.01 and [c]p <0.001 versus hairless *fat-1*$^{-/-}$ mice.

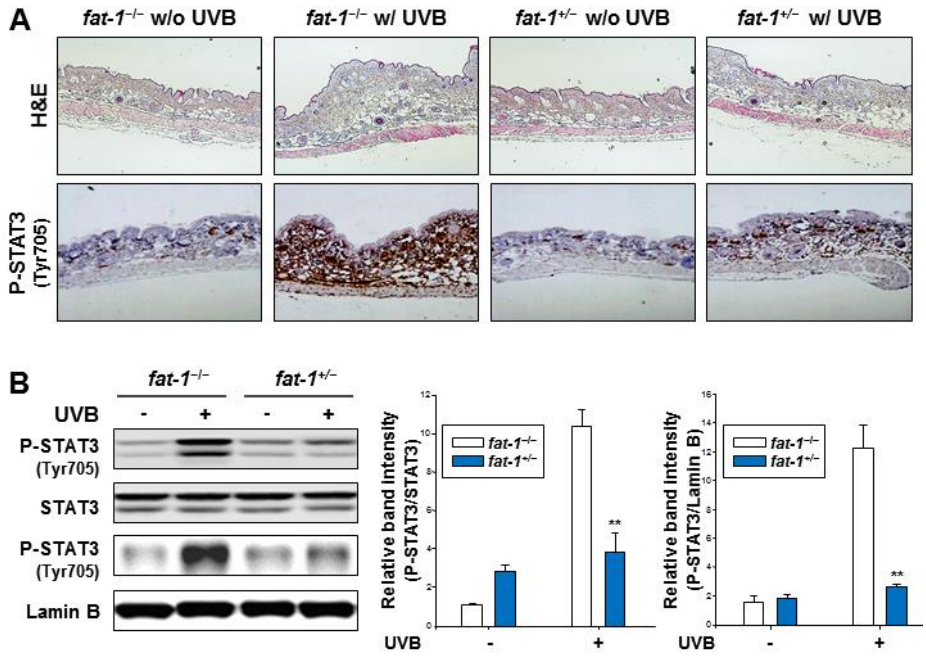

Fig. 3-2. UVB-induced inflammation was ameliorated in *fat-1*$^{+/-}$ mouse skin. Newly developed female hairless mice (n = 3 per treatment group) were topically treated on their backs with UVB radiation (180 mJ/cm^2). (A) Skin thickness in hairless *fat-1*$^{-/-}$ and *fat-1*$^{+/-}$ mice was visualized by H&E staining at 2 h following UVB exposure. Formalin-fixed and paraffin-embedded tissues from UVB-irradiated mice were also immunostained for phospho-STAT3 (Tyr^{705}), and counterstained with hematoxylin. Magnifications, ×100. (B) Whole lysates and nuclear extracts from different groups were subjected to SDS-PAGE and immunoblotted to detect total and phosphorylated forms of STAT3 (Tyr^{705}). Quantification of P-STAT3 was normalized to that of STAT3 and lamin B, followed by statistical analysis of relative band density. Data are expressed as means ± SE. $^{**}p$ <0.01 versus UVB-irradiated hairless *fat-1*$^{-/-}$ mice.

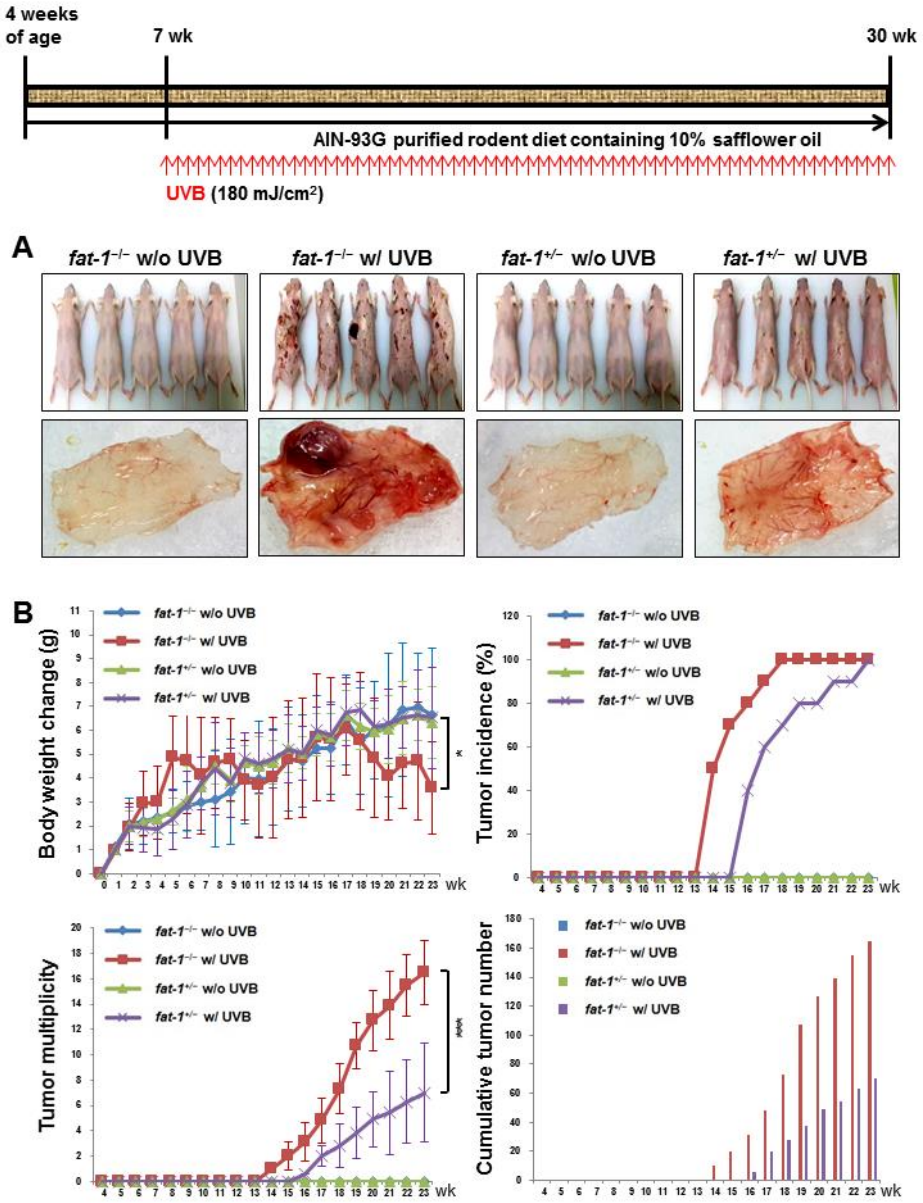

Fig. 3-3. UVB-induced skin tumor development was suppressed in hairless *fat-1*$^{+/-}$ mice compared with that in *fat-1*$^{-/-}$ mice. The female hairless *fat-1*$^{-/-}$ or *fat-1*$^{+/-}$ mice (n = 10 per group) were irradiated with UVB (180 mJ/cm^2) three times a week until termination of the experiment. (A) The photographic images represent papillomas formed at the 23rd week of UVB treatment. (B)

The body weight change was measured on a weekly basis. Starting four week following UVB treatment, tumors of at least 1 mm diameter were counted every week till the 23rd weeks. The results were expressed as the percentage of papilloma-bearing mice (incidence), the average number of papillomas per mouse (multiplicity) and the cumulative number of papillomas. Data are expressed as means ± SD. *p <0.05 and ***p <0.001 versus UVB-irradiated hairless *fat-1*$^{-/-}$ mice.

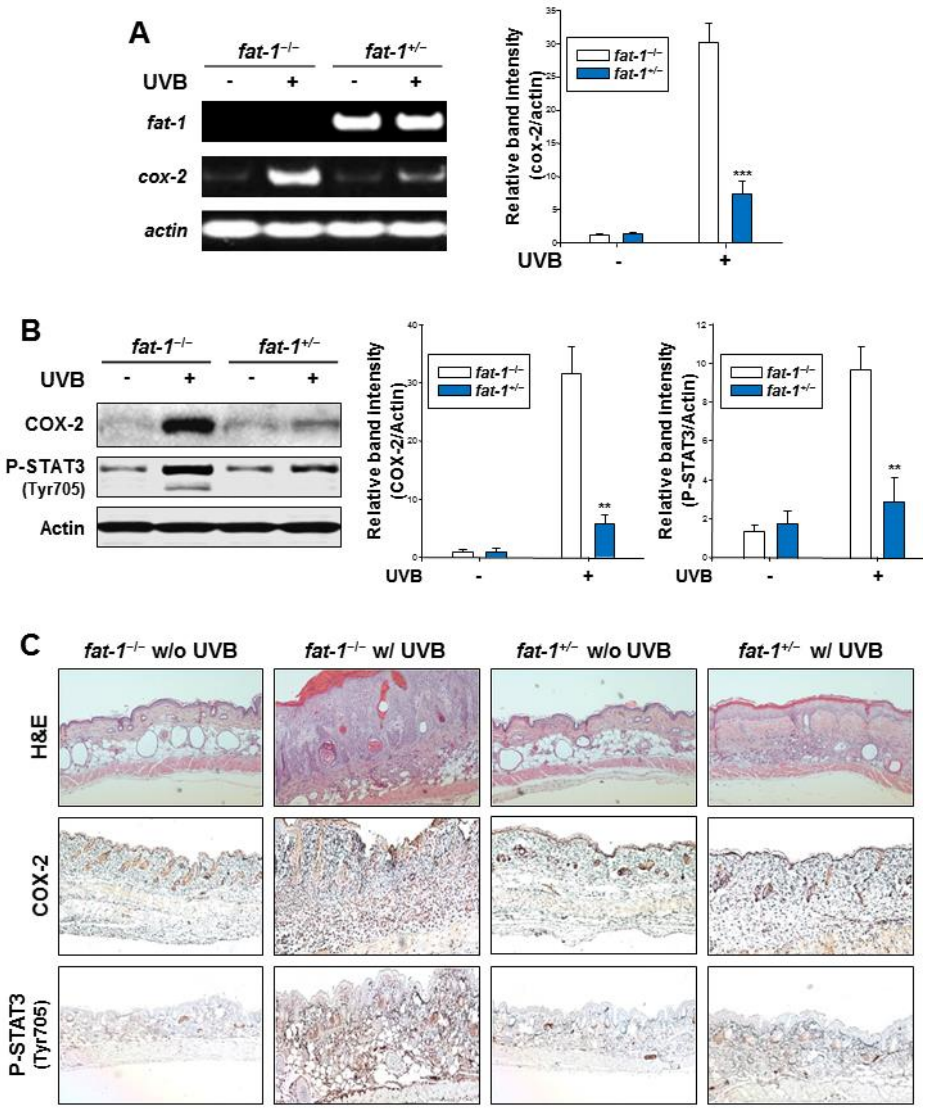

Fig. 3-4. UVB-induced expression of COX-2 and phosphorylation of STAT3 were diminished in the papillomas of hairless *fat-1*$^{+/-}$ mice compared with those in the *fat-1*$^{-/-}$ mice. Animal treatment and other experimental details are described in the legend to **Fig. 3-3**. (A) Total RNA was isolated from skin tissues, and mRNA expression of *cox-2* was examined by RT-PCR analysis. Quantification of *cox-2* was normalized to that of *actin*,

followed by statistical analysis of relative band density. (B) Whole surrounding tissue extracts (30 μg protein) were analyzed for the expression of COX-2 and P-STAT3 (Tyr^{705}) by immunoblotting. Quantification of COX-2 and P-STAT3 was normalized to that of actin, followed by statistical analysis of relative band density. Results are expressed as means ± SE. $^{**}p < 0.01$ and $^{***}p < 0.001$ versus UVB-irradiated hairless *fat-1*$^{-/-}$ mice. (C) H&E staining of papillomas showed hypertrophic squamous epithelium forming papillary fronds. The sections of skin tissues were also subjected to immunohistochemical analysis of COX-2 and P-STAT3 (Tyr^{705}). Positive COX-2 and P-STAT3 (Tyr^{705}) staining yielded a brown-colored product. Magnifications, ×100.

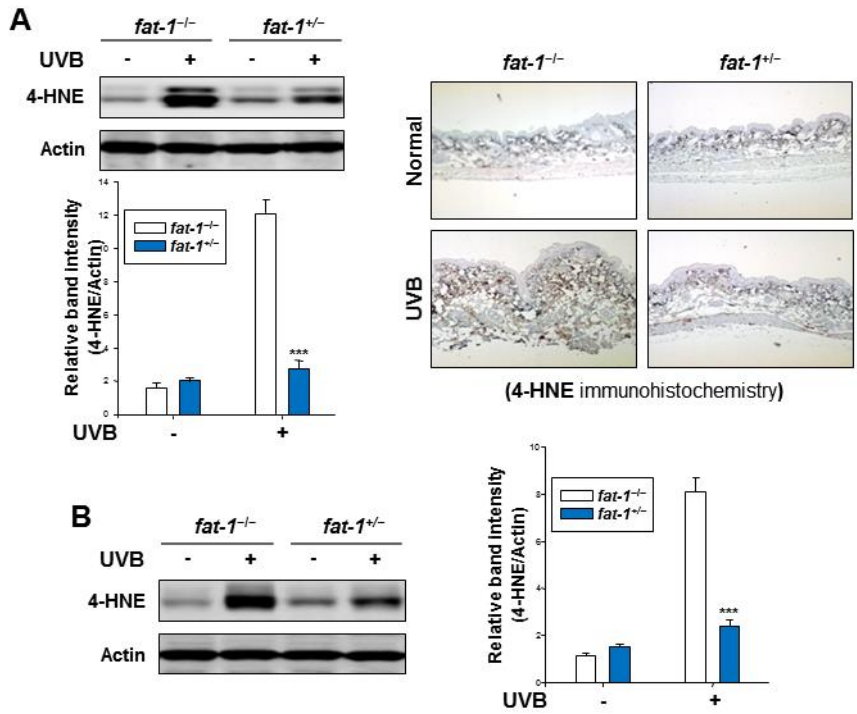

Fig. 3-5. UVB-induced oxidative skin damage was attenuated in *fat-1*$^{+/-}$ mice. (A) Animal treatment is same as described in the legend to **Fig. 3-2**. Isolated protein extracts were electrophoresed and transferred to a PVDF membrane, which was probed using antibody for 4-HNE. Quantification of 4-HNE was normalized to that of actin followed by statistical analysis of relative band density. Results are expressed as means ± SE. ***p <0.001 versus UVB-irradiated hairless *fat-1*$^{-/-}$ mice. Formalin-fixed and paraffin-embedded tissues from UVB-irradiated mice were immunostained for detecting the 4-HNE-modified protein expression. Magnifications, ×100. (B) Experimental conditions are same as described in the legend to **Fig. 3-3**. Western blot analysis of 4-HNE-modified protein expression in the skin papillomas of hairless *fat-1*$^{-/-}$ and *fat-1*$^{+/-}$ mice. Quantification of 4-HNE was normalized to that of actin

followed by statistical analysis of relative band density. ***p <0.001 versus UVB-irradiated hairless *fat-1*$^{-/-}$ mice.

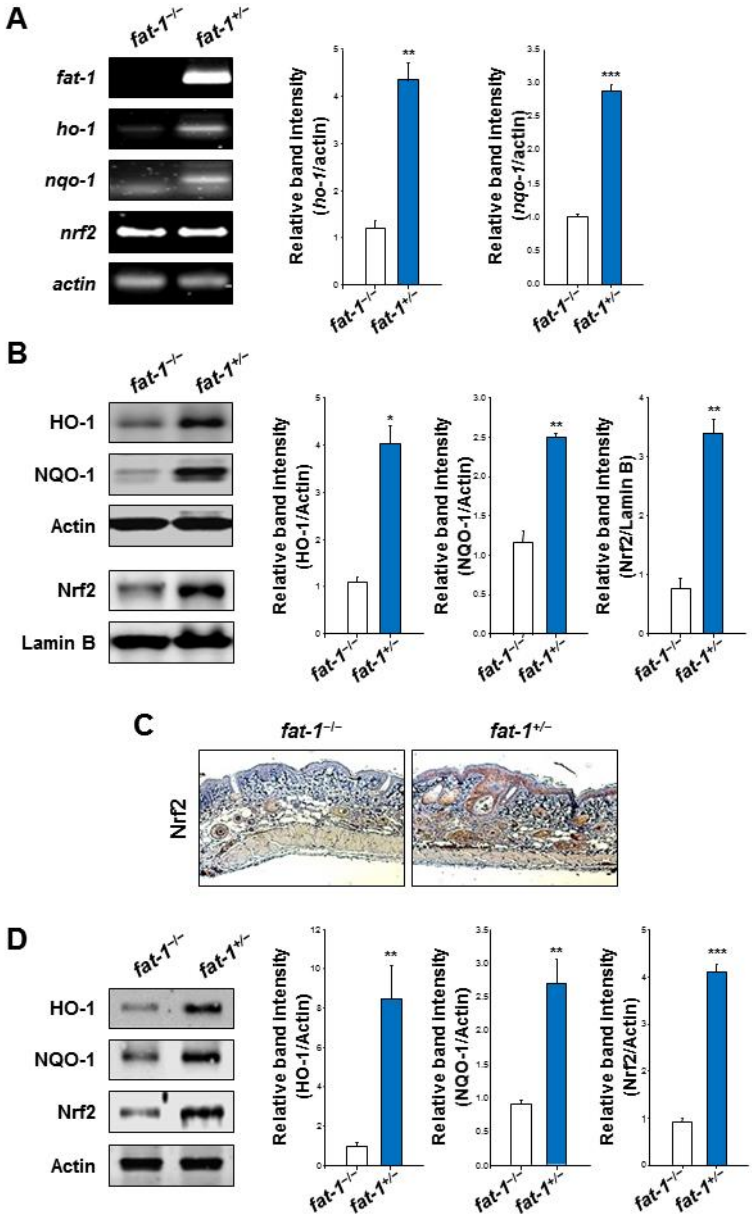

Fig. 3-6. The Nrf2-mediated induction of cytoprotective gene expression was elevated in the skin tissues of hairless *fat-1*$^{+/-}$ mice. Hairless *fat-1*$^{-/-}$ and *fat-1*$^{+/-}$ mice (n = 3 per treatment group) were maintained on AIN-93 diet supplemented with 10% safflower oil (rich in ω-6 fatty acids) for 5 weeks. (A) RT-PCR analysis was conducted to measure the mRNA levels of *ho-1, nqo1*

and *nrf2*. Quantification of *ho-1* and *nqo1* was normalized to that of *actin,* followed by statistical analysis of relative band density. (B) Collected skin tissues were placed on ice and fat was removed to get an epidermal layer. The epidermal lysates and nuclear extracts were separated by electrophoresis on SDS-PAGE and immunoblotted to detect protein expression of HO-1, NQO1 and Nrf2. Quantification of HO-1, NQO1 and Nrf2 immunoblot was normalized to that of actin and lamin B, followed by statistical analysis of relative band density. (C) Paraffin-embedded skin tissue blocks were analyzed by immunohistochemistry and the levels of Nrf2 (brown spots) were compared between hairless *fat-1*$^{-/-}$ and *fat-1*$^{+/-}$ mice. Magnifications, ×100. (D) After 23 weeks of feeding the 10% safflower oil diet, whole tissue extracts (30 μg protein) were analyzed for the protein levels of Nrf2-regulated antioxidant genes by immunoblotting. Quantification of HO-1, NQO1, and Nrf2 immunoblot was normalized to that of actin, followed by statistical analysis of relative band density. Data are expressed as means ± SE. **p* <0.05, ***p* <0.01 and ****p* <0.001 versus hairless *fat-1*$^{-/-}$ mice.

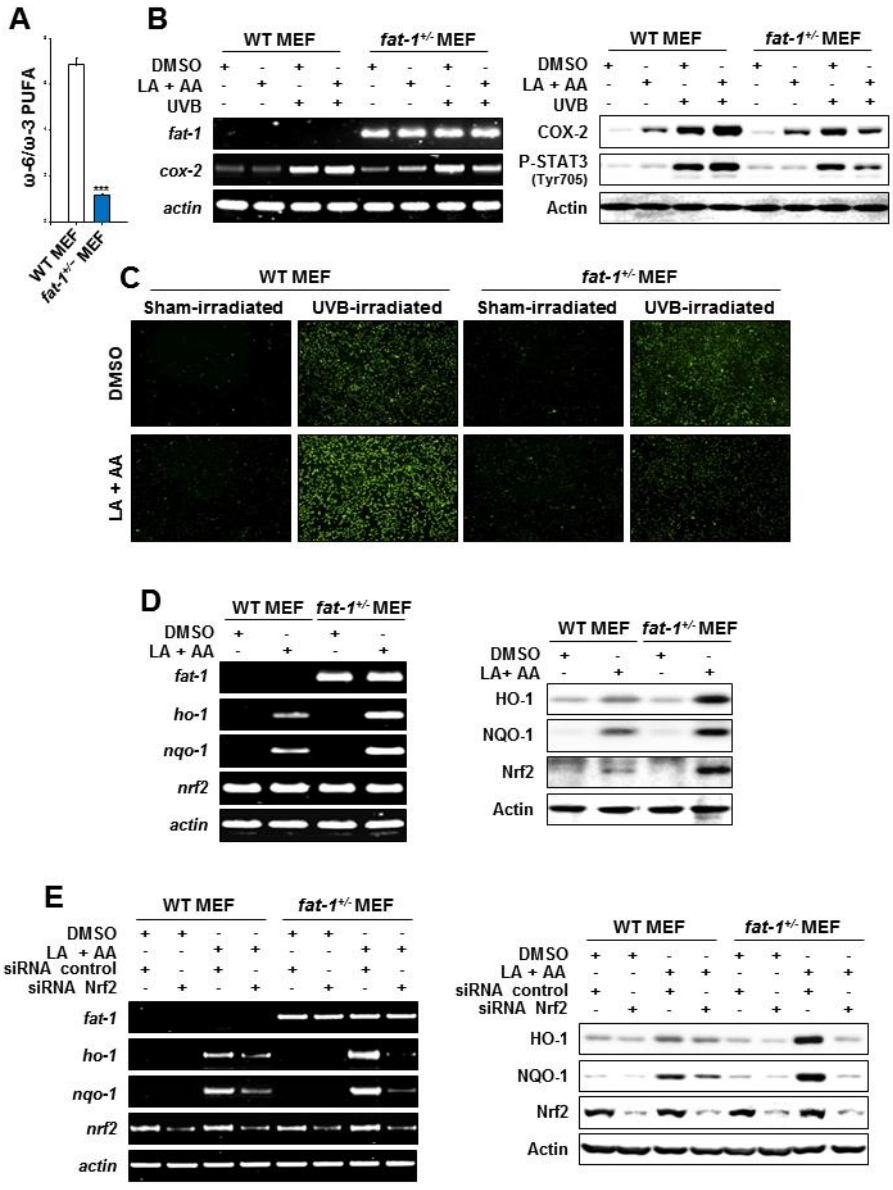

Fig. 3-7. UVB-induced inflammation and oxidative stresses were less severe in *fat-1* MEFs than that in WT MEFs. At 4 weeks of age, male *fat-1* transgenic and female WT littermates fed with the 10% safflower oil and maintained throughout mating, pregnancy, and lactation on the same diet. Embryos were isolated from those mice and used to prepare fibroblasts. (A)

PUFA profiles of MEFs were attained by using gas chromatography. Significantly decreased levels of ω-6 vs. ω-3 fatty acids were observed in MEFs derived from *fat-1* mice compared with those in WT MEFs. Results are expressed as means ± SE. ***p <0.001 versus WT MEFs. (B) MEF cells were incubated with LA and AA (50 μM each) for 24 h before exposure to UVB radiation (20 mJ/cm^2). After 1 h of UVB irradiation, cells were subjected to RT-PCR for mRNA expression of *cox-2*, and Western blot analysis for the protein expression of COX-2 and a phosphorylated form of STAT3 (Tyr^{705}). (C) MEF cells treated as described above were subjected to the DCF-DA assay. Enhancement of UVB-induced intracellular ROS generation was observed in absence of *fat-1* gene. (D) MEF cells were incubated with or without LA and AA (50 μM each) for 24 h. The protein levels of HO-1, NQO1 and Nrf2 were analyzed by Western blot analysis. (E) MEF cells were transiently transfected with *nrf2* siRNA or control siRNA for 48 h and were incubated with or without LA and AA (50 μM each) for 24 h.

Table 3-2. PUFA composition in mouse embryonic fibroblasts (MEFs) from *fat-1* transgenic and wild-type mice

		WT MEF	*fat-1*$^{+/-}$ MEF
Linoleic acid	C18:2	2.95 ± 0.08	1.51 ± 0.01^{c}
γ-Linolenic acid	C18:3	0.07 ± 0.01	0.03 ± 0.01^{a}
Arachidonic acid	C20:4	6.24 ± 0.13	3.89 ± 0.06^{c}
ω-6 PUFAs (%)		9.26 ± 0.21	5.44 ± 0.05^{c}
α-Linolenic acid	C18:3	0.17 ± 0.01	0.37 ± 0.03^{b}
Eicosapentaenoic acid	C20:5	0.44 ± 0.01	1.56 ± 0.21^{b}
Docosahexaenoic acid	C22:6	0.74 ± 0.02	2.67 ± 0.22^{c}
ω-3 PUFAs (%)		1.35 ± 0.02	4.60 ± 0.08^{c}
ω-6/ω-3 PUFAs		6.85 ± 0.10	1.19 ± 0.01^{c}
ω-3/ω-6 PUFAs		0.15 ± 0.003	0.85 ± 0.01^{c}

Data are expressed as means ± SE (n = 3).

^{a}p <0.05, ^{b}p <0.01 and ^{c}p <0.001 versus WT MEFs.

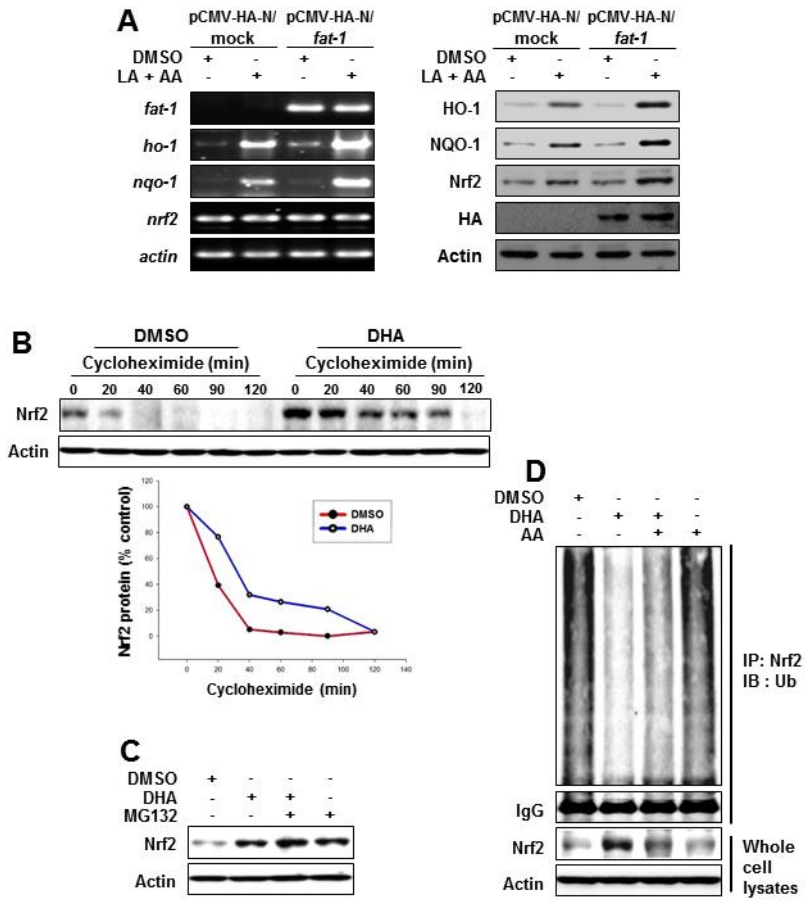

Fig. 3-8. DHA increased the stability of Nrf2 protein in mouse epidermal JB6 cells. (A) JB6 cells were transfected transiently for 24 h with expression plasmids for pCMV-HA-mock or pCMV-HA-*fat-1*. Transfected cells were treated with or without LA and AA (25 μM) for 48 h prior to the RT-PCR and Western blot analysis to determine the levels of Nrf2 and cytoprotective proteins. Transfection with pCMV-HA-*fat-1* increased protein expression of Nrf2 without altering its mRNA transcriptional level in JB6 cells. (B, C) JB6 cells were challenged with 0.1 mg/mL cycloheximide for the indicated times or MG-132 (20 μM) for 30 min in the absence or presence of 50 μM of DHA for

6 h. Western blot analysis was performed for detecting Nrf2 levels. (D) After treatment of JB6 cells with DHA (50 μM) in the absence or presence of AA (25 μM) for 6 h, 500 μg of proteins was immunoprecipitated with anti-Nrf2 antibody and visualized by Western blot analysis with anti-ubiquitin antibody.

5. Discussion

A wide variety of natural anti-inflammatory and anti-oxidative agents which are constituents of our daily diet have been demonstrated to combat skin cancer triggered by UVB irradiation (Chapkin *et al.* 2009, Mittal *et al.* 2003, Singh *et al.* 2006, Staniforth *et al.* 2006b, Won *et al.* 2004). Mounting evidence from epidemiological and laboratory-based studies suggest that ω-3-PUFAs, present in fish oil and plant seed oil, possess a broad range of health beneficial properties (Jho *et al.* 2004) and exert protective effects against oxidative stress-induced disease processes, such as inflammation (Kang & Weylandt 2008), aging (Lukiw & Bazan 2008) and cancer (Rose & Connolly 1999)**.** DHA, one of the major ω-3-PUFAs, has been reported to inhibit UVB-induced inflammatory and oxidative responses in mouse skin (Rahman *et al.* 2011). Rahman *et al.* have demonstrated that topical application of DHA inhibited UVB-induced expression of COX-2 and that of NAD(P)H oxidase-4, an enzyme involved in the generation of ROS, in hairless mouse skin *(Rahman et al.* 2011). These findings are in good agreement with the previously published anti-inflammatory and anti-oxidative effects of this compound (Chen *et al.* 2013, Sunada *et al.* 2006).

Meanwhile, the present study also examines the chemopreventive effects of endogenously produced ω-3 PUFAs against photocarcinogenesis using *fat-1* transgenic mice without the need of supplementation with exogenous ω-3 PUFAs. Modification of the tissue ω-6/ω-3 fatty acid ratio by increasing ω-3

fatty acid levels and decreasing ω-6 fatty acid levels may be an effective therapeutic approach, because this will not only reduce the ω-6-derived tumor-promoting eicosanoids but also increase the formation of ω-3-derived anti-tumor eicosanoids. Experimental data have already showed that the efficacy of ω-3 PUFAs in suppressing cancer growth depends not only on the amount of ω-3 PUFAs but also on background levels of ω-6 PUFAs (Bougnoux 1999).

Homozygous mutations in hairless gene cause a permanent hair loss, referred to as alopecia in both humans and mice (Panteleyev *et al.* 1999). The hairless animals are used historically as a convenient mouse model to study skin carcinogenesis (Benavides *et al.* 2009). To enhance susceptibility to both cutaneous inflammation and papilloma development, we have generated hairless *fat-1*$^{-/-}$ and *fat-1*$^{+/-}$ mice by cross-breeding of male *fat-1*$^{+/-}$ transgenic mice with female SKH-1 hairless mice. The present study showed that an inflammatory response in the hairless *fat-1*$^{+/-}$ mice was significantly lower than in the hairless *fat-1*$^{-/-}$ mice thereby subsequently reducing the susceptibility to UVB-induced papilloma formation.

Recently, COX-2 has been identified as a molecular link between inflammation and tumor promotion (Kundu & Surh 2005). COX-2 has been upregulated in various cells in culture or in mouse skin *in vivo* after irradiation with UVB (Cho *et al.* 2005, Tang *et al.* 2001b, Bachelor *et al.* 2005, Staniforth *et al.* 2006a, Tang *et al.* 2001a). Elevated expression of COX-2 observed in mouse skin papillomas formed after chronic exposure to UVB (An *et al.* 2002, Won *et al.* 2004). A number of animal models have shown that inhibition of

COX-2 by biochemical inhibitors or genetic deletion helps suppress chemical- or UVB-induced skin tumor development (Tiano *et al.* 2002, Wright *et al.* 2006). Oral or topical administration of celecoxib, a COX-2 inhibitor, has been reported to prevent new tumor formation after the onset of UVB-induced photocarcinogenesis in hairless mice (Wilgus *et al.* 2003). In the present study, the stimulation of hairless mice with UVB (180 mJ/cm^2) until 23 weeks resulted in a significant increase in COX-2 expression. Hairless *fat-1*$^{+/-}$ mice capable of spontaneously producing ω-3 PUFAs exhibited significantly reduced expression of COX-2 compared with those from hairless *fat-1*$^{-/-}$ mice, and were protected from UVB-induced photocarcinogenesis. These findings suggest that ω-3 PUFAs could be potential candidates for chemoprevention of inflammation-associated carcinogenesis.

Our *in vivo* data showed that enhanced inflammatory response regulated tumor progression via activation of the transcription factor STAT3 in UVB-irradiated skin of hairless mice. A critical role of STAT3 in promoting proliferation, metastasis and immune evasion of tumor cells has been shown in various pathophysiologic conditions (Yu & Jove 2004). Kim *et al.* reported that constitutive activation of STAT3 enhanced UVB-induced skin carcinogenesis (Kim *et al.* 2009a). Likewise, STAT3 activation promoted keratinocyte survival and proliferation in response to UVB radiation (Sano *et al.* 2005). Thus, inhibition of aberrant STAT3 signaling is considered as a pragmatic approach for achieving the prevention of skin cancer. In this study, the repeated UVB irradiation caused Tyr^{705} phosphorylation of STAT3 in the skin papillomas and

this was attenuated in *fat-1*$^{+/-}$ mice.

ROS-mediated oxidative stress is capable of fostering the development of various pathological conditions mainly by overwhelming skin homeostatic defenses. Body protects against oxidative stress and maintains the reduced state of cells through activation of a series of antioxidant enzymes, such as HO-1 and NQO1 (Surh *et al.* 2008). In line with this notion, WT mice exhibit relatively reduced multiplicity of skin papillomas as compared to HO-1 knockout animals at the early stage of skin carcinogenesis (Was *et al.* 2011). Likewise, NQO1-null mice were more sensitive to chemically induced skin tumorigenesis as compared to WT mice *(*Long *et al. 2000,* Long *et al.* 2001). Nrf2 plays a fundamental role in regulatory expression of many anti-oxidative and cytoprotective proteins including HO-1 and NQO1. Nrf2 knockout mice were more susceptible to develop chemically induce skin tumors (Xu *et al.* 2006). In our results, one of the notable changes accompanying a lower level of oxidative stress related hallmarks and the reduction of papilloma formation by UVB irradiation was the Nrf2-mediated induction of cytoprotective gene expression in the skin tissues of *fat-1* mice.

Since DHA, a prototypic ω-3 PUFA, exhibited pronounced induction of HO-1 and NQO1 *in vitro* (Yang *et al.* 2013), we sought to explore the mechanistic basis of anti-oxidative effects of an elevated ω-3-PUFA level in subsequent experiments using the *fat-1* MEFs. In order to delineate the molecular mechanisms underlying the induction of HO-1 and NQO1, we examined the activation of Nrf2 in the *fat-1* MEFs. The inhibition of HO-1 and NQO1

expression in the Nrf2 siRNA-transfected *fat-1* MEFs suggests that the expression of HO-1 and NQO1 was induced mainly through upregulation of Nrf2 signaling in the *fat-1* MEFs. Furthermore, DHA enhanced stabilization of Nrf2 protein by inhibiting ubiquitination and 26S proteasomal degradation in the JB6 cells. The downregulation of Nrf2 ubiquitination and subsequent 26S proteasomal degradation through disruption of the protein-protein interaction present in Cullin3-Rbx1 E3 ligase complex is generally accepted (Villeneuve *et al.* 2010). As little is known about the mechanisms by which dietary phytochemicals such as DHA leads to Nrf2 activation by targeting ubiquitin ligase complex, much more precise experiments are required.

Nrf2 is normally sequestered in the cytoplasm as an inactive complex with its cytosolic repressor, named Kelch-like ECH associated protein 1 (Keap1) (Lee & Surh 2005, Surh *et al.* 2008). An early independent study suggested that modification of Keap1 cysteines by ARE inducers directly disrupts the interaction between Keap1 and Nrf2 (Dinkova-Kostova *et al.* 2002). However, subsequent experiments demonstrated that in fact the disruption of the Keap1-Nrf2 complex does not occur upon modification of Keap1 cysteines (Eggler *et al.* 2005). While modification of Keap1 cysteines does not alter the affinity of Keap1 for Nrf2, recent data indicate that the Keap1-Cullin3 interaction is altered (Zhang *et al.* 2004a, Gao *et al.* 2007). These results suggested that reaction of Nrf2 activators with Keap1 cysteines leads to a reduced association between Keap1 and Cullin3, thereby downregulating Nrf2 ubiquitination. This would lead to Nrf2 accumulation and increased expression of cytoprotective

proteins. Therefore, whether the activation of Nrf2 by DHA is mediated through direct interaction of DHA or its electrophilic metabolites with Nrf2 inhibitory protein Keap1 merits further investigation.

In conclusion, the present study demonstrates that constitutive ω-3 fatty acid production in the *fat-1* mice protects against UVB-induced papillomagenesis through the downregulation of STAT3 activation, inhibition of lipid perdoxidation and upregulation of cytoprotective proteins. These results may offer practical and feasible approaches for the prevention of skin disorders characterized by inflammation or persistent oxidative stress.

Chapter Ⅳ

Constitutive ω-3 fatty acid production in *fat-1* transgenic mice and docosahexaenoic acid administration to wild type mice protect against 2,4,6-trinitrobenzene sulfonic acid-induced colitis

1. Abstract

Omega-6 (ω-6) and omega-3 (ω-3) polyunsaturated fatty acids (PUFAs) are known to have opposite effects on the inflammatory process. In general, ω-6 PUFAs are pro-inflammatory, whereas ω-3 PUFAs possess anti-inflammatory as well as anti-oxidative activity. In the present study, we investigated the protective effects of ω-3 PUFAs on experimentally induced murine colitis. Intrarectal administration of 2.5% 2,4,6-trinitrobenzene sulfonic acid (TNBS) caused inflammation in the colon of wild type mice, but this was less severe in *fat-1* transgenic mice that constitutively produce ω-3 PUFAs from ω-6 PUFAs. The intraperitoneal administration of docosahexaenoic acid (DHA), a representative ω-3 PUFA, was also protective against TNBS-induced murine colitis. In addition, endogenously formed and exogenously introduced ω-3 PUFAs attenuated lipid peroxidation (malondialdehyde) and protein oxidation (4-hydroxy-2-nonenal) in the colon of TNBS-treated mice. The effective protection against inflammatory and oxidative colonic tissue damages in *fat-1* and DHA-treated mice was associated with suppression of nuclear factor-kappa B activation and cyclooxygenase-2 expression and with elevated activation of nuclear factor erythroid-related factor 2 and upregulation of its target gene, *heme oxygenase-1*. Taken together, these results provide mechanistic basis of protective action of ω-3 fatty PUFAs against experimental colitis.

Keywords

2,4,6-Trinitrobenzene sulfonic acid; Colitis; Docosahexaenoic acid; *fat-1* transgenic mice; Inflammation; Omega-3 polyunsaturated fatty acids

2. Introduction

Inflammatory bowel diseases (IBD) are chronically relapsing disorders of the colon and small intestine (Binder 2004). Their pathogenic features involve dysregulation of the intestinal immune response, characterized by T cell-rich infiltrates and overproduction of reactive oxygen species (ROS) in the inflamed mucosa of the terminal ileum and colon, where many intestinal microbes reside (Rafii *et al.* 1999, Atreya *et al.* 2000). Altered intestinal microflora and ROS overproduction may contribute to initiation and perpetuation of colonic inflammation. Intestinal bacterial endotoxins, such as lipopolysaccharides, penetrate the epithelial barrier and directly stimulate the mucosal immune system (Rafii *et al.* 1999, Radema *et al.* 1991). This results in the production of pro-inflammatory cytokines and other inflammatory mediators, which act through Toll-like receptors or cytokine receptors (Jung *et al.* 1997, Chow *et al.* 1999, Cario & Podolsky 2000). Recently, a better understanding of the mechanisms involved in pathogenesis of IBD has been achieved with the animal models of intestinal inflammation. 2,4,6-Trinitrobenzenesulfonic acid (TNBS)-induced colitis in mice is one such animal model that mimics the human IBD and is hence utilized in preclinical studies (Neurath *et al.* 2000, Wirtz & Neurath 2007, Wirtz *et al.* 2007).

Polyunsaturated fatty acids (PUFAs) are important as structural components of membrane phospholipids and as precursors of families of intracellular signaling molecules, including eicosanoids (Lands 1987, Samuelsson *et al.*

1987, James *et al.* 2000). The eicosanoids derived from omega-6 (ω-6) and omega-3 (ω-3) PUFAs are functionally distinct, and some have opposing physiological functions (James *et al.* 2000, Calder 1997). For example, eicosanoids derived from the ω-6 PUFA arachidonic acid, such as prostaglandin E_2 and leukotriene B_4, have been shown to promote formation, growth, and metastasis of cancer cells (Haeggstrom 2004, Kunikata *et al.* 2005), whereas those from ω-3 PUFAs have suppressive effects (Calder 1997, Rose & Connolly 2000, Karmali 1987, Nie *et al.* 2000, Ge *et al.* 2002, Yang *et al.* 2004). It has been shown that the health benefit of dietary ω-3 PUFAs is most prominent when its proportion exceeds substantially that of ω-6 PUFAs (Cave 1997, Belluzzi *et al.* 1996, Endres *et al.* 1999, Stenson *et al.* 1992). According to recent findings (Simopoulos 2000, Leaf & Weber 1987), the ratio of ω-6 to ω-3 PUFAs in modern diet is approximately 20:1. This may account for the increased incidence of inflammatory diseases (Simopoulos 2000, Leaf & Weber 1987) including IBD in Western societies where diets are largely deficient in ω-3 PUFAs (Shoda *et al.* 1996, Tragnone *et al.* 1995). Thus, balancing the tissue ratio of ω-6 to ω-3 fatty acids may be a feasible approach to the control of many inflammation-associated disorders.

Kang *et al.* generated transgenic mice carrying a *fat-1* gene which encodes desaturase (Kang *et al.* 2004). Unlike the wild type (WT) littermates, these mice can convert ω-6 to ω-3 PUFAs. Different tissues of *fat-1* mice show a marked increase in ω-3 PUFAs and decrease in ω-6 PUFAs (Kang *et al.* 2004). For instance, *fat-1* transgenic mice fed diet containing ω-6 PUFAs had significantly

higher amounts of ω-3 PUFAs in the colonic tissues compared with those in WT mice (Hudert *et al.* 2006). Thus, the *fat-1* transgenic mice offer a model for investigating the importance of the ratio of ω-6/ω-3 PUFA in the management of many inflammation-associated disorders. In the present study, we investigated the beneficial effect of endogenously produced ω-3 fatty acids in *fat-1* transgenic mice on the development of experimentally induced colitis. In a series of parallel experiments, effects of exogenously administered docosahexaenoic acid (DHA), a prototypic ω-3 PUFA, was also examined.

3. Materials and Methods

Animals and diets

fat-1 transgenic mice were backcrossed onto a the C57BL/6 background (Charles River Laboratories, Wilmington, MA). The tails of offsprings were subjected to genotyping to verify the *fat-1* heterozygosity using the Tissue-Direct^{TM} PCR Kit (Lamda Biotech, Inc. St. Louis, MO). The genotyping primers were as follows: 5'-CTG CAC CAC GCC TTC ACC AAC C-3' (forward) and 5'-ACA CAG CAG CAG ATT CCA GAG ATT-3' (reverse). Male heterozygous *fat-1* mice were used in our study and were housed in plastic cages under controlled conditions of temperature (23 ± 2°C), humidity (50 ± 10%) and light (12/12 h light/dark cycle). They fed a 10% safflower oil diet high in ω-6 and low in ω-3 fatty acids until the desired age (8–9 weeks). The studies were approved by the Institutional Animal Care and Use Committee of Seoul National University.

Induction of TNBS-induced colitis

Both WT and transgenic mice were anaesthetized with ketamine and xylazine. Colitis was induced by intrarectal administration of 2.5% TNBS (Sigma Aldrich, St. Louis, MO) in 50% ethanol via a thin round-tip needle equipped with a 1 ml syringe, and the animals were then kept in a vertical position for 30 seconds. The total injection volume was 100 μl. To evaluate the prophylactic effect of DHA (Cayman Chemical Co., Ann Arbor, MI), the TNBS colitis mice

were injected intraperitoneally with 200 µl of phosphate-buffered saline (PBS) or DHA (4 mg/kg body weight) for 7 days before induction of colitis and thereafter until the end of the study. The defecation pattern and the body weight change were monitored daily to see any inflammation signs. The mice were sacrificed 3 days after TNBS administration. The colons were removed, opened longitudinally and cleared of the fecal matter with PBS. Immediately after washing, an inflamed segment was cut for histopathological examination, whereas another portion was flash frozen in lipid nitrogen and kept at -70°C until use.

Histopathological examination

Specimens of the colon fixed with 10% buffered formalin were embedded in paraffin. Each section (4 µm) was stained with hematoxylin and eosin (H&E). The fixed sections were examined by light microscopy for the presence of lesions.

Immunohistochemical analysis

The dissected colon tissues were prepared for immunohistochemical analysis of the expression patterns of 4-hydroxy-2-nonenal (4-HNE)- or malondialdehyde (MDA)-modified protein, cyclooxygenase-2 (COX-2), nuclear factor-kappa B (NF-κB) p65 and nuclear factor erythroid-related factor 2 (Nrf2). Four-µm sections of 10% formalin-fixed, paraffin-embedded tissues were cut on silanized glass slides, deparaffinized three times with xylene and

rehydrated through graded alcohol bath. The deparaffinized sections were heated by using microwave and boiled twice for 6 min in 10 mM citrate buffer (pH 6.0) for antigen retrieval. To diminish nonspecific staining, each section was treated with 3% hydrogen peroxide and 4% peptone casein blocking solution for 15 min. For the detection of respective protein expression, slides were incubated with proteins modified with 4-HNE or MDA (JaICA, Nikken SEIL Co. Ltd., Shizuoka, Japan), COX-2 (Cayman Chemical Co., Ann Arbor, MI), NF-κB p65 and Nrf2 (Santa Cruz Biotechnology, Inc., Santa Cruz, CA) antibodies at room temperature for 40 min in Tris-buffered saline containing 0.05% Tween 20, and then developed using horseradish peroxidase-conjugated secondary antibodies (rabbit or mouse) (Dako, Glostrup, Denmark). The peroxidase binding sites were detected by staining with 3,3'-diaminobenzidine tetrahydrochloride. Finally, counterstaining was performed using Mayer's hematoxylin.

Tissue lysis and protein extraction

Colon tissues were homogenized in ice-cold lysis buffer [150 mM NaCl, 0.5% Triton-X 100, 50 mM Tris–HCl (pH 7.4), 20 mM ethylene glycol tetra-acetic acid, 1 mM dithiothreitol (DTT), 1 mM Na_3VO_4 and protease inhibitors, 1 mM phenylmethyl sulfonylfluoride (PMSF) and ethylenediaminetetraacetic acid (EDTA)-free cocktail tablet] followed by periodical vortex for 30 min at 0°C. Lysates were centrifuged at 14,800 *g* for 15 min at 4°C. Supernatants were collected and stored at -70°C until use.

Preparation of cytosolic and nuclear extracts

Cytosolic extracts were obtained from lysates dissolved in hypotonic buffer A [10 mM 4-(2-hydroxyethyl)-1-piperazineethanesulfonic acid (HEPES, pH 7.8), 1.5 mM $MgCl_2$, 10 mM KCl, 1 mM DTT, 0.1 mM EDTA and 0.1 mM PMSF] with 10% Nonidet P-40 (NP-40) by homogenization and vortex-mixing at 10 min intervals for 3 h. After centrifugation at 14,800 *g* for 15 min, the supernatants (the cytosolic extracts) were collected and stored at -70°C until use. Precipitated pellets were washed with buffer A plus 10% NP-40 three times to remove remaining cytosolic components. Pellets were then resuspended in buffer C [50 mM HEPES, pH 7.8, 50 mM KCl, 300 mM NaCl, 0.1 mM EDTA, 1 mM DTT, 0.1 mM PMSF and 20% glycerol]. After centrifugation at 14,800 *g* for 15 min, the supernatants (nuclear extracts) were collected and stored at -70°C until use.

Western blot analysis

For Western blot analysis, the total protein concentration was quantified by using the bichinconinic acid protein assay kit (Pierce, Rockford, IL). Cell lysates (30 μg protein) were mixed and boiled in sodium dodecyl sulfate (SDS) sample buffer for 5 min before 8-15% SDS-polyacrylamide gel electrophoresis (SDS-PAGE). They were separated by SDS-PAGE and transferred to a polyvinylidene difluoride membrane (Gelman Laboratory, Ann Arbor, MI). The blots were blocked in 5% fat-free dry milk in tris-buffered saline containing 0.1%

tween 20 (TBST) for 1 h at room temperature. The membranes were incubated for 12-24 h at 4°C with dilutions of primary antibodies for proteins modified with 4-HNE (JaICA, Nikken SEIL Co. Ltd., Shizuoka, Japan), COX-2 (Cayman Chemical Co., Ann Arbor, MI), actin (Sigma Aldrich, St. Louis, MO), α-tubulin (Santa Cruz Biotechnology, Inc., Santa Cruz, CA), lamin B (Invitrogen, Carlsbad, CA), P-IκBα, p65 (Cell Signaling Technology, Danvers, MA), heme oxygenase-1 (HO-1) (Stressgen Biotechnologies Co., San Diego, CA), and Nrf2 (Santa Cruz Biotechnology, Inc., Santa Cruz, CA). Membranes were washed followed by incubation with 1:3000 dilutions of respective horseradish peroxidase-conjugated secondary antibodies (rabbit or mouse) (Zymed Laboratories Inc., San Francisco, CA) for 2 h and again washed with TBST. Protein expressed was visualized with an enhanced chemiluminescent (ECL) detection kit (Amersham Pharmacia Biotech, Buckinghamshire, UK) and LAS-4000 image reader (Fujifilm, Tokyo, Japan) according to the manufacturer's instructions.

Reverse transcription-polymerase chain reaction analysis (RT-PCR)

Total RNA was isolated from mouse colon tissues using TRIzol® reagent (Invitrogen, Carlsbad, CA) according to the manufacturer's protocol. To generate the cDNA from RNA, 1 μg of total RNA was reverse transcribed with murine leukemia virus reverse transcriptase (Promega, Madison, WI) for 50 min at 42°C and again for 15 min at 72°C. About 1 μl of cDNA was amplified with a PCR mixture (HS Prime Taq 2X Premix, Daejeon, South Korea) in

sequential reactions. The primers used for each RT-PCR reactions are as follows: *cox-2*, 5'-CTG GTG CCT GGT CTG ATG ATG-3' and 5'-GGC AAT GCG GTT CTG ATA CTG-3'; *actin*, 5'-AGA GCA TAG CCC TCG TAG AT-3' and 5'-CCC AGA GCA AGA GAG GTA TC-3'; *ho-1*, 5'-TAC ACA TCC AAG CCG AGA AT-3' and 5'-GTT CCT CTG TCA GCA TCA CC-3'; *nrf2,* 5'-CCT CTG TCA CCA AGC TCA AGG-3' and 5'-TTC TGG GCG GCG ACT TTA TT-3' (forward and reverse, respectively). Amplification products were analyzed by 2-3% agarose gel electrophoresis, followed by staining with SYBR Green (Invitrogen, Carlsbad, CA) and photographed using fluorescence in LAS-4000 (Fujifilm, Tokyo, Japan).

Statistical analysis

All the values were expressed as the mean ± standard error (SE) of at least three independent experiments. Statistical significance was determined by the Student's *t*-test and $p < 0.05$ was considered to be statistically significant.

4. Results

fat-1 *transgenic and DHA-treated WT mice were protected from TNBS-induced colonic inflammation*

An increased ω-3 PUFA tissue status in *fat-1* transgenic mice conferred effective protection against colitis caused by TNBS injection. Thus, *fat-1* mice exhibited body weight reduction and shortening of the colorectal length caused by TNBS to a lesser extent than the WT mice (**Fig. 4-1A and B**). There were significant differences between TNBS-treated WT and *fat-1* transgenic mice in the bowel habit as well as in the gross findings of colon (**Fig. 4-1C and D**). Histopathological analysis showed that TNBS administration completely disrupted the architecture of colonic mucosa as evidenced by distortion of crypts, loss of goblet cells and infiltration of mononuclear cells. These abnormalities were significantly alleviated in *fat-1* transgenic mice (**Fig. 4-1E**). According to the previously reported PUFA profiles of the colonic tissues of *fat-1* transgenic mice, DHA is the most predominant ω-3 PUFA (Hudert *et al.* 2006). Therefore, we also investigated the protective potential of DHA administered in WT mice which were subjected to TNBS-induced colitis. As in the case of *fat-1* transgenic mice, WT mice administered DHA were protected from TNBS-induced colitis (**Fig. 4-2**).

TNBS-induced oxidative colonic tissue damage was ameliorated in **fat-1** *and DHA-treated mouse colon*

Oxidative stress has been implicated in the pathogenesis of human IBD and experimentally induced colitis. Sustained elevation of ROS production in IBD by activated phagocytic leukocytes, the xanthene oxidase activity and oxidation of arachidonic acid overwhelms the endogenous antioxidant defense, and this leads to oxidative tissue injury, causing impairment in membrane stability and cell death (McKenzie *et al.* 1996). Instillation of TNBS causes production of ROS, initiating and perpetuating colonic inflammation (Liu & Wang 2011). Some reactive aldehydes, such as 4-HNE and MDA, are produced as the secondary products of ROS-mediated lipid peroxidation (Ayala *et al.* 2014, Negre-Salvayre *et al.* 2008). As shown in **Fig. 4-3A and B**, the levels of MDA- and 4-HNE-modified proteins were much lower in the colonic tissues of *fat-1* mice than that in WT animals. Likewise, DHA treatment attenuated oxidative colonic tissue damage as demonstrated by the reduced expression of 4-HNE-modified protein (**Fig. 4-3C and D**).

TNBS-induced expression of COX-2 was decreased in* fat-1 *and DHA-treated mouse colon

Increased expression of the pro-inflammatory enzyme, COX-2 is often observed in the inflamed colonic mucosa of patients with IBD (Wang & Dubois 2010b) as well as TNBS-induced colitis in animals (Paiotti *et al.* 2009, Zhang *et al.* 2004b). To assess whether protection of *fat-1* and DHA-treated mice against TNBS-induced colonic inflammation involves alteration in expression of COX-2, tissue samples were analyzed by RT-PCR and immunoblot analysis.

The mRNA and protein expression levels of COX-2 were markedly diminished in *fat-1* transgenic mice (**Fig. 4-4A**). Immunohistochemical analysis further confirmed the inhibitory effect of endogenously formed ω-3 PUFAs on TNBS-induced COX-2 expression in the *fat-1* mouse colon (**Fig. 4-4B**). DHA administration also inhibited the expression of COX-2 in the colon of TNBS-treated mice (**Fig. 4-4C and D**).

TNBS-induced NF-κB activation was diminished in the colonic mucosa of* fat-1 *and DHA-treated mice

NF-κB is one of the representative redox-sensitive transcription factors that plays a key role in intracellular inflammatory signal transduction. Concordant with the reduced ROS-mediated oxidative stress in *fat-1* mouse colon (**Fig. 4-3**), there was a substantial decrease in NF-κB activation upon TNBS treatment. Activation of NF-κB is dependent on its dissociation from the inhibitory protein IκBα, which requires phosphorylation of the latter protein. We determined the level of phosphorylated IκBα in the colon of mice injected with TNBS. As shown in **Fig. 4-5A and C**, *fat-1* and DHA-treated mice exhibited a significant reduction of TNBS-induced IκBα phosphorylation at the serine 32/36 residue and its subsequent degradation in the colonic mucosa. In addition, TNBS treatment induced nuclear translocation of p65, the functionally active subunit of NF-κB, which was dampened in *fat-1* (**Fig. 4-5A**) and DHA-treated (**Fig. 4-5C**) mice. A significantly lower intensity of p65 immunostaining was also observed in the colonic tissues from *fat-1* and DHA-treated mice, as compared

with WT control mice (**Fig. 4-5B and D**).

The protein level of Nrf2 and its nuclear translocation were increased in the colon of* fat-1 *and DHA-treated mice

NF-κB activation is mediated by ROS to some extent, and antioxidant enzymes can attenuate inflammatory as well as oxidative tissue damage (Kundu & Surh 2010). Nrf2 is a prime transcription factor that plays a key role in regulating the expression of antioxidant genes, such as *HO-1*. There was a robust induction of Nrf2-mediated HO-1 expression in *fat-1* mouse colon (**Fig. 4-6A and B**). Although the colonic mRNA expression levels of Nrf2 were not much different between WT and *fat-1* mice (**Fig. 4-6A**), its protein expression was significantly elevated by endogenous production of ω-3 PUFAs in the latter animals (**Fig. 4-6B**). The nuclear translocation of Nrf2 was also augmented in colonic tissues of *fat-1* mice as compared to that of WT mice (**Fig. 4-6B**). We attempted to evaluate the anti-oxidative effects of DHA in terms of nuclear accumulation of Nrf2 in the colonic mucosa, and a significant difference was found between control and DHA-treated mice (**Fig. 4-6C**). The increased expression of Nrf2 in the colons of DHA-treated mice was verified by immunohistochemical analysis (**Fig. 4-6D**).

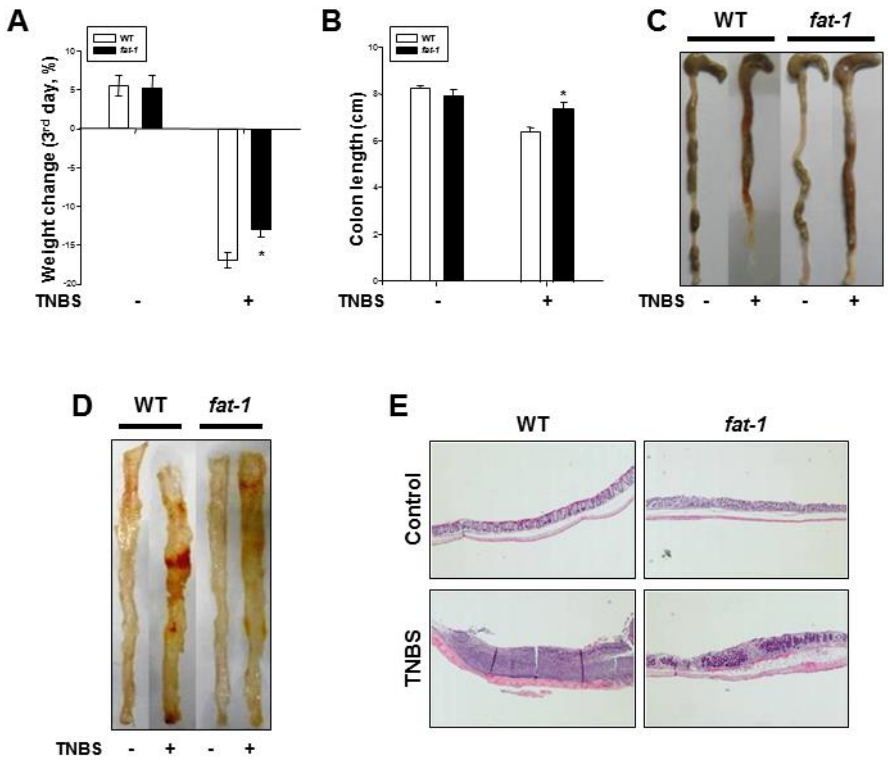

Fig. 4-1. TNBS-induced colonic inflammation was less severe in *fat-1* transgenic mice than that in WT mice. Male WT and *fat-1* transgenic mice were anaesthetized with ketamine and xylazine, and colitis was induced by intrarectal administration of TNBS (2.5% in 50% ethanol). The comparison of (A) body weight change and (B) colon length at day 3 in WT and *fat-1* mice after TNBS exposure. Results are expressed as means ± SE (n = 3 for each group). *p <0.05 versus TNBS-treated WT mice. (C) Representative photographs of the mouse colon in WT and *fat-1* transgenic mice with and without TNBS treatment. (D) Macroscopic view of the mouse colon in WT and *fat-1* mice. (E) Representative distal colon sections stained with H&E. Magnifications; ×100.

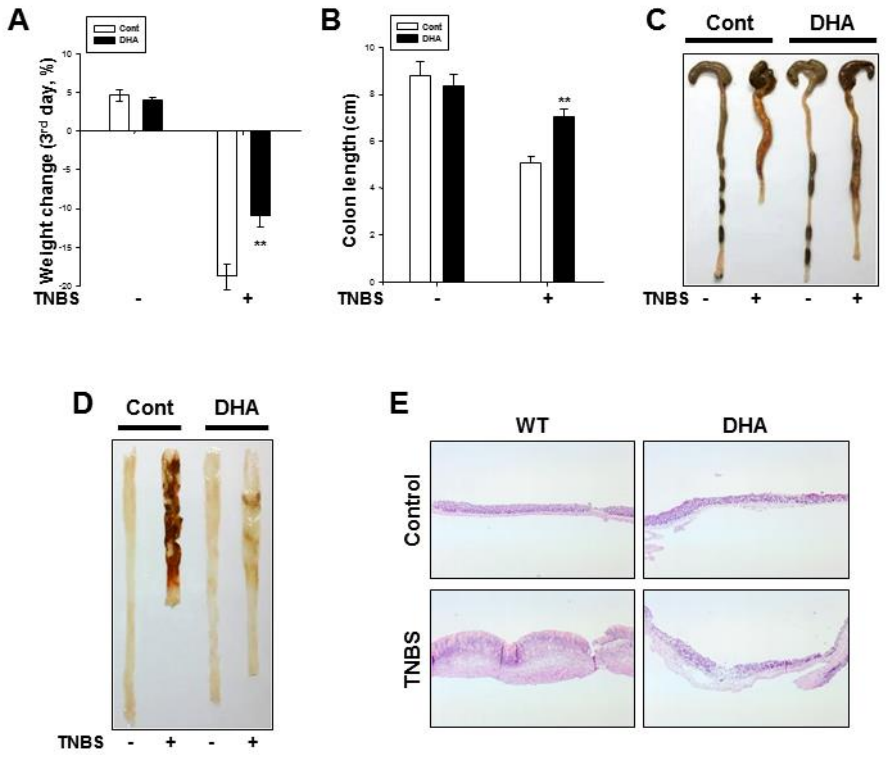

Fig. 4-2. DHA administration ameliorated pathological symptoms in a TNBS-induced murine colitis model. Male C57BL/6 mice were injected intraperitoneally with DHA (4 mg/kg body weight) for 7 days before induction of TNBS colitis and thereafter until the end of the study. The comparison of (A) body weight change and (B) colon length at day 3 in mice after TNBS exposure. Data are expressed as means ± SE (n = 3 for each group). **p <0.01 versus TNBS-treated control mice. (C) Representative photographs and (D) macroscopic view of the mouse colon in control, TNBS-treated, DHA (4 mg/kg)-treated, and DHA (4 mg/kg) plus TNBS-treated group. (E) Representative distal colon sections stained with H&E. Magnifications; ×100.

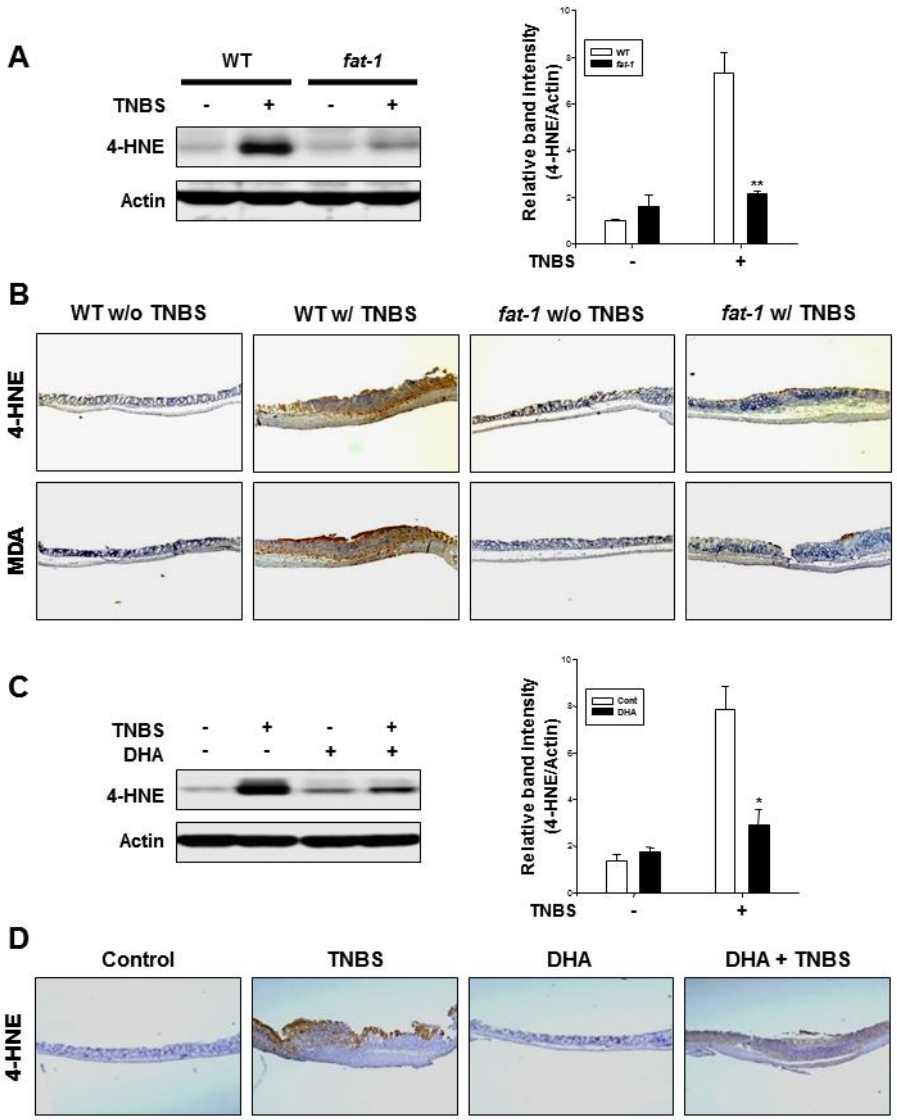

Fig. 4-3. TNBS-induced oxidative colonic tissue damage was attenuated in *fat-1* and DHA-treated mice. (A) Western blot analysis of 4-HNE-modified protein expression in the colon strips of WT and *fat-1* mice. Results are expressed as means ± SE (n = 3, in each group). **Significantly different from TNBS-treated WT mice (p <0.01). (B) Immunohistochemical detection of 4-HNE- and MDA-modified proteins (brown spots) in mouse colon.

Magnifications; ×100. (C) 4-HNE levels in the colonic mucosa of control and DHA-treated mice. *p <0.05 versus TNBS-treated control mice. (D) A representative photomicrograph showing 4-HNE immunopositive cells in mouse colon of each group. Magnifications; ×100.

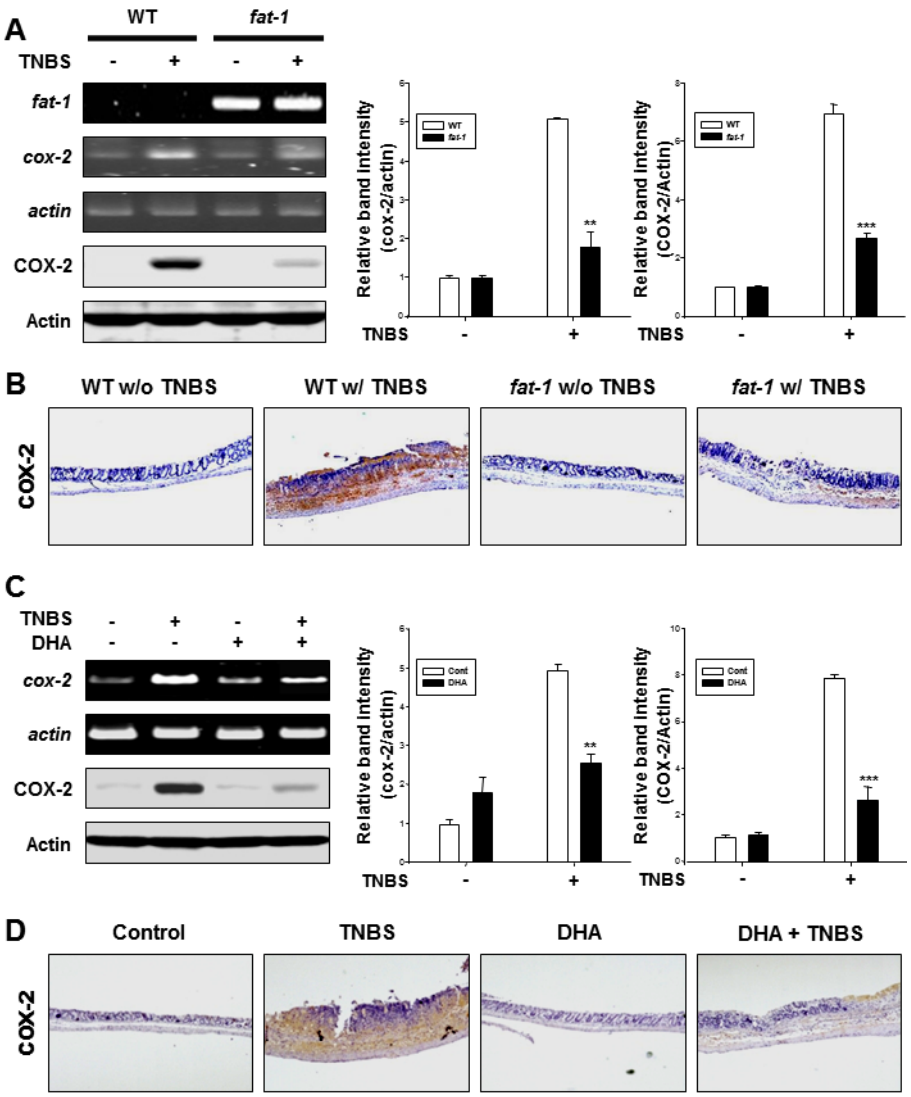

Fig. 4-4. TNBS-induced colonic expression of COX-2 was decreased in *fat-1*- and DHA-treated mice compared with that in WT control mice. (A) RT-PCR and Western blot analysis of COX-2 in colon strips of WT control mice, TNBS-treated WT littermates, *fat-1* transgenic mice, and TNBS-treated *fat-1* littermates. Data are expressed as means ± SE ($n = 3$ for each group). $^{**}p < 0.01$ and $^{***}p < 0.001$ versus TNBS-treated WT mice. (B) Immunohistochemical detection of COX-2 (brown spots) in mouse colon. Magnifications; ×100. (C)

The mRNA and protein levels of COX-2 in colon strips of control, TNBS-treated, DHA (4 mg/kg)-treated, and DHA (4 mg/kg) plus TNBS-treated mice. $^{**}p < 0.01$ and $^{***}p < 0.001$ versus TNBS-treated WT control mice. (D) The respective sections were immunostained for COX-2 and counterstained with hematoxylin. Positive COX-2 staining yielded a brown-colored product. Magnifications; ×100.

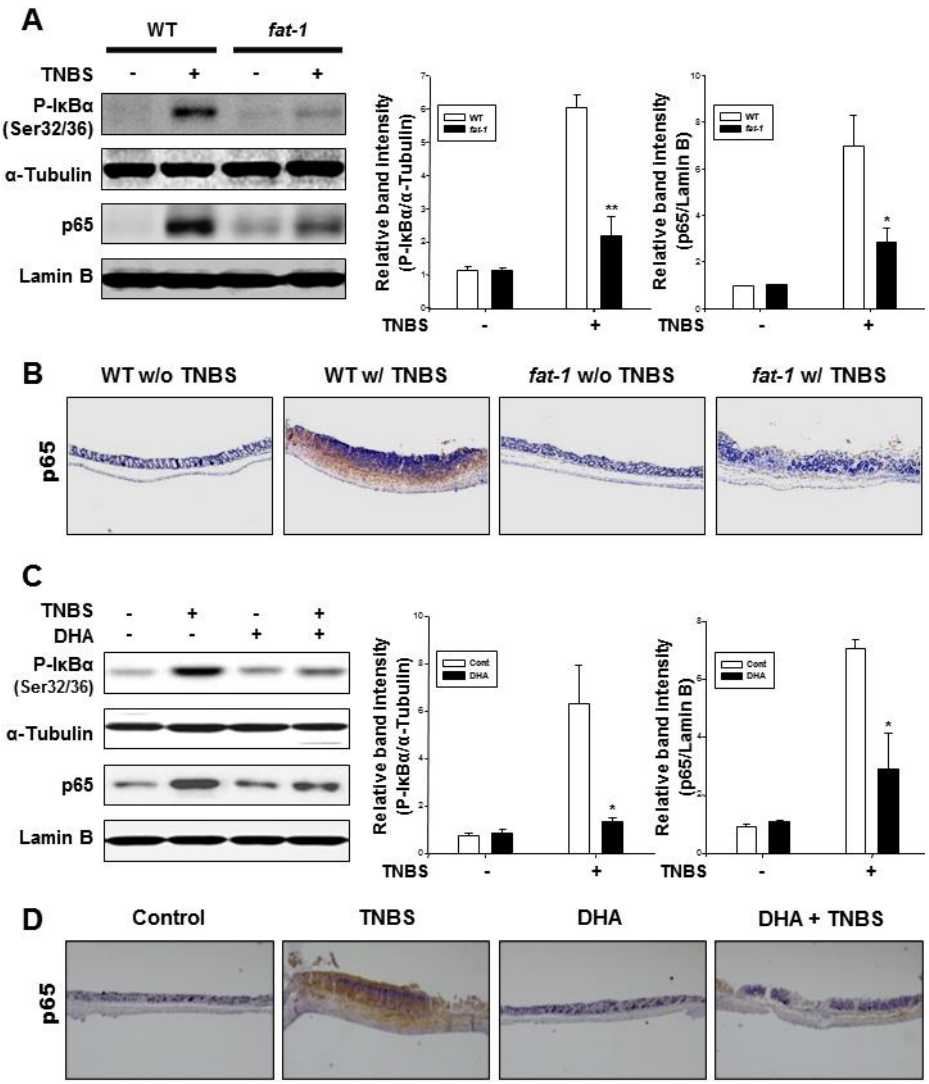

Fig. 4-5. TNBS-induced NF-κB activation was diminished in the colonic tissues of *fat-1* and DHA-treated mice compared with that in the WT control mouse colon. (A) Colonic NF-κB activation in terms of cytosolic P-IκBα (Ser32/36) and nuclear p65 levels was assessed by Western blot analysis. Results are expressed as means ± SE (n = 3, in each group). *p <0.05 and **p <0.01 versus TNBS-treated WT mice. (B) Immunohistochemical analysis of p65 expression. Magnifications; ×100. (C) P-IκBα (Ser32/36) and p65 levels in

the supernatants of colon strips of colon strips of control, TNBS-treated, DHA (4 mg/kg)-treated, and DHA (4 mg/kg) plus TNBS-treated mice. *p <0.05 versus TNBS-treated control mice. (D) Immunohistochemical detection of p65 (brown spots) in the control, TNBS alone, DHA (4 mg/kg) alone, and DHA (4 mg/kg) plus TNBS group. Magnifications; ×100.

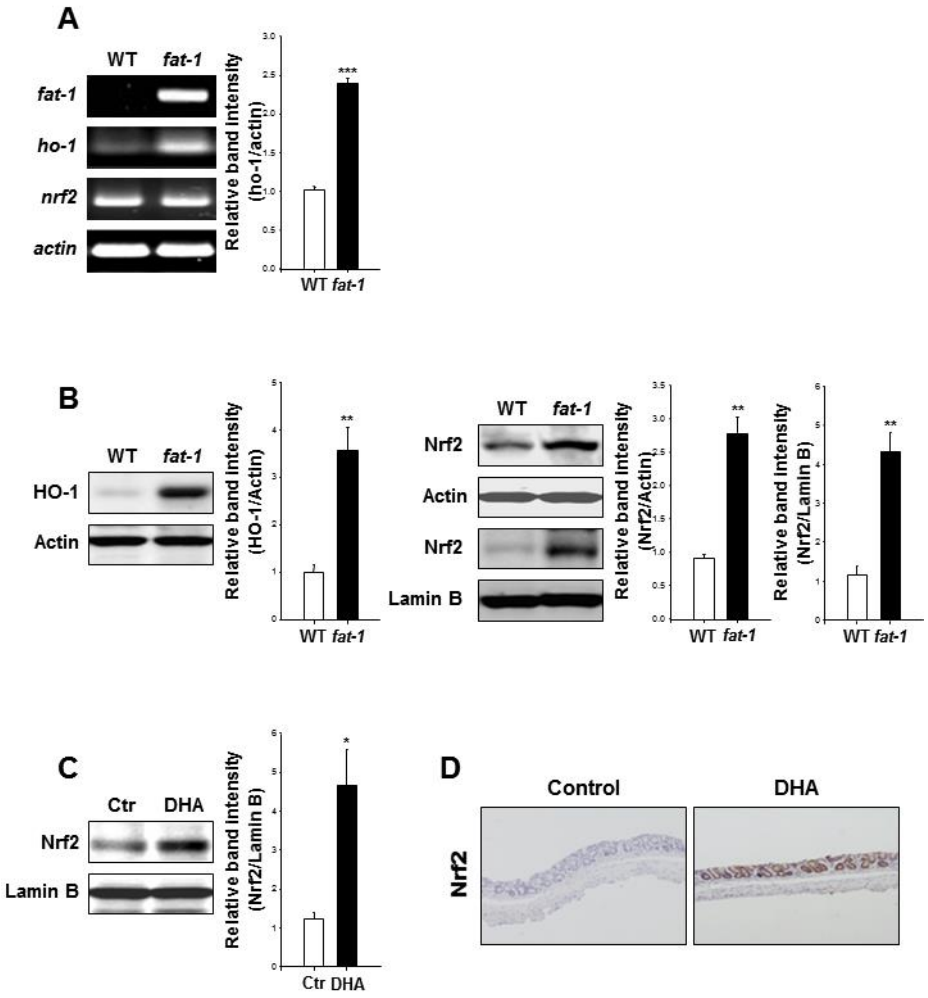

Fig. 4-6. The protein levels of Nrf2 and its nuclear translocation were increased in the colon of *fat-1* and DHA-treated mice. (A) RT-PCR analysis of mRNA expression of *ho-1* and *nrf2* in WT mice and *fat-1* littermates. (B) Western blot analysis of HO-1 and Nrf2 levels in the colon strips of WT and *fat-1* transgenic mice. Data are expressed as means ± SE (n = 3 for each group). $^{**}p$ <0.01 and $^{***}p$ <0 .001 versus WT animals. (C) Nrf2 levels in the nuclear fraction of colon strips of control and DHA-treated mice. $^{*}p$ <0.05 versus control animals. (D) Immunohistochemical detection of Nrf2 (brown spots) in

mouse colon. Magnifications; x100. The experimental conditions are described in Materials and Methods.

5. Discussion

The advent of animal models of mucosal inflammation in the colon has helped researchers a better understanding of the mechanisms involved in intestinal homeostasis and pathogenesis of IBD. TNBS-induced colitis is a well-established animal model of mucosal inflammation and resembles human Crohn's disease in regard to many features, both histologically and immunologically (Neurath *et al.* 2000, Wirtz & Neurath 2007, Wirtz *et al.* 2007). In the present study, *fat-1* transgenic and DHA-treated WT mice were protected from TNBS-induced colonic inflammation. The protection from TNBS-induced colitis in *fat-1* and DHA-treated mice were associated with regulation of the redox-sensitive transcription factors NF-κB and Nrf2 in the colonic mucosa of these animals. NF-κB and Nrf2 regulate pro- and anti-inflammatory gene expression, respectively in a cooperative way (Cuadrado *et al.* 2014). Therefore, proper modulation of NF-κB and Nrf2 signaling is considered an effective strategy in the management of disorders tied to inflammation and oxidative stress.

Evidence for the involvement of COX-2 in colonic inflammation came from the observations that selective inhibitors of this enzyme reduced the severity of the symptoms in the animal model of TNBS-induced colitis (Paiotti *et al.* 2009, Kruschewski *et al.* 2006) as well as patients with Crohn's disease (McCartney *et al.* 1999). Thus, inhibition of the abnormally elevated expression or activity of COX-2 appears to be an effective approach to the prevention and treatment

of IBD. In the present study, *fat-1* mice capable of spontaneously producing ω-3 PUFAs and DHA-treated mice exhibited significantly reduced colonic expression of COX-2 compared with those from WT control animals, and were protected from TNBS-induced colitis. Considering COX-2 as a principal molecular link between inflammation and cancer (Williams *et al.* 1999), these findings suggest that ω-3 PUFAs could be potential candidates for chemoprevention of inflammation-associated colon carcinogenesis.

Our present study demonstrates decreased phosphorylation of IκBα and nuclear translocation of p65, two key events in NF-κB signaling, in *fat-1* and DHA-treated mice, which account for their protection from TNBS-induced colitis. ω-3 PUFAs undergo both enzymatic and non-enzymatic conversion, some of resulting products have powerful anti-inflammatory and proresolving activities (Yum *et al.* 2016). Examples are resolvins and protectins, endogenous ω-3 PUFA-derived lipid mediators (Kohli & Levy 2009, Serhan *et al.* 2008). It will be worthwhile evaluating the protective effects of these endogenous anti-inflammatory and proresolving substances on experimentally induced colitis and colon carcinogenesis. In this context, it is noticeable that resolvin E_1 protects against TNBS-induced colitis (Arita *et al.* 2005).

The inflammatory process not only induces NF-κB activation but also generates ROS and related products, such as superoxide anion, hydrogen peroxide, 4-HNE, and hypochlorous acid, which are involved in the pathogenesis of IBD (Kruidenier *et al.* 2003, Naito *et al.* 2007). We observed in the present study that TNBS significantly increased accumulation of 4-HNE

and MDA as well as NF-κB activation in the colon of mice intrarectally injected with TNBS. Furthermore, it has been reported that treatment with superoxide dismutase significantly ameliorates TNBS-induced colitis (Han *et al.* 2006). The results of the present study support a role for ω-3 PUFAs in the preservation of the intestinal epithelial barrier as demonstrated by higher levels of the anti-oxidative Nrf2 and its target gene, *ho-1* in the colon mucosa of *fat-1* transgenic and DHA-treated mice. Thus, potentiation of cyprotective capacity in the ω-3 PUFA-enriched tissues may be one of the underlying mechanisms responsible for the protection against ROS-induced oxidative damages in TNBS-induced colonic inflammation.

In summary, the protection from colitis observed in *fat-1* and DHA-treated mice is associated with inhibition of NF-κB activation, down-regulation of COX-2 expression, activation of Nrf2 and up-regulation of HO-1 in the intestinal mucosa. Our present work provides the molecular mechanisms of anti-inflammatory and anti-oxidative activities of ω-3 PUFAs in the context of their potential in the management of IBD and other inflammatory aliments.

CONCLUSION

Sustained inflammation is a common denominator of the metabolic syndrome, and implicated in diverse pathological conditions and some types of human cancer. However, long-term use of the NSAIDs for the purpose of preventing/treating inflammation-associated chronic disorders is limited by side effects, so there is the need for new, effective and well-tolerated anti-inflammatory agents. There has been a growing body of epidemiological, clinical and experimental evidence underscoring protective effects of dietary fish oil enriched with ω-3 PUFAs against pathogenesis of the aforementioned disorders. The pleiotropic effects of ω-3 PUFAs on multi-stage carcinogenesis and cancer progression are related to its ability to modulate inflammation-associated signal transduction and gene expression.

Interestingly, the use of *fat-1* transgenic mice can eliminate the need of dietary manipulation and thereby avoid the potential confounding effects of dietary supplementation. This mouse model can provide a well-controlled experimental condition for studying the beneficial effects of ω-3 PUFAs. Thus, the transgenic mice provide powerful new tools for elucidating the benefits of ω-3 PUFAs and the molecular mechanisms of their action.

Recent studies on the distinct set of metabolites derived from ω-3 PUFAs have revealed the endogenous formation of several novel lipid mediators which have proresolving as well as anti-inflammatory effects. If not resolved properly

and in a timely manner, inflammation becomes chronic and can cause various human diseases including cancer. In this regard, it'll be worthwhile evaluating the chemopreventive and anti-carcinogenic potential of those proresolving as well as anti-inflammatory substances that originate from ω-3 PUFAs. Development of therapeutically relevant, stable synthetic analogues of ω-3 PUFAs and their metabolites capable of activating proresolving signal transduction while inhibiting unresolved inflammation will be of prime interest.

REFERENCES

Afaq, F., Adhami, V. M. and Mukhtar, H. (2005) Photochemoprevention of ultraviolet B signaling and photocarcinogenesis. *Mutat Res,* **571,** 153-173.

An, K. P., Athar, M., Tang, X. *et al.* (2002) Cyclooxygenase-2 expression in murine and human nonmelanoma skin cancers: implications for therapeutic approaches. *Photochem Photobiol,* **76,** 73-80.

Arber, N., Eagle, C. J., Spicak, J. *et al.* (2006) Celecoxib for the prevention of colorectal adenomatous polyps. *N Engl J Med,* **355,** 885-895.

Arita, M., Yoshida, M., Hong, S., Tjonahen, E., Glickman, J. N., Petasis, N. A., Blumberg, R. S. and Serhan, C. N. (2005) Resolvin E1, an endogenous lipid mediator derived from ω-3 eicosapentaenoic acid, protects against 2,4,6-trinitrobenzene sulfonic acid-induced colitis. *Proc Natl Acad Sci U S A,* **102,** 7671-7676.

Atreya, R., Mudter, J., Finotto, S. *et al.* (2000) Blockade of interleukin 6 trans signaling suppresses T-cell resistance against apoptosis in chronic intestinal inflammation: evidence in crohn disease and experimental colitis in vivo. *Nat Med,* **6,** 583-588.

Ayala, A., Munoz, M. F. and Arguelles, S. (2014) Lipid peroxidation: production, metabolism, and signaling mechanisms of malondialdehyde and 4-hydroxy-2-nonenal. *Oxid Med Cell Longev,*

2014, 360438.

Bachelor, M. A., Cooper, S. J., Sikorski, E. T. and Bowden, G. T. (2005) Inhibition of p38 mitogen-activated protein kinase and phosphatidylinositol 3-kinase decreases UVB-induced activator protein-1 and cyclooxygenase-2 in a SKH-1 hairless mouse model. *Mol Cancer Res,* **3,** 90-99.

Bannenberg, G. L., Chiang, N., Ariel, A., Arita, M., Tjonahen, E., Gotlinger, K. H., Hong, S. and Serhan, C. N. (2005) Molecular circuits of resolution: formation and actions of resolvins and protectins. *J Immunol,* **174,** 4345-4355.

Beaglehole, R., Bonita, R. and Magnusson, R. (2011) Global cancer prevention: an important pathway to global health and development. *Public Health,* **125,** 821-831.

Belluzzi, A., Brignola, C., Campieri, M., Pera, A., Boschi, S. and Miglioli, M. (1996) Effect of an enteric-coated fish-oil preparation on relapses in Crohn's disease. *N Engl J Med,* **334,** 1557-1560.

Benavides, F., Oberyszyn, T. M., VanBuskirk, A. M., Reeve, V. E. and Kusewitt, D. F. (2009) The hairless mouse in skin research. *J Dermatol Sci,* **53,** 10-18.

Bertagnolli, M. M., Eagle, C. J., Zauber, A. G. *et al.* (2006) Celecoxib for the prevention of sporadic colorectal adenomas. *N Engl J Med,* **355,** 873-884.

Bhattacharya, A., Rahman, M., Banu, J., Lawrence, R. A., McGuff, H. S.,

Garrett, I. R., Fischbach, M. and Fernandes, G. (2005) Inhibition of osteoporosis in autoimmune disease prone MRL/Mpj-Fas(lpr) mice by *N*-3 fatty acids. *J Am Coll Nutr,* **24,** 200-209.

Bhattacharya, A., Sun, D., Rahman, M. and Fernandes, G. (2007) Different ratios of eicosapentaenoic and docosahexaenoic ω-3 fatty acids in commercial fish oils differentially alter pro-inflammatory cytokines in peritoneal macrophages from C57BL/6 female mice. *J Nutr Biochem,* **18,** 23-30.

Binder, V. (2004) Epidemiology of IBD during the twentieth century: an integrated view. *Best Pract Res Clin Gastroenterol,* **18,** 463-479.

Bishayee, A., Thoppil, R. J., Waghray, A., Kruse, J. A., Novotny, N. A. and Darvesh, A. S. (2012) Dietary phytochemicals in the chemoprevention and treatment of hepatocellular carcinoma: *in vivo* evidence, molecular targets, and clinical relevance. *Curr Cancer Drug Targets,* **12,** 1191-1232.

Bougnoux, P. (1999) *n*-3 polyunsaturated fatty acids and cancer. *Curr Opin Clin Nutr Metab Care,* **2,** 121-126.

Burn, J., Bishop, D. T., Chapman, P. D. *et al.* (2011a) A randomized placebo-controlled prevention trial of aspirin and/or resistant starch in young people with familial adenomatous polyposis. *Cancer Prev Res,* **4,** 655-665.

Burn, J., Gerdes, A. M., Macrae, F. *et al.* (2011b) Long-term effect of aspirin on cancer risk in carriers of hereditary colorectal cancer: an analysis

from the CAPP2 randomised controlled trial. *Lancet,* **378,** 2081-2087.

Calder, P. C. (1997) *n*-3 polyunsaturated fatty acids and cytokine production in health and disease. *Ann Nutr Metab,* **41,** 203-234.

Calder, P. C. (2006) Polyunsaturated fatty acids and inflammation. *Prostaglandins Leukot Essent Fatty Acids,* **75,** 197-202.

Calder, P. C. (2008) Polyunsaturated fatty acids, inflammatory processes and inflammatory bowel diseases. *Mol Nutr Food Res,* **52,** 885-897.

Cario, E. and Podolsky, D. K. (2000) Differential alteration in intestinal epithelial cell expression of toll-like receptor 3 (TLR3) and TLR4 in inflammatory bowel disease. *Infect Immun,* **68,** 7010-7017.

Carpenter, C. L. and Cantley, L. C. (1996) Phosphoinositide kinases. *Curr Opin Cell Biol,* **8,** 153-158.

Carpenter, R. L. and Lo, H. W. (2014) STAT3 target genes relevant to human cancers. *Cancers (Basel),* **6,** 897-925.

Cave, W. T., Jr. (1997) ω-3 polyunsaturated fatty acids in rodent models of breast cancer. *Breast Cancer Res Treat,* **46,** 239-246.

Cerutti, P., Ghosh, R., Oya, Y. and Amstad, P. (1994) The role of the cellular antioxidant defense in oxidant carcinogenesis. *Environ Health Perspect,* **102 Suppl 10,** 123-129.

Chang, E. J., Kundu, J. K., Liu, L., Shin, J. W. and Surh, Y. J. (2011) Ultraviolet B radiation activates NF-κB and induces iNOS expression in HR-1 hairless mouse skin: role of IκB kinase-β. *Mol Carcinog,* **50,** 310-317.

Chapkin, R. S., Kim, W., Lupton, J. R. and McMurray, D. N. (2009) Dietary

docosahexaenoic and eicosapentaenoic acid: emerging mediators of inflammation. *Prostaglandins Leukot Essent Fatty Acids,* **81,** 187-191.

Chen, J., Zeng, T., Bi, Y., Zhong, Z., Xie, K. and Zhao, X. (2013) Docosahexaenoic acid (DHA) attenuated paraquat induced lung damage in mice. *Inhal Toxicol,* **25,** 9-16.

Cho, J. W., Park, K., Kweon, G. R., Jang, B. C., Baek, W. K., Suh, M. H., Kim, C. W., Lee, K. S. and Suh, S. I. (2005) Curcumin inhibits the expression of COX-2 in UVB-irradiated human keratinocytes (HaCaT) by inhibiting activation of AP-1: p38 MAP kinase and JNK as potential upstream targets. *Exp Mol Med,* **37,** 186-192.

Chow, J. C., Young, D. W., Golenbock, D. T., Christ, W. J. and Gusovsky, F. (1999) Toll-like receptor-4 mediates lipopolysaccharide-induced signal transduction. *J Biol Chem,* **274,** 10689-10692.

Chun, K. S., Cha, H. H., Shin, J. W., Na, H. K., Park, K. K., Chung, W. Y. and Surh, Y. J. (2004) Nitric oxide induces expression of cyclooxygenase-2 in mouse skin through activation of NF-κB. *Carcinogenesis,* **25,** 445-454.

Chung, H. Y., Cesari, M., Anton, S., Marzetti, E., Giovannini, S., Seo, A. Y., Carter, C., Yu, B. P. and Leeuwenburgh, C. (2009) Molecular inflammation: underpinnings of aging and age-related diseases. *Ageing Res Rev,* **8,** 18-30.

Connor, W. E. (2000) Importance of *n*-3 fatty acids in health and disease. *Am J Clin Nutr,* **71,** 171S-175S.

Connor, W. E. and Connor, S. L. (2007) The importance of fish and docosahexaenoic acid in Alzheimer disease. *Am J Clin Nutr,* **85,** 929-930.

Cottin, S. C., Sanders, T. A. and Hall, W. L. (2011) The differential effects of EPA and DHA on cardiovascular risk factors. *Proc Nutr Soc,* **70,** 215-231.

Coutinho, A. E. and Chapman, K. E. (2011) The anti-inflammatory and immunosuppressive effects of glucocorticoids, recent developments and mechanistic insights. *Mol Cell Endocrinol,* **335,** 2-13.

Cuadrado, A., Martin-Moldes, Z., Ye, J. and Lastres-Becker, I. (2014) Transcription factors NRF2 and NF-κB are coordinated effectors of the Rho family, GTP-binding protein RAC1 during inflammation. *J Biol Chem,* **289,** 15244-15258.

Dalli, J., Zhu, M., Vlasenko, N. A., Deng, B., Haeggstrom, J. Z., Petasis, N. A. and Serhan, C. N. (2013) The novel 13S,14S-epoxy-maresin is converted by human macrophages to maresin 1 (MaR1), inhibits leukotriene A_4 hydrolase (LTA_4H), and shifts macrophage phenotype. *FASEB J,* **27,** 2573-2583.

Del Prete, A., Allavena, P., Santoro, G., Fumarulo, R., Corsi, M. M. and Mantovani, A. (2011) Molecular pathways in cancer-related inflammation. *Biochem Med (Zagreb),* **21,** 264-275.

Dinkova-Kostova, A. T., Holtzclaw, W. D., Cole, R. N., Itoh, K., Wakabayashi, N., Katoh, Y., Yamamoto, M. and Talalay, P. (2002) Direct evidence

that sulfhydryl groups of Keap1 are the sensors regulating induction of phase 2 enzymes that protect against carcinogens and oxidants. *Proc Natl Acad Sci U S A,* **99,** 11908-11913.

Eggler, A. L., Liu, G., Pezzuto, J. M., van Breemen, R. B. and Mesecar, A. D. (2005) Modifying specific cysteines of the electrophile-sensing human Keap1 protein is insufficient to disrupt binding to the Nrf2 domain Neh2. *Proc Natl Acad Sci U S A,* **102,** 10070-10075.

Endres, S., Lorenz, R. and Loeschke, K. (1999) Lipid treatment of inflammatory bowel disease. *Curr Opin Clin Nutr Metab Care,* **2,** 117-120.

Eschenhagen, T., Force, T., Ewer, M. S. *et al.* (2011) Cardiovascular side effects of cancer therapies: a position statement from the Heart Failure Association of the European Society of Cardiology. *Eur J Heart Fail,* **13,** 1-10.

Fischer, S. M., Pavone, A., Mikulec, C., Langenbach, R. and Rundhaug, J. E. (2007) Cyclooxygenase-2 expression is critical for chronic UV-induced murine skin carcinogenesis. *Mol Carcinog,* **46,** 363-371.

Gago-Dominguez, M., Yuan, J. M., Sun, C. L., Lee, H. P. and Yu, M. C. (2003) Opposing effects of dietary *n*-3 and *n*-6 fatty acids on mammary carcinogenesis: The Singapore Chinese Health Study. *Br J Cancer,* **89,** 1686-1692.

Gao, L., Wang, J., Sekhar, K. R. *et al.* (2007) Novel *n*-3 fatty acid oxidation products activate Nrf2 by destabilizing the association between Keap1

and Cullin3. *J Biol Chem,* **282,** 2529-2537.

Ge, Y., Chen, Z., Kang, Z. B., Cluette-Brown, J., Laposata, M. and Kang, J. X. (2002) Effects of adenoviral gene transfer of *C. elegans n*-3 fatty acid desaturase on the lipid profile and growth of human breast cancer cells. *Anticancer Res,* **22,** 537-543.

Gilroy, D. W., Colville-Nash, P. R., Willis, D., Chivers, J., Paul-Clark, M. J. and Willoughby, D. A. (1999) Inducible cyclooxygenase may have anti-inflammatory properties. *Nat Med,* **5,** 698-701.

Gong, J., Xie, J., Bedolla, R. *et al.* (2014) Combined targeting of STAT3/NF-κB/COX-2/EP4 for effective management of pancreatic cancer. *Clin Cancer Res,* **20,** 1259-1273.

Gorjao, R., Azevedo-Martins, A. K., Rodrigues, H. G., Abdulkader, F., Arcisio-Miranda, M., Procopio, J. and Curi, R. (2009) Comparative effects of DHA and EPA on cell function. *Pharmacol Ther,* **122,** 56-64.

Gupta, S. C., Kim, J. H., Prasad, S. and Aggarwal, B. B. (2010) Regulation of survival, proliferation, invasion, angiogenesis, and metastasis of tumor cells through modulation of inflammatory pathways by nutraceuticals. *Cancer Metastasis Rev,* **29,** 405-434.

Haeggstrom, J. Z. (2004) Leukotriene A_4 hydrolase/aminopeptidase, the gatekeeper of chemotactic leukotriene B_4 biosynthesis. *J Biol Chem,* **279,** 50639-50642.

Halliday, G. M. (2005) Inflammation, gene mutation and photoimmunosuppression in response to UVR-induced oxidative

damage contributes to photocarcinogenesis. *Mutat Res,* **571,** 107-120.

Han, W., Mercenier, A., Ait-Belgnaoui, A. *et al.* (2006) Improvement of an experimental colitis in rats by lactic acid bacteria producing superoxide dismutase. *Inflamm Bowel Dis,* **12,** 1044-1052.

Harnack, L., Block, G., Subar, A., Lane, S. and Brand, R. (1997) Association of cancer prevention-related nutrition knowledge, beliefs, and attitudes to cancer prevention dietary behavior. *J Am Diet Assoc,* **97,** 957-965.

Henson, P. M. (2005) Dampening inflammation. *Nat Immunol,* **6,** 1179-1181.

Holub, D. J. and Holub, B. J. (2004) ω-3 fatty acids from fish oils and cardiovascular disease. *Mol Cell Biochem,* **263,** 217-225.

Hudert, C. A., Weylandt, K. H., Lu, Y., Wang, J., Hong, S., Dignass, A., Serhan, C. N. and Kang, J. X. (2006) Transgenic mice rich in endogenous ω-3 fatty acids are protected from colitis. *Proc Natl Acad Sci U S A,* **103,** 11276-11281.

Ibrahim, A., Mbodji, K., Hassan, A., Aziz, M., Boukhettala, N., Coeffier, M., Savoye, G., Dechelotte, P. and Marion-Letellier, R. (2011) Anti-inflammatory and anti-angiogenic effect of long chain *n*-3 polyunsaturated fatty acids in intestinal microvascular endothelium. *Clin Nutr,* **30,** 678-687.

Ihbe-Heffinger, A., Paessens, B., Berger, K., Shlaen, M., Bernard, R., von Schilling, C. and Peschel, C. (2013) The impact of chemotherapy-induced side effects on medical care usage and cost in German hospital care--an observational analysis on non-small-cell lung cancer patients.

Support Care Cancer, **21,** 1665-1675.

James, M. J., Gibson, R. A. and Cleland, L. G. (2000) Dietary polyunsaturated fatty acids and inflammatory mediator production. *Am J Clin Nutr,* **71,** 343S-348S.

Jean, C., Hernandez-Pigeon, H., Blanc, A., Charveron, M. and Laurent, G. (2007) Epidermal growth factor receptor pathway mitigates UVA-induced G2/M arrest in keratinocyte cells. *J Invest Dermatol,* **127,** 2418-2424.

Jho, D. H., Cole, S. M., Lee, E. M. and Espat, N. J. (2004) Role of ω-3 fatty acid supplementation in inflammation and malignancy. *Integr Cancer Ther,* **3,** 98-111.

Jia, Q., Lupton, J. R., Smith, R. *et al.* (2008) Reduced colitis-associated colon cancer in *fat-1* (*n*-3 fatty acid desaturase) transgenic mice. *Cancer Res,* **68,** 3985-3991.

Jung, H. C., Kim, J. M., Song, I. S. and Kim, C. Y. (1997) *Helicobacter pylori* induces an array of pro-inflammatory cytokines in human gastric epithelial cells: quantification of mRNA for interleukin-8, -1 α/β, granulocyte-macrophage colony-stimulating factor, monocyte chemoattractant protein-1 and tumour necrosis factor-α. *J Gastroenterol Hepatol,* **12,** 473-480.

Kang, J. X. (2007) *Fat-1* transgenic mice: a new model for ω-3 research. *Prostaglandins Leukot Essent Fatty Acids,* **77,** 263-267.

Kang, J. X. and Wang, J. (2005) A simplified method for analysis of

polyunsaturated fatty acids. *BMC Biochem,* **6,** 5.

Kang, J. X., Wang, J., Wu, L. and Kang, Z. B. (2004) *Fat-1* mice convert *n*-6 to *n*-3 fatty acids. *Nature,* **427,** 504.

Kang, J. X. and Weylandt, K. H. (2008) Modulation of inflammatory cytokines by ω-3 fatty acids. *Subcell Biochem,* **49,** 133-143.

Kang, Z. B., Ge, Y., Chen, Z., Cluette-Brown, J., Laposata, M., Leaf, A. and Kang, J. X. (2001) Adenoviral gene transfer of *Caenorhabditis elegans n*-3 fatty acid desaturase optimizes fatty acid composition in mammalian cells. *Proc Natl Acad Sci U S A,* **98,** 4050-4054.

Karmali, R. A. (1987) Eicosanoids in neoplasia. *Prev Med,* **16,** 493-502.

Katiyar, S. K., Matsui, M. S., Elmets, C. A. and Mukhtar, H. (1999) Polyphenolic antioxidant (-)-epigallocatechin-3-gallate from green tea reduces UVB-induced inflammatory responses and infiltration of leukocytes in human skin. *Photochem Photobiol,* **69,** 148-153.

Khor, T. O., Yu, S. and Kong, A. N. (2008) Dietary cancer chemopreventive agents - targeting inflammation and Nrf2 signaling pathway. *Planta Med,* **74,** 1540-1547.

Kim, D. J., Angel, J. M., Sano, S. and DiGiovanni, J. (2009a) Constitutive activation and targeted disruption of signal transducer and activator of transcription 3 (Stat3) in mouse epidermis reveal its critical role in UVB-induced skin carcinogenesis. *Oncogene,* **28,** 950-960.

Kim, H., Casta, A., Tang, X., Luke, C. T., Kim, A. L., Bickers, D. R., Athar, M. and Christiano, A. M. (2012) Loss of hairless confers susceptibility to

UVB-induced tumorigenesis via disruption of NF-κB signaling. *PLoS One,* **7,** e39691.

Kim, Y. S., Young, M. R., Bobe, G., Colburn, N. H. and Milner, J. A. (2009b) Bioactive food components, inflammatory targets, and cancer prevention. *Cancer Prev Res,* **2,** 200-208.

Kohli, P. and Levy, B. D. (2009) Resolvins and protectins: mediating solutions to inflammation. *Br J Pharmacol,* **158,** 960-971.

Koon, H. W., Zhao, D., Zhan, Y., Rhee, S. H., Moyer, M. P. and Pothoulakis, C. (2006) Substance P stimulates cyclooxygenase-2 and prostaglandin E_2 expression through JAK-STAT activation in human colonic epithelial cells. *J Immunol,* **176,** 5050-5059.

Kruidenier, L., van Meeteren, M. E., Kuiper, I., Jaarsma, D., Lamers, C. B., Zijlstra, F. J. and Verspaget, H. W. (2003) Attenuated mild colonic inflammation and improved survival from severe DSS-colitis of transgenic Cu/Zn-SOD mice. *Free Radic Biol Med,* **34,** 753-765.

Kruschewski, M., Anderson, T., Buhr, H. J. and Loddenkemper, C. (2006) Selective COX-2 inhibition reduces leukocyte sticking and improves the microcirculation in TNBS colitis. *Dig Dis Sci,* **51,** 662-670.

Kundu, J. K., Chang, E. J., Fujii, H., Sun, B. and Surh, Y. J. (2008) Oligonol inhibits UVB-induced COX-2 expression in HR-1 hairless mouse skin-AP-1 and C/EBP as potential upstream targets. *Photochem Photobiol,* **84,** 399-406.

Kundu, J. K. and Surh, Y. J. (2005) Breaking the relay in deregulated cellular

signal transduction as a rationale for chemoprevention with anti-inflammatory phytochemicals. *Mutat Res,* **591,** 123-146.

Kundu, J. K. and Surh, Y. J. (2010) Nrf2-Keap1 signaling as a potential target for chemoprevention of inflammation-associated carcinogenesis. *Pharm Res,* **27,** 999-1013.

Kundu, J. K. and Surh, Y. J. (2012) Emerging avenues linking inflammation and cancer. *Free Radic Biol Med,* **52,** 2013-2037.

Kunikata, T., Yamane, H., Segi, E. *et al.* (2005) Suppression of allergic inflammation by the prostaglandin E receptor subtype EP3. *Nat Immunol,* **6,** 524-531.

Lands, W. E. (1987) Biochemical and cellular actions of membrane lipids. *Am Rev Respir Dis,* **136,** 200-204.

Leaf, A. and Weber, P. C. (1987) A new era for science in nutrition. *Am J Clin Nutr,* **45,** 1048-1053.

Lee, J. S. and Surh, Y. J. (2005) Nrf2 as a novel molecular target for chemoprevention. *Cancer Lett,* **224,** 171-184.

Liu, X. and Wang, J. (2011) Anti-inflammatory effects of iridoid glycosides fraction of Folium syringae leaves on TNBS-induced colitis in rats. *J Ethnopharmacol,* **133,** 780-787.

Lo, H. W., Cao, X., Zhu, H. and Ali-Osman, F. (2010) Cyclooxygenase-2 is a novel transcriptional target of the nuclear EGFR-STAT3 and EGFRvIII-STAT3 signaling axes. *Mol Cancer Res,* **8,** 232-245.

Lo, H. W., Hsu, S. C., Ali-Seyed, M., Gunduz, M., Xia, W., Wei, Y.,

Bartholomeusz, G., Shih, J. Y. and Hung, M. C. (2005) Nuclear interaction of EGFR and STAT3 in the activation of the iNOS/NO pathway. *Cancer Cell,* **7,** 575-589.

Long, D. J., 2nd, Waikel, R. L., Wang, X. J., Perlaky, L., Roop, D. R. and Jaiswal, A. K. (2000) NAD(P)H:quinone oxidoreductase 1 deficiency increases susceptibility to benzo(*a*)pyrene-induced mouse skin carcinogenesis. *Cancer Res,* **60,** 5913-5915.

Long, D. J., 2nd, Waikel, R. L., Wang, X. J., Roop, D. R. and Jaiswal, A. K. (2001) NAD(P)H:quinone oxidoreductase 1 deficiency and increased susceptibility to 7,12-dimethylbenz[*a*]-anthracene-induced carcinogenesis in mouse skin. *J Natl Cancer Inst,* **93,** 1166-1170.

Love, R. R., Leventhal, H., Easterling, D. V. and Nerenz, D. R. (1989) Side effects and emotional distress during cancer chemotherapy. *Cancer,* **63,** 604-612.

Lukiw, W. J. and Bazan, N. G. (2008) Docosahexaenoic acid and the aging brain. *J Nutr,* **138,** 2510-2514.

Lukiw, W. J., Pelaez, R. P., Martinez, J. and Bazan, N. G. (1998) Budesonide epimer R or dexamethasone selectively inhibit platelet-activating factor-induced or interleukin 1β-induced DNA binding activity of *cis*-acting transcription factors and cyclooxygenase-2 gene expression in human epidermal keratinocytes. *Proc Natl Acad Sci U S A,* **95,** 3914-3919.

Luster, A. D., Alon, R. and von Andrian, U. H. (2005) Immune cell migration

in inflammation: present and future therapeutic targets. *Nat Immunol,* **6,** 1182-1190.

Ma, Y., Lindsey, M. L. and Halade, G. V. (2012) DHA derivatives of fish oil as dietary supplements: a nutrition-based drug discovery approach for therapies to prevent metabolic cardiotoxicity. *Expert Opin Drug Discov,* **7,** 711-721.

Maillard, V., Bougnoux, P., Ferrari, P., Jourdan, M. L., Pinault, M., Lavillonniere, F., Body, G., Le Floch, O. and Chajes, V. (2002) *N*-3 and *N*-6 fatty acids in breast adipose tissue and relative risk of breast cancer in a case-control study in Tours, France. *Int J Cancer,* **98,** 78-83.

Manca, A., Asseburg, C., Bravo Vergel, Y., Seymour, M. T., Meade, A., Stephens, R., Parmar, M. and Sculpher, M. J. (2012) The cost-effectiveness of different chemotherapy strategies for patients with poor prognosis advanced colorectal cancer (MRC FOCUS). *Value Health,* **15,** 22-31.

Matsumura, Y. and Ananthaswamy, H. N. (2004) Toxic effects of ultraviolet radiation on the skin. *Toxicol Appl Pharmacol,* **195,** 298-308.

McCartney, S. A., Mitchell, J. A., Fairclough, P. D., Farthing, M. J. and Warner, T. D. (1999) Selective COX-2 inhibitors and human inflammatory bowel disease. *Aliment Pharmacol Ther,* **13,** 1115-1117.

McKenzie, S. J., Baker, M. S., Buffinton, G. D. and Doe, W. F. (1996) Evidence of oxidant-induced injury to epithelial cells during inflammatory bowel disease. *J Clin Investig,* **98,** 136-141.

Medeiros, R., Figueiredo, C. P., Passos, G. F. and Calixto, J. B. (2009) Reduced skin inflammatory response in mice lacking inducible nitric oxide synthase. *Biochem Pharmacol,* **78,** 390-395.

Medzhitov, R. (2008) Origin and physiological roles of inflammation. *Nature,* **454,** 428-435.

Mittal, A., Elmets, C. A. and Katiyar, S. K. (2003) Dietary feeding of proanthocyanidins from grape seeds prevents photocarcinogenesis in SKH-1 hairless mice: relationship to decreased fat and lipid peroxidation. *Carcinogenesis,* **24,** 1379-1388.

Monje, M. and Dietrich, J. (2012) Cognitive side effects of cancer therapy demonstrate a functional role for adult neurogenesis. *Behav Brain Res,* **227,** 376-379.

Monsuez, J. J., Charniot, J. C., Vignat, N. and Artigou, J. Y. (2010) Cardiac side-effects of cancer chemotherapy. *Int J Cardiol,* **144,** 3-15.

Muller-Decker, K., Neufang, G., Berger, I., Neumann, M., Marks, F. and Furstenberger, G. (2002) Transgenic cyclooxygenase-2 overexpression sensitizes mouse skin for carcinogenesis. *Proc Natl Acad Sci U S A,* **99,** 12483-12488.

Naito, Y., Takagi, T. and Yoshikawa, T. (2007) Molecular fingerprints of neutrophil-dependent oxidative stress in inflammatory bowel disease. *J Gastroenterol,* **42,** 787-798.

Nathan, C. and Ding, A. (2010) Nonresolving inflammation. *Cell,* **140,** 871-882.

Neergheen, V. S., Bahorun, T., Taylor, E. W., Jen, L. S. and Aruoma, O. I. (2010)

Targeting specific cell signaling transduction pathways by dietary and medicinal phytochemicals in cancer chemoprevention. *Toxicology,* **278,** 229-241.

Negre-Salvayre, A., Coatrieux, C., Ingueneau, C. and Salvayre, R. (2008) Advanced lipid peroxidation end products in oxidative damage to proteins. Potential role in diseases and therapeutic prospects for the inhibitors. *Br J Pharmacol,* **153,** 6-20.

Neurath, M., Fuss, I. and Strober, W. (2000) TNBS-colitis. *Int Rev Immunol,* **19,** 51-62.

Nguyen, T., Sherratt, P. J., Nioi, P., Yang, C. S. and Pickett, C. B. (2005) Nrf2 controls constitutive and inducible expression of ARE-driven genes through a dynamic pathway involving nucleocytoplasmic shuttling by Keap1. *J Biol Chem,* **280,** 32485-32492.

Nie, D., Tang, K., Szekeres, K., Trikha, M. and Honn, K. V. (2000) The role of eicosanoids in tumor growth and metastasis. *Ernst Schering Res Found Workshop***,** 201-217.

Oberley, T. D., Xue, Y., Zhao, Y., Kiningham, K., Szweda, L. I. and St Clair, D. K. (2004) *In situ* reduction of oxidative damage, increased cell turnover, and delay of mitochondrial injury by overexpression of manganese superoxide dismutase in a multistage skin carcinogenesis model. *Antioxid Redox Signal,* **6,** 537-548.

Paiotti, A. P., Miszputen, S. J., Oshima, C. T., de Oliveira Costa, H., Ribeiro, D. A. and Franco, M. (2009) Effect of COX-2 inhibitor after TNBS-

induced colitis in Wistar rats. *J Mol Histol,* **40,** 317-324.

Pan, M. H., Lai, C. S., Dushenkov, S. and Ho, C. T. (2009) Modulation of inflammatory genes by natural dietary bioactive compounds. *J Agric Food Chem,* **57,** 4467-4477.

Panteleyev, A. A., Botchkareva, N. V., Sundberg, J. P., Christiano, A. M. and Paus, R. (1999) The role of the hairless (*hr*) gene in the regulation of hair follicle catagen transformation. *Am J Pathol,* **155,** 159-171.

Park, J. H., Lee, C. K., Hwang, Y. S., Park, K. K. and Chung, W. Y. (2008) Hemin inhibits cyclooxygenase-2 expression through NF-κB activation and ornithine decarboxylase expression in 12-*O*-tetradecanoylphorbol-13-acetate-treated mouse skin. *Mutat Res,* **642,** 68-73.

Paul, G., Bataille, F., Obermeier, F. *et al.* (2005) Analysis of intestinal haem-oxygenase-1 (HO-1) in clinical and experimental colitis. *Clin Exp Immunol,* **140,** 547-555.

Petersen, D. R. and Doorn, J. A. (2004) Reactions of 4-hydroxynonenal with proteins and cellular targets. *Free Radic Biol Med,* **37,** 937-945.

Radema, S. A., van Deventer, S. J. and Cerami, A. (1991) Interleukin 1β is expressed predominantly by enterocytes in experimental colitis. *Gastroenterology,* **100,** 1180-1186.

Rafii, F., Lunsford, P., Hehman, G. and Cerniglia, C. E. (1999) Detection and purification of a catalase-peroxidase from *Mycobacterium sp.* Pyr-1. *FEMS Microbiol Lett,* **173,** 285-290.

Rahman, M., Halade, G. V., Bhattacharya, A. and Fernandes, G. (2009) The *fat-1* transgene in mice increases antioxidant potential, reduces pro-inflammatory cytokine levels, and enhances PPARγ and SIRT-1 expression on a calorie restricted diet. *Oxid Med Cell Longev,* **2,** 307-316.

Rahman, M., Kundu, J. K., Shin, J. W., Na, H. K. and Surh, Y. J. (2011) Docosahexaenoic acid inhibits UVB-induced activation of NF-κB and expression of COX-2 and NOX-4 in HR-1 hairless mouse skin by blocking MSK1 signaling. *PLoS One,* **6,** e28065.

Ramaprasad, T. R., Baskaran, V., Krishnakantha, T. P. and Lokesh, B. R. (2005) Modulation of antioxidant enzyme activities, platelet aggregation and serum prostaglandins in rats fed spray-dried milk containing *n*-3 fatty acid. *Mol Cell Biochem,* **280,** 9-16.

Ramsauer, K., Sadzak, I., Porras, A., Pilz, A., Nebreda, A. R., Decker, T. and Kovarik, P. (2002) p38 MAPK enhances STAT1-dependent transcription independently of Ser-727 phosphorylation. *Proc Natl Acad Sci U S A,* **99,** 12859-12864.

Ricciotti, E. and FitzGerald, G. A. (2011) Prostaglandins and inflammation. *Arterioscler Thromb Vasc Biol,* **31,** 986-1000.

Romieu, I., Garcia-Esteban, R., Sunyer, J., Rios, C., Alcaraz-Zubeldia, M., Velasco, S. R. and Holguin, F. (2008) The effect of supplementation with ω-3 polyunsaturated fatty acids on markers of oxidative stress in elderly exposed to PM(2.5). *Environ Health Perspect,* **116,** 1237-1242.

Rose, D. P. and Connolly, J. M. (1999) ω-3 fatty acids as cancer chemopreventive agents. *Pharmacol Ther,* **83,** 217-244.

Rose, D. P. and Connolly, J. M. (2000) Regulation of tumor angiogenesis by dietary fatty acids and eicosanoids. *Nutr Cancer,* **37,** 119-127.

Rossi, A. G., Sawatzky, D. A., Walker, A. *et al.* (2006) Cyclin-dependent kinase inhibitors enhance the resolution of inflammation by promoting inflammatory cell apoptosis. *Nat Med,* **12,** 1056-1064.

Rundhaug, J. E. and Fischer, S. M. (2010) Molecular mechanisms of mouse skin tumor promotion. *Cancers (Basel),* **2,** 436-482.

Russell, F. D. and Burgin-Maunder, C. S. (2012) Distinguishing health benefits of eicosapentaenoic and docosahexaenoic acids. *Mar Drugs,* **10,** 2535-2559.

Samuelsson, B., Dahlen, S. E., Lindgren, J. A., Rouzer, C. A. and Serhan, C. N. (1987) Leukotrienes and lipoxins: structures, biosynthesis, and biological effects. *Science,* **237,** 1171-1176.

Sander, C. S., Chang, H., Hamm, F., Elsner, P. and Thiele, J. J. (2004) Role of oxidative stress and the antioxidant network in cutaneous carcinogenesis. *Int J Dermatol,* **43,** 326-335.

Sano, S., Chan, K. S., Kira, M. *et al.* (2005) Signal transducer and activator of transcription 3 is a key regulator of keratinocyte survival and proliferation following UV irradiation. *Cancer Res,* **65,** 5720-5729.

Serhan, C. N. (2007) Resolution phase of inflammation: novel endogenous anti-inflammatory and proresolving lipid mediators and pathways. *Annu*

Rev Immunol, **25,** 101-137.

Serhan, C. N., Brain, S. D., Buckley, C. D., Gilroy, D. W., Haslett, C., O'Neill, L. A., Perretti, M., Rossi, A. G. and Wallace, J. L. (2007) Resolution of inflammation: state of the art, definitions and terms. *FASEB J,* **21,** 325-332.

Serhan, C. N., Chiang, N. and Van Dyke, T. E. (2008) Resolving inflammation: dual anti-inflammatory and pro-resolution lipid mediators. *Nat Rev Immunol,* **8,** 349-361.

Serhan, C. N., Maddox, J. F., Petasis, N. A., Akritopoulou-Zanze, I., Papayianni, A., Brady, H. R., Colgan, S. P. and Madara, J. L. (1995) Design of lipoxin A_4 stable analogs that block transmigration and adhesion of human neutrophils. *Biochemistry,* **34,** 14609-14615.

Serhan, C. N. and Savill, J. (2005) Resolution of inflammation: the beginning programs the end. *Nat Immunol,* **6,** 1191-1197.

Serini, S., Fasano, E., Piccioni, E., Cittadini, A. R. and Calviello, G. (2011) Differential anti-cancer effects of purified EPA and DHA and possible mechanisms involved. *Curr Med Chem,* **18,** 4065-4075.

Sher, D. J., Wee, J. O. and Punglia, R. S. (2011) Cost-effectiveness analysis of stereotactic body radiotherapy and radiofrequency ablation for medically inoperable, early-stage non-small cell lung cancer. *Int J Radiat Oncol Biol Phys,* **81,** e767-774.

Shoda, R., Matsueda, K., Yamato, S. and Umeda, N. (1996) Epidemiologic analysis of Crohn disease in Japan: increased dietary intake of *n*-6

polyunsaturated fatty acids and animal protein relates to the increased incidence of Crohn disease in Japan. *Am J Clin Nutr,* **63,** 741-745.

Simonsen, N., van't Veer, P., Strain, J. J. *et al.* (1998) Adipose tissue ω-3 and ω-6 fatty acid content and breast cancer in the EURAMIC study. European Community Multicenter Study on Antioxidants, Myocardial Infarction, and Breast Cancer. *Am J Epidemiol,* **147,** 342-352.

Simopoulos, A. P. (2000) Human requirement for *N*-3 polyunsaturated fatty acids. *Poult Sci,* **79,** 961-970.

Singh, R. P., Dhanalakshmi, S., Mohan, S., Agarwal, C. and Agarwal, R. (2006) Silibinin inhibits UVB- and epidermal growth factor-induced mitogenic and cell survival signaling involving activator protein-1 and NF-κB in mouse epidermal JB6 cells. *Mol Cancer Ther,* **5,** 1145-1153.

Smith, W. L., DeWitt, D. L. and Garavito, R. M. (2000) Cyclooxygenases: structural, cellular, and molecular biology. *Annu Rev Biochem,* **69,** 145-182.

Souied, E. H., Delcourt, C., Querques, G., Bassols, A., Merle, B., Zourdani, A., Smith, T., Benlian, P. and Nutritional, A. M. D. T. S. G. (2013) Oral docosahexaenoic acid in the prevention of exudative age-related macular degeneration: the Nutritional AMD Treatment 2 study. *Ophthalmology,* **120,** 1619-1631.

Spychalla, J. P., Kinney, A. J. and Browse, J. (1997) Identification of an animal ω-3 fatty acid desaturase by heterologous expression in Arabidopsis. *Proc Natl Acad Sci U S A,* **94,** 1142-1147.

Staniforth, V., Chiu, L. T. and Yang, N. S. (2006a) Caffeic acid suppresses UVB radiation-induced expression of interleukin-10 and activation of mitogen-activated protein kinases in mouse. *Carcinogenesis,* **27,** 1803-1811.

Staniforth, V., Chiu, L. T. and Yang, N. S. (2006b) Caffeic acid suppresses UVB radiation-induced expression of interleukin-10 and activation of mitogen-activated protein kinases in mouse. *Carcinogenesis,* **27,** 1803-1811.

Stenson, W. F., Cort, D., Rodgers, J., Burakoff, R., DeSchryver-Kecskemeti, K., Gramlich, T. L. and Beeken, W. (1992) Dietary supplementation with fish oil in ulcerative colitis. *Ann Intern Med,* **116,** 609-614.

Sunada, S., Kiyose, C., Kubo, K., Takebayashi, J., Sanada, H. and Saito, M. (2006) Effect of docosahexaenoic acid intake on lipid peroxidation in diabetic rat retina under oxidative stress. *Free Radic Res,* **40,** 837-846.

Sundberg, J. P. and King, L. E., Jr. (2001) Morphology of hair in normal and mutant laboratory mice. *Eur J Dermatol,* **11,** 357-361.

Surh, Y. J. (2003) Cancer chemoprevention with dietary phytochemicals. *Nat Rev Cancer,* **3,** 768-780.

Surh, Y. J., Chun, K. S., Cha, H. H., Han, S. S., Keum, Y. S., Park, K. K. and Lee, S. S. (2001) Molecular mechanisms underlying chemopreventive activities of anti-inflammatory phytochemicals: down-regulation of COX-2 and iNOS through suppression of NF-κB activation. *Mutat Res,* **480-481,** 243-268.

Surh, Y. J., Kundu, J. K. and Na, H. K. (2008) Nrf2 as a master redox switch in turning on the cellular signaling involved in the induction of cytoprotective genes by some chemopreventive phytochemicals. *Planta Med,* **74,** 1526-1539.

Tang, Q., Chen, W., Gonzales, M. S., Finch, J., Inoue, H. and Bowden, G. T. (2001a) Role of cyclic AMP responsive element in the UVB induction of cyclooxygenase-2 transcription in human keratinocytes. *Oncogene,* **20,** 5164-5172.

Tang, Q., Gonzales, M., Inoue, H. and Bowden, G. T. (2001b) Roles of Akt and glycogen synthase kinase 3β in the ultraviolet B induction of cyclooxygenase-2 transcription in human keratinocytes. *Cancer Res,* **61,** 4329-4332.

Tiano, H. F., Loftin, C. D., Akunda, J. et al. (2002) Deficiency of either cyclooxygenase (COX)-1 or COX-2 alters epidermal differentiation and reduces mouse skin tumorigenesis. *Cancer Res,* **62,** 3395-3401.

Toriyama-Baba, H., Iigo, M., Asamoto, M. et al. (2001) Organotropic chemopreventive effects of *n*-3 unsaturated fatty acids in a rat multi-organ carcinogenesis model. *Jpn J Cancer Res,* **92,** 1175-1183.

Tragnone, A., Valpiani, D., Miglio, F., Elmi, G., Bazzocchi, G., Pipitone, E. and Lanfranchi, G. A. (1995) Dietary habits as risk factors for inflammatory bowel disease. *Eur J Gastroenterol Hepatol,* **7,** 47-51.

Tripp, C. S., Blomme, E. A., Chinn, K. S., Hardy, M. M., LaCelle, P. and Pentland, A. P. (2003) Epidermal COX-2 induction following

ultraviolet irradiation: suggested mechanism for the role of COX-2 inhibition in photoprotection. *J Invest Dermatol,* **121,** 853-861.

Tyrrell, R. M. (1995) Ultraviolet radiation and free radical damage to skin. *Biochem Soc Symp,* **61,** 47-53.

Villeneuve, N. F., Lau, A. and Zhang, D. D. (2010) Regulation of the Nrf2-Keap1 antioxidant response by the ubiquitin proteasome system: an insight into cullin-ring ubiquitin ligases. *Antioxid Redox Signal,* **13,** 1699-1712.

Wagener, F. A., Carels, C. E. and Lundvig, D. M. (2013) Targeting the redox balance in inflammatory skin conditions. *Int J Mol Sci,* **14,** 9126-9167.

Wang, D. and Dubois, R. N. (2010a) Eicosanoids and cancer. *Nat Rev Cancer,* **10,** 181-193.

Wang, D. and Dubois, R. N. (2010b) The role of COX-2 in intestinal inflammation and colorectal cancer. *Oncogene,* **29,** 781-788.

Was, H., Sokolowska, M., Sierpniowska, A. et al. (2011) Effects of heme oxygenase-1 on induction and development of chemically induced squamous cell carcinoma in mice. *Free Radic Biol Med,* **51,** 1717-1726.

Wilgus, T. A., Koki, A. T., Zweifel, B. S., Kusewitt, D. F., Rubal, P. A. and Oberyszyn, T. M. (2003) Inhibition of cutaneous ultraviolet light B-mediated inflammation and tumor formation with topical celecoxib treatment. *Mol Carcinog,* **38,** 49-58.

Williams, C. S., Mann, M. and DuBois, R. N. (1999) The role of cyclooxygenases in inflammation, cancer, and development. *Oncogene,*

18, 7908-7916.

Wirtz, S., Neufert, C., Weigmann, B. and Neurath, M. F. (2007) Chemically induced mouse models of intestinal inflammation. *Nat Protoc,* **2,** 541-546.

Wirtz, S. and Neurath, M. F. (2007) Mouse models of inflammatory bowel disease. *Adv Drug Deliv Rev,* **59,** 1073-1083.

Wittgen, H. G. and van Kempen, L. C. (2007) Reactive oxygen species in melanoma and its therapeutic implications. *Melanoma Res,* **17,** 400-409.

Won, Y. K., Ong, C. N., Shi, X. and Shen, H. M. (2004) Chemopreventive activity of parthenolide against UVB-induced skin cancer and its mechanisms. *Carcinogenesis,* **25,** 1449-1458.

Wright, T. I., Spencer, J. M. and Flowers, F. P. (2006) Chemoprevention of nonmelanoma skin cancer. *J Am Acad Dermatol,* **54,** 933-946; quiz 947-950.

Xia, S. H., Wang, J. and Kang, J. X. (2005) Decreased *n*-6/*n*-3 fatty acid ratio reduces the invasive potential of human lung cancer cells by downregulation of cell adhesion/invasion-related genes. *Carcinogenesis,* **26,** 779-784.

Xiong, H., Du, W., Sun, T. T., Lin, Y. W., Wang, J. L., Hong, J. and Fang, J. Y. (2014) A positive feedback loop between STAT3 and cyclooxygenase-2 gene may contribute to *Helicobacter pylori*-associated human gastric tumorigenesis. *Int J Cancer,* **134,** 2030-2040.

Xu, C., Huang, M. T., Shen, G., Yuan, X., Lin, W., Khor, T. O., Conney, A. H. and Kong, A. N. (2006) Inhibition of 7,12-dimethylbenz(*a*)anthracene-induced skin tumorigenesis in C57BL/6 mice by sulforaphane is mediated by nuclear factor E2-related factor 2. *Cancer Res,* **66,** 8293-8296.

Yaar, M. and Gilchrest, B. A. (2007) Photoageing: mechanism, prevention and therapy. *Br J Dermatol,* **157,** 874-887.

Yang, P., Chan, D., Felix, E., Cartwright, C., Menter, D. G., Madden, T., Klein, R. D., Fischer, S. M. and Newman, R. A. (2004) Formation and antiproliferative effect of prostaglandin $E_{(3)}$ from eicosapentaenoic acid in human lung cancer cells. *J Lipid Res,* **45,** 1030-1039.

Yang, Y. C., Lii, C. K., Wei, Y. L., Li, C. C., Lu, C. Y., Liu, K. L. and Chen, H. W. (2013) Docosahexaenoic acid inhibition of inflammation is partially via cross-talk between Nrf2/heme oxygenase 1 and IKK/NF-κB pathways. *J Nutr Biochem,* **24,** 204-212.

Yu, H. and Jove, R. (2004) The STATs of cancer--new molecular targets come of age. *Nat Rev Cancer,* **4,** 97-105.

Yum, H. W., Na, H. K. and Surh, Y. J. (2016) Anti-inflammatory effects of docosahexaenoic acid: Implications for its cancer chemopreventive potential. *Semin Cancer Biol,* **40-41,** 141-159.

Zhang, D. D., Lo, S. C., Cross, J. V., Templeton, D. J. and Hannink, M. (2004a) Keap1 is a redox-regulated substrate adaptor protein for a Cul3-dependent ubiquitin ligase complex. *Mol Cell Biol,* **24,** 10941-10953.

Zhang, L., Lu, Y. M. and Dong, X. Y. (2004b) Effects and mechanism of the selective COX-2 inhibitor, celecoxib, on rat colitis induced by trinitrobenzene sulfonic acid. *Chin J Dig Dis,* **5,** 110-114.

Zhang, Q. S., Maddock, D. A., Chen, J. P., Heo, S., Chiu, C., Lai, D., Souza, K., Mehta, S. and Wan, Y. S. (2001) Cytokine-induced p38 activation feedback regulates the prolonged activation of AKT cell survival pathway initiated by reactive oxygen species in response to UV irradiation in human keratinocytes. *Int J Oncol,* **19,** 1057-1061.

Ziesche, E., Bachmann, M., Kleinert, H., Pfeilschifter, J. and Muhl, H. (2007) The interleukin-22/STAT3 pathway potentiates expression of inducible nitric-oxide synthase in human colon carcinoma cells. *J Biol Chem,* **282,** 16006-16015.

국 문 초 록

염증과 암의 인과관계에 대한 많은 연구가 보고되고 있다. Cyclooxygenase-2 (COX-2)에 의해 생성되는 프로스타글란딘이 염증반응을 매개하고, COX-2의 비정상적인 과도한 발현은 발암 촉진 과정에서도 중요한 역할을 하는 것으로 알려져 왔다. 세포 내 산화적 스트레스는 염증 반응 뿐만 아니라, 이를 스스로 제어하고 조절하고자 하는 생체 내 방어기전을 유발한다. 이러한 세포의 항산화 방어 기전에 중요한 역할을 하는 nuclear factor-erythroid related factor-2 (Nrf2)로, 이는 세포 내 다양한 스트레스에 의해 활성화 되어, 항산화, 해독화 효소들의 발현을 촉진하는 전사인자로 알려져 있다. 본 연구에서는 COX-2가 비정상적 과발현된 염증 및 발암과정에서 화학암예방 후보물질로 알려진 오메가3 지방산이 Nrf2의 활성화를 유도함으로써 산화적 스트레스 및 염증 상황을 조절할 수 있는 지의 여부를 검토하고 그 작용 기전을 분자적 수준에서 규명하고자 하였다.

자외선은 피부노화와 광발암과정에 중요한 환경요인이다. 포유류 피부에 자외선을 조사할 때 세포내 활성산소종의 증가하여 산화적 스트레스가 유발되고, 이는 DNA손상, 단백질 불활성화, 유전자 발현의 변형, 세포막의 손상 그리고 세포자살까지 이르게 한다. 본 연구자는 오메가6 지방산들을 오메가3 지방산들로의 전환을 촉매하는 *fat-1* 유전자가 도입된 형질전환 마우스를 이용하여 자외선

B (Ultraviolet B; UVB)에 의한 피부 손상에 대한 오메가 3 지방산의 보호 효과를 검토하였다. 상기 마우스에 오메가6 지방산이 풍부한 식이를 공급하였을 때, Docosahexaenoic acid (DHA)를 포함한 오메가3 지방산들이 피부 조직에 다량 생성되었다. 암컷 wild-type (WT)과 *fat-1* 마우스 등에 UVB (500 mJ/cm^2)를 조사하였을 시, *fat-1* 마우스는 WT 마우스에 비해 UVB로 인한 염증 및 산화적 조직 손상이 현저히 감소되어 있음을 관찰하였다. 또한, UVB에 의한 signal transducer and activator of transcription 3 (STAT3)의 활성화 및 이 전사 인자의 조절을 받는 표적 단백질 COX-2의 발현이 경감된 것도 확인하였다. 자외선B 조사에 더 민감한 피부 반응을 위해, *fat-1* 수컷과 무모 암컷 마우스들을 교배하여 *fat-1* 무모 마우스들을 만들었다. 일주일에 3번, 23주 동안 암컷 *fat-1* 무모 마우스 등에 UVB (180 mJ/cm^2) 를 조사하여 피부암을 유발시켰다. UVB는 WT의 무모 마우스에 유의적으로 유두종 형성을 촉진하였으며 이는 *fat-1* 무모 마우스에서 그 수가 감소하였다. 또한 피부염 모델 에서와 마찬가지로 기존의 무모 마우스들에 비해 적은 양으로 염증 관련 세포들이 피부에 침윤되었고, STAT3의 활성화와 COX-2의 발현도 경감되었음을 알 수 있었다. 별도의 실험에서 기존의 WT 마우스와 비교하였을 시, Nrf2 전사인자가 유도하는 hemeoxygenase-1 (HO-1) 와 NAD(P)H quinoneoxidoreductase-1 (NQO1) 발현 수준이 *fat-1* 마우스 피부 조직과 mouse embryonic fibroblast (MEF) 세포에서 증가되어 있음을 확인하였다. 마우스 상피 JB6

세포에 *fat-1* 유전자 과발현 벡터를 형질도입 하였을 때도 항산화 효소들 발현이 확연히 증가되었다. *fat-1* MEF 세포에 Nrf2 siRNA를 형질도입 하였을 때, Nrf2 단백질 발현의 감소뿐 만 아니라 세포보호단백질의 발현도 저해됨으로써, Nrf2가 *fat-1* 유전자에 의한 HO-1과 NQO1 단백질 발현을 조절함을 알 수 있었다. 이상의 연구결과들을 통해 자외선B가 유도하는 발암과정에 대한 오메가3 지방산의 화학적암예방효과는 염증 및 발암 과정을 매개하는 표적 단백질들의 활성화를 경감시키고, 활성산소종을 제거하는 항산화 단백질들의 발현 증가를 통해 매개 된다고 사료된다.

장내 감염으로 인한 과민성 장 증후군이 염증 혹은 면역 활성화의 결과로 다양한 소화 증상을 일으키고, 대장암 발생에 영향을 주는 것으로 보고되고 있다. 2,4,6-Trinitrobenzene sulfonic acid (TNBS)는 장염 유발 약물로써 널리 사용되고 있으며 과민반응에 의한 막내 염증을 유발한다. 막 투과를 원활하게 하기 위해 에탄올에 녹여 마우스의 항문에 주입 시, TNBS가 장벽으로 들어가 병변들을 유발하였지만, 이는 *fat-1* 형질전환 마우스에서 경감되었다. 대표적인 오메가3 지방산인 DHA 처리시에도 *fat-1* 형질전환 마우스의 경우와 마찬가지로 대장염에 대한 보호효과를 관찰 할 수 있었다. 별도의 실험에서, 높은 비율의 오메가3 지방산들의 생성과 DHA의 투여 시 TNBS에 의한 산화적 조직 손상 및 염증 관련 효소 COX-2의 발현도 억제되었다. 한편 COX-2 유전자 발현 조절에 중요한 역할을 하는 전사인자 nuclear

factor-kappa B (NF-κB)의 저해제 IκBα의 인산화 및 NF-κB의 주요 구성성분 p65의 핵내 유입이 저해되었음을 관찰할 수 있었다. 이러한 결과로부터 DHA를 포함한 오메가3 지방산의 마우스 대장염 보호 효과는 TNBS에 의한 유도된 NF-κB 활성화 및 COX-2 발현 억제를 통해 일어난다고 볼 수 있으며, 더 나아가 대장암을 예방하는 효과를 나타낼 수 있음을 시사한다.

주요어 (Key words): 오메가3 지방산; *fat-1* 형질전환 마우스; Docosahexaenoic acid (DHA); Ultraviolet B; UVB); 피부암; 2,4,6-Trinitrobenzene sulfonic acid (TNBS); 대장염

학번 (Student Number): 2012-30464